Radio Science Bulletin

ISSN 1024-4530

INTERNATIONAL
UNION OF
RADIO SCIENCE

UNION
RADIO-SCIENTIFIQUE
INTERNATIONALE

U.R.S.I.

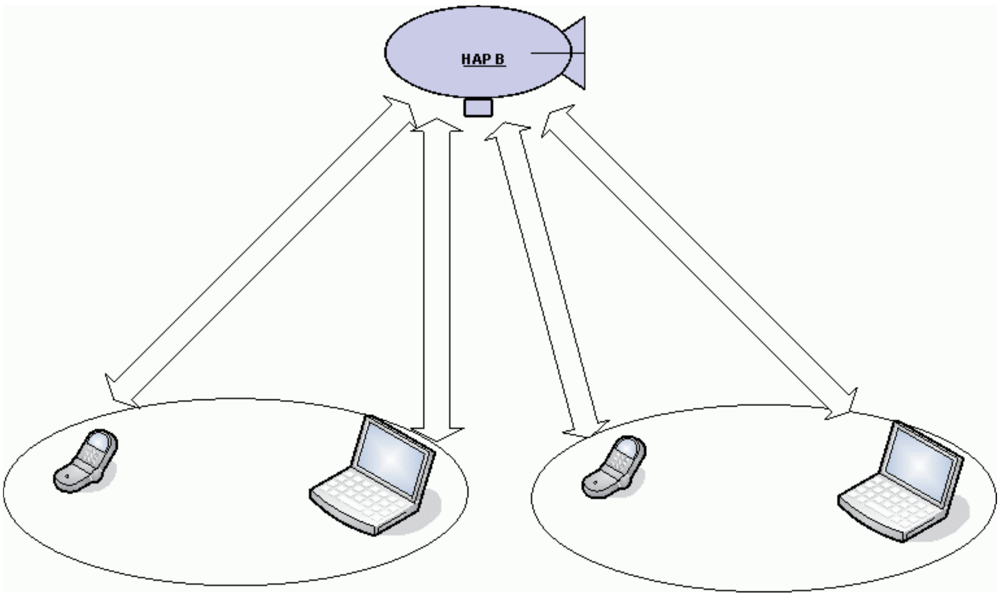

No 334
September 2010

URSI, c/o Ghent University (INTEC)
St.-Pietersnieuwstraat 41, B-9000 Gent (Belgium)

Contents

Front cover: A multi-cell HAP network. See the paper by Popovic et al. on pp. 19-24.

For information, please contact :
The URSI Secretariat
c/o Ghent University (INTEC)
Sint-Pietersnieuwstraat 41, B-9000 Gent, Belgium
Tel.: (32) 9-264 33 20, Fax: (32) 9-264 42 88
E-mail: info@ursi.org

The International Union of Radio Science (URSI) is a foundation Union (1919) of the International Council of Scientific Unions as direct and immediate successor of the Commission Internationale de Télégraphie Sans Fil which dates from 1913.

Editorial

The second Special Section on High-Altitude Platforms (HAPs) appears in this issue. The first special section appeared in the March 2010 issue, No. 332. The Guest Editors of the special section, Jacob Gavan, David Grace, and Ryszard Struzak, have provided a separate introduction to the section. Their efforts in bringing these special sections to the *Radio Science Bulletin* are greatly appreciated.

Our Other Papers

VLF waves propagate in a waveguide formed between the surface of the Earth and the lower boundary of the ionosphere (the D region). This waveguide is perturbed by a variety of solar, ionospheric, atmospheric, and other natural phenomena. Observations of the effects of these perturbations on the propagation of VLF waves have proven to be a powerful means of studying the sources of these perturbations, as well as studying the ionosphere. F. C. P. Bertoni, J.-P. Raulin, H. Rivero Gavilan, W. Guevara Day, R. Rodrigues, and G. Fernandez have provided us with a most interesting paper on SAVNET, the South American VLF NETwork. SAVNET is an international project coordinating such observations at different stations. The paper begins with a brief introduction to effects on VLF propagation. This is followed by an overview of the current scientific observations being carried out with SAVENET. These include the use of propagation effects as a proxy for observing both quiescent and transient solar phenomena, the determination of recombination coefficients in the D region, and measurements of variations in atmospheric temperature. The SAVENET instrumentation is described. The use of SAVENET for studying solar activity is then explained, along with examples of the results obtained to date. Magnetars are neutron stars that have huge magnetic fields, and that suddenly release very large amounts of energy. The authors show that SAVENET has been able to detect magnetar events.

Frank Leferink, Ferran Silva, Johan Catrysse, Sven Battermann, Veronique Beauvois, and Anne Roc'h are the authors of the invited *Review of Radio Science* paper from Commission E that appears in this issue. As these authors point out, the ITU's (International Telecommunication Union's) man-made electromagnetic noise levels are based on measurements from more than 30 years ago, and these measurements were basically made outdoors. The nature, sources, and levels of man-made noise have changed dramatically over time. Furthermore, many of today's sources of man-made electromagnetic noise are located in enclosed and semi-enclosed environments. This paper provides an overview and some new measurements of man-made noise in semi-enclosed environments that are common today. These include common living areas, such as houses, offices, industrial environments, cars, airplanes, trains, and near the now-ubiquitous computers and wireless-communications equipment with which we live. The paper begins with an overview of the characterization of natural and man-made electromagnetic noise. This is followed by a summary of the current data available for man-made electromagnetic noise. The role of man-made electromagnetic noise in producing interference is then examined. The authors report on a new survey of ambient electromagnetic noise in semi-enclosed environments. The fundamental changes over time in the sources and nature of man-made electromagnetic noise illuminated by this paper are fascinating.

The efforts of Christos Christopoulos, the previous Associate Editor for Commission E, and those of Phil Wilkinson, in bringing us this paper are gratefully acknowledged.

Electric-field sensors at HF and lower frequencies are the topic of the paper by Ben-Zion Kaplan, Uri Suissa, David Yardeny, and Arie Sheinker. The authors present what they term an unusual viewpoint of the operation of such sensors. They show that the operating principles of such sensors differ depending on the frequency range of the field being measured. They begin by noting that VHF electric-field sensors are often based on an adjustable half-wavelength dipole, which is small enough to be portable. In contrast, HF sensors that use half-wave dipoles require much larger antennas, which typically have to be built "in place" for each measurement. This has important implications for the calibration of such sensors. The authors then note that sensors for measurement of electric fields at even lower frequencies usually employ capacitive coupling to the field being measured. For sensing even-lower ULF and dc fields, sensors often employ some motion of the sensor's electrodes to create a "dynamic reactance." Having explained their categorization of the sensors qualitatively, the authors then provide some quantitative analysis of the sensors. They conclude with a number of remarks on the application of such sensors. I think that you will find this paper to provide a new and useful way of viewing the operation of electromagnetic sensors, which might inspire new sensor designs.

Also in this Issue

Kristian Schlegel has again provided us with reviews of two new books of interest to radio scientists. If you have a book you think should be reviewed in the *Radio Science Bulletin*, please contact Kristian.

Some of the results from the long-awaited INTERPHONE study of the health effects of cell phones have finally been published. Jim Lin summarizes those relating to brain tumors in his column, and provides some interesting comments regarding their interpretation. He also reports on two additional studies that are underway in the same area.

Now is the time to start planning to submit papers to and attend the XXXth URSI General Assembly and Scientific Symposium! This will be held August 13-20, 2011, in Istanbul, Turkey. The call for papers appears again in this issue. The paper-submission deadline is February 11, 2011. There is also a call for applications to be an URSI Young Scientist at the General Assembly and Scientific Symposium in this issue, along with a call for entries to the URSI Student Paper Competition. I urge you to take note of these, and plan your involvement now. You are going to want to be in Istanbul!

Ross

XXX General Assembly and Scientific Symposium of the International Union of Radio Science

Union Radio Scientifique Internationale

August 13-20, 2011 Lütfi Kırdar Convention and Exhibition Centre, Istanbul, TURKEY

Call for Papers

The XXX General Assembly and Scientific Symposium of the International Union of Radio Science (Union Radio Scientifique Internationale: URSI) will be held at the Lütfi Kırdar Convention and Exhibition Centre in the beautiful historical center of Istanbul, Turkey, August 13-20, 2011.

The XXX General Assembly and Scientific Symposium will have a scientific program organized around the ten Commissions of URSI and consisting of plenary lectures, public lectures, tutorials, posters, invited and contributed papers. In addition, there will be workshops, short courses, special programs for young scientists, student paper competition, programs for accompanying persons, and industrial exhibits. More than 1,500 scientists from more than fifty countries are expected to participate in the Assembly. The detailed program, the link to an electronic submission site, the registration form, and hotel information will be available on the General Assembly Web site: **http://www.ursigass2011.org**

Information for all authors -*Submission information*
All contributions (four pages full paper and up to 100 words abstract) should be submitted electronically via the link provided on the General Assembly Web site. Please consult the symposium Web site, **http://www.ursigass2011.org**, for the latest instructions, templates, and sample formats.

Important Deadlines

Paper submission	February 11, 2011
Notification of acceptance	April 30, 2011

Topics of Interest
Commission A : Electromagnetic Metrology Commission B : Fields and Waves Commission C : Radiocommunication Systems and Signal Processing Commission D : Electronics and Photonics Commission E : Electromagnetic Environments and Interference Commission F : Wave Propagation and Remote Sensing Commission G : Ionospheric Radio and Propagation Commission H : Waves in Plasmas Commission J : Radio Astronomy Commission K : Electromagnetics in Biology and Medicine

Student Paper Competition
A student must be first author of the paper. The student's advisor should attach a statement that his/her contribution is primarily advisory. All other submission requirements and instructions can be found at symposium Web site.

Special Sessions
Individuals interested in organizing special sessions should request permission from the Chair of the appropriate URSI Commission.

Contact
For any questions related to the XXX General Assembly, please contact the Chair of the Conference: Prof. Hamit Serbest Department of Electrical and Electronics Engineering Cukurova University, Adana, Turkey
E-mail: ursigass2011@ursigass2011.org

FIRST ANNOUNCEMENT

The XXX General Assembly and Scientific Symposium of the International Union of Radio Science (Union Radio Scientifique Internationale-URSI) will be held at the Lütfi Kırdar Convention & Exhibition Centre, Istanbul, Turkey on August 13-20, 2011.

The General Assemblies and Scientific Symposia of URSI are held at intervals of

plans for future research and special projects in all areas of radio science, especially where international cooperation is desirable. The first Assembly was held in Brussels, Belgium in 1922 and the latest in Chicago, IL, USA in 2008.

The XXX General Assembly and Scientific Symposium will have a scientific program organized around the ten Commissions of URSI and consisting of plenary lectures, public lectures, tutorials, invited and contributed papers. In addition, there will be workshops, short courses, special programs for young scientists, student paper competition, and programs for accompanying persons. More than 1,500 scientists from more than fifty countries are expected to participate in the Assembly and Scientific Symposium.

The Call for Papers will be issued in mid 2010, will be published in the Radio Science Bulletin and in the IEEE Antennas and Propagation Magazine, and will be posted on the URSI website. It is expected that all papers should be received by the beginning of February 2011, that Authors will be notified of the disposition of their submissions by the end of April 2011.

Preliminary information

Detailed information on the scientific program and on abstract submissions will be available toward the end of March 2010. A web site with current information on the XXX General Assembly is available at: **www.ursigass2011.org** and all abstracts will be received electronically.

Organizing Committee

Chair	A. Hamit Serbest, *Cukurova University, Turkey*, hamitserbest@gmail.com
Vice Chair	Ayhan Altıntaş, *Bilkent University, Turkey*, altintas@ee.bilkent.edu.tr
Finance	Sedef Kent, *Technical University of Istanbul, Turkey*, kents@itu.edu.tr
Publications	Erdem Yazgan, *Hacettepe University, Turkey*, yazgan@hacettepe.edu.tr
Young Scientists	Özlem Aydın Çivi, *Middle East Technical University, Turkey*, ozlem@metu.edu.tr
Student Paper Competition	Birsen Saka, *Hacettepe University, Turkey*, birsen@hacettepe.edu.tr
Workshops/Short Courses	Vakur B. Ertürk, *Bilkent University, Turkey*, vakur@ee.bilkent.edu.tr
Exhibits	Şimşek Demir, *Middle East Technical University*, *Turkey*, simsek@metu.edu.tr
Fundraising	Erdal Panayırcı, *Kadir Has University, Turkey*, eepanay@khas.edu.tr
Registration	Tour Select Ltd, organization@ursigass2011.org
Social activities	Tour Select Ltd, organization@ursigass2011.org
Hotel Reservation	Tour Select Ltd, organization@ursigass2011.org
Contact with URSI	P. Van Daele, peter.vandaele@intec.ugent.be W. Ross Stone, r.stone@ieee.org

Scientific Program Committee

Coordinator	P.L.E. Uslenghi *(U.S.A)*
Associate Coordiator	A. Hamit Serbest *(Turkey)*
Commission A	Chair: P. Banerjee *(National Physical Laboratory, New Delhi, India)* Vice Chair: W. A. Davis *(Virginia Tech, Blacksburg, VA, USA)*
Commission B	Chair: Karl J. Langenberg *(University of Kassel, Germany)* Vice-Chair: Giuliano Manara *(Università di Pisa, Italy)*
Commission C	Chair: Prof. Takashi Ohira *(Toyohashi University of Technology, Japan)* Vice-Chair: Prof. Marco Luise *(University of Pisa-Dip. Ingegneria Informazione, Italy)*
Commission D	Chair: Franz Kaertner *(USA)* Vice Chair: Mr. S. Tedjini *(INPG-ESISAR, France)*
Commission E	Chair: Professor Christos Christopoulos *(University of Nottingham, UK)* Vice-Chair: Professor A P J van Deursen *(Technische Universiteit Eindhoven, Netherlands)*
Commission F	Chair: Madhu Chandra *(Germany)* Vice Chair: Dr R.H. Lang *(George Washington University, USA)*
Commission G	Chair: Dr Michael T Rietveld *(EISCAT Scientific Association, Norway)* Vice Chair: Prof John D Mathews *(Pennsylvania State University, USA)*
Commission H	Chair: Yoshiharu Omura *(Japan)* Vice Chair: Dr. O. Santolik *(Academy of Sciences of the Czech Republic, Czech Republic)*
Commission J	Chair: Subra Anathakrishnan *(India)* Vice Chair: Dr. D.C. BACKER, *(University of California, USA)*
Commission K	Chair: Guglielmo D'Inzeo *(Italy)* Vice Chair: Prof. M. TAKI, *(Tokyo Metropolitan University, JAPAN)*

www.ursigass2011.org

AWARDS FOR YOUNG SCIENTISTS

CONDITIONS

A limited number of awards are available to assist young scientists from both developed and developing countries to attend the General Assembly and Scientific Symposium of URSI.

To qualify for an award the applicant:

1. must be less than 35 years old on September 1 of the year of the URSI General Assembly and Scientific Symposium;
2. should have a paper, of which he or she is the principal author, submitted and accepted for oral or poster presentation at a regular session of the General Assembly and Scientific Symposium.

Applicants should also be interested in promoting contacts between developed and developing countries. Applicants from all over the world are welcome, also from regions that do not (yet) belong to URSI. All successful applicants are expected to participate fully in the scientific activities of the General Assembly and Scientific Symposium. They will receive free registration, and financial support for board and lodging at the General Assembly and Scientific Symposium. A basic accommodation is provided by the assembly organizers permitting the Young Scientists from around the world to collaborate and interact. Young scientists may arrange alternative accommodation, but such arrangements are entirely at their own expense. Limited funds will also be available as a contribution to the travel costs of young scientists from developing countries.

The application needs to be done electronically by going to the same website used for the submission of abstracts/papers. This website is www.papers-GASS2011.ursi.org. The deadline for paper submission for the URSI GASS2011 in Istanbul is 07 February 2011.
A web-based form will appear when applicants check "Young Scientist paper" at the time they submit their paper. All Young Scientists must submit their paper(s) and this application together with a CV and a list of publications in PDF format to the GA submission Web site.

Applications will be assessed by the URSI Young Scientist Committee taking account of the national ranking of the application and the technical evaluation of the abstract by the relevant URSI Commission. Awards will be announced on the URSI Web site in April 2011.

For more information about URSI, the General Assembly and Scientific Symposium and the activities of URSI Commissions, please look at the URSI Web site at: http://www.ursi.org or the GASS 2011 website at http://www.ursigass2011.org/

If you need more information concerning the Young Scientist Program, please contact:

The URSI Secretariat
c/o Ghent University / INTEC
Sint-Pietersnieuwstraat 41
B-9000 GENT
BELGIUM
fax: +32 9 264 42 88
E-mail: ingeursi@intec.ugent.be

XXXth URSI General Assembly and Scientific Symposium

Istanbul, Turkey August 13-20, 2011

URSI Student Paper Competition

Chair: Prof. Steven C. Reising
Colorado State University, Fort Collins, CO, USA

Student Paper Prize winners, 1st Place through 5th Place, will be awarded a certificate and check in the amounts of $1500, $1250, $1000, $750 and $500, respectively.

Rules and Guidelines

- First author and presenter must be a full-time university student.
- The topic of the paper must be related to the field of one of the ten URSI Commissions.
- A full paper must be submitted by the abstract deadline. The paper must be not longer than 25 pages and in the single-column, double-spaced manuscript format of the journal *Radio Science*.
- A letter from the student's advisor on university letterhead must be appended to the paper. The letter must state that the author is enrolled as a full-time university student in a degree program. If co-authored, the letter must state that all co-authors played only an advisory role. *No other students are permitted as co-authors*.
- Ten finalists will be chosen based upon quality, originality and scientific merit. They will receive free access to the workshop/short course of their choice. They will be required to attend the banquet, where all finalists will be recognized, and the prizes will be presented.
- The URSI Panel of Judges will consist of the ten URSI Commission Chairs or their authorized representatives, in case of absence.
- In addition, the prizes will be awarded based on the clarity of their presentation, accessibility to the broad audience of the ten URSI Commissions and the ability to answer questions on their work.
- All participants will have the option of submitting their full paper manuscripts for review for publication in a special section of the journal *Radio Science* edited by Prof. Piergiorgio L. E. Uslenghi, Univ. of Illinois at Chicago, IL, USA, 2011 URSI GASS Scientific Program Coordinator.

Introduction to the Special Section on High-Altitude Platforms

The URSI *Radio Science Bulletin* has been covering the subject of radio communications from High-Altitude Platforms (HAPs). This began with the presentation of an introduction and review paper on HAPs, "Concepts and Main Applications of High-Altitude-Platform Radio Relays," which was published in issue No. 330, September 2009, pp. 20-31. This was followed by the first of two special sections, in issue No. 332, published in March 2010, pp. 17-74. That special section included five papers:

- "Circularly Polarized Homogeneous Lens Antenna System Providing Multi-Beam Radiation Pattern for HAPS"
- "Inter-High Altitude Platform Handoff for Communications Systems with Directional Antennas"
- "Low-Latency MAC Layer Handoff for a High-Altitude Platform Delivering Broadband Communications"
- "WIMAX HAPs-Based Downlink Performance Employing Geometrical and Statistical Channel Propagation Characteristics"
- "ITUs Regulatory Framework, Technical Studies in ITU-R, and Future Activities in Relation to High-Altitude-Platform Station (HAPS)"

These papers thoroughly analyzed the state of the art of HAPs antennas and radio systems, especially for future communication generations. An overview was also provided of the development of HAPs from the global standardization and regulation viewpoint.

This second special section on HAPs includes three papers. The first paper, "Directional Traffic-Aware Intra-HAP Handoff Scheme for HAP Communications Systems," is a complement to the second and third papers of the first special section on HAPs. In this paper, a novel directional traffic-aware intra-HAP handoff scheme (DTAHS) is proposed. In this, users in overlap areas of overloaded cells may be forced to hand off earlier than their optimal handoff boundaries, in order to partially balance the traffic among the adjacent cells. The new scheme provides a compromise between the new-call-blocking probability and the handoff-call-dropping probability when the overlap interval between adjacent cells is relatively short. Simulation results showed that the new scheme outperforms both the load-balancing handoff scheme (LBHS) and the cooperative-directional intra-HAP handoff scheme (CDHS). It can be also concluded that the variation of new-call-blocking probability for different overlap intervals is lower than that of the handoff-call-dropping probability.

David Grace is with the Department of Electronics, the University of York, York, YO10 5DD, UK; e-mail: dg6@ohm.york.ac.uk. Jacob Gavan is with the Sami Shamoon College of Engineering, Jabutinsky 84, Ashdod, Israel; e-mail: gavan@hit.ac.il. Ryszard Struzak is with the National Institute of Telecommunications, Swojczycka 38, 51-501, Wroclaw, Poland; e-mail: struzak@gmail.com.

The second paper, "On Security Advantages of HAPs over Satellites," may contribute to the important security issues of HAPs, using hierarchical security tactics for HAPs, and providing a comparison to satellites. This paper analyses and compares security features of network architectures based on HAPs and satellites. The concrete contributions are twofold. First, this paper proposes a security comparison method of network architectures that are based on airborne infrastructure, e.g., HAPs and satellites. Second, the paper presents the results of the comparison, which show that network architecture based on HAPs out-perform network architectures based on satellites in respect to most of the analyzed security features.

The third paper, "Microwave Wireless-Power Transmission to High-Altitude-Platform Systems," may contribute to the long operation of HAPs by the utilization of microwave wireless-power-transmission systems. This paper starts with the description of the concept of the different wireless-power-transmission systems, followed by a review of the genesis of and developments in wireless-power-transmission systems. However, the paper mainly concentrates on microwave wireless-power-transmission systems for feeding stratospheric HAP airships. Several research and development results, obtained in the evaluation steps of the fascinating solar-power satellites (SPS), are useful for the future design and implementation of HAPs microwave wireless-power-transmission systems. Comparisons between microwave wireless-power-transmission systems for terrestrial links, stratospheric HAPs, and solar-power-satellites in a geostationary orbit are provided. In an Appendix, simple methods are developed for computing the areas of the microwave wireless-power-transmission transmitter antenna arrays, microwave beams, and rectenna as functions of the required power-transmission efficiency, separation distances, and frequency bands. The results show that the required microwave wireless-power-transmission systems areas, weights, complexity, and cost are significantly less for HAPs than for solar-power satellites. The design and realization of microwave wireless-power-transmission systems feeding HAPs may thus contribute for the future realization and preliminary tests of solar-power-satellite systems.

The guest editors would again like to thank the authors for their contributions. They would also like to thank the reviewers, who have provided useful feedback in the form of suggestions and corrections to help improve the quality of the manuscripts. We would also like to thank Dr. Ross Stone, the Editor of the URSI *Radio Science Bulletin*, for giving us this opportunity to put together these special sections. Finally, we hope that the *Radio Science Bulletin*'s readers will find the articles inspiring and helpful to their future research.

Jacob Gavan, David Grace and Ryszard Struzak

Directional Traffic-Aware Intra-HAP Handoff Scheme for HAP Communications Systems

Shufeng Li
David Grace
Jibo Wei
Dongtang Ma

Abstract

In this paper, a novel directional traffic-aware intra-HAP handoff scheme (DTAHS) is proposed. In this, users in overlapping areas of overloaded cells may be forced to hand off earlier than their optimal handoff boundaries, in order to partially balance the traffic among the adjacent cells. The new scheme provides a good compromise between the new-call-blocking probability and the handoff-call-dropping probability, when the overlap interval between adjacent cells is relatively short. Simulation results show that the new scheme outperforms both the load-balancing handoff scheme (LBHS) and the cooperative directional intra-HAP handoff scheme (CDHS) when the factor value associated with call blocking is smaller than 0.8 and bigger than 0.4 for a relatively short overlap interval. It can be also concluded that the variation of new-call-blocking probability for different overlap intervals is lower than that of the handoff-call-dropping probability. The load-balancing handoff scheme and the directional traffic-aware intra-HAP handoff scheme are suitable for the long and short overlap interval cases, respectively.

1. Introduction

High-altitude platforms (HAPs), operating in the stratosphere at altitudes of up to 22 km, are proposed to provide 3G mobile or broadband fixed wireless-access (BFWA) services [1-3]. A HAP communications system can exploit the best features of both terrestrial and satellite communications systems, such as a large area of coverage, a low cost of deployment, and no shadowing for high elevation angles. This type of system has the prospect of becoming one of the most important types of communications infrastructure in the near future.

The platform, either an airship or an aircraft, is not able to remain completely stationary in the stratosphere. Generally, the platform's movement can be decomposed into horizontal/vertical displacement and inclination, where the horizontal displacement has been shown to degrade the downlink capacity [4]. The effects of the platform's instability can be counterbalanced by a mechanical propulsion mechanism [4], by using multiple platforms to provide diversity for signal reception [5], or by different antenna-pointing strategies that are employed to compensate for platform displacement [6]. Moreover, handoff has been proposed for HAP communications systems to maintain service continuity when users move between cells, caused by the movement of the platform. Katzis et al. revealed that the handoff and dropping probability increases due to the platform movement [7]. The effects of the platform motion on IMT-2000 soft handover were also addressed in [8]. Moreover, a number of issues relating to the inter-HAP handoff have been examined when the platform is replaced, either for maintenance, or periodic replacement in the case of short-term manned HAPs [9].

In multi-cell communications systems, many radio-resource management schemes – which manipulate either the capacity [10, 11] or the traffic [12-14] among the adjacent cells to achieve load balancing – have been proposed to improve the system's performance. The reader can refer to [15] for a thorough understanding of a mathematical theory of dynamic load balancing. Some of these schemes, such as guard channels [11] and queuing [13], are adopted to give priority to handoff calls, and to reduce the handoff-dropping performance, which is perceived to be more important than the new-call blocking performance. However, these handoff-call-prioritizing schemes either cannot improve the new-call-blocking performance [13], or they even degrade the new-call-blocking performance [11]. A load-balancing scheme can improve both the new-call-blocking

Shufeng Li, Jibo Wei, and Dongtang Ma are with the School of Electronic Science and Engineering, National University of Defense Technology, Changsha, Hunan Province, 410073, China (CIE); e-mail: {lishufeng, wjbhw, dongtangma}@nudt.edu.cn. Shufeng Li and David Grace are with the Communications Research Group, Department of Electronics, University of York, Heslington, York, YO10 5DD, United Kingdom; e-mail: lishufeng@nudt.edu.cn; dg@ohm.york.ac.uk.

and handoff-call-dropping performance [14]. However, the handoff-dropping performance improvement is restricted by more ongoing calls introduced to the system, especially for situations when excessive handoff calls happen.

To date, there is no paper that has discussed the handoff issues in HAP communications systems that has combined load balancing with the intra-HAP handoff, considering altogether both the new-call and handoff-call performance. Therefore, in this paper we propose a directional traffic-aware intra-HAP handoff scheme. This partially exploits the traffic fluctuation, and considers characteristics of HAP communications systems, such as a co-located cellular structure and directional handoff. Simulation results show how the new scheme provides a good compromise between the new-call-blocking probability and the handoff-call-dropping probability.

2. Explanation of Radio Resource-Management Schemes and Orthogonalization

Obviously, radio resource-management schemes [10-14] try to avoid new calls and/or handoff calls accessing potentially blocked cells in which all the channels are occupied, or they try to maximize the difference between the channel resources and the carried traffic. Orthogonalization theory is used in this paper to give a distinct explanation to these radio resource-management schemes.

For multi-cell communications systems with a cell-reuse factor N, it is assumed that only one new-call arrival and/or handoff call happens during a time Δt for the cells in a cell-reuse group. The cell in a cell-reuse group can be represented by C_i, $i = 1,...,N$, where $\lambda_i^n(j\Delta t)$, $\lambda_i^h(j\Delta t)$ and $\mu_i(j\Delta t)$ are the new-call-arrival state, the handoff-call-arrival state, and the call-departure state, respectively, for the cell C_i at time $j\Delta t$. They are equal to one if the respective event happens, and equal to zero, otherwise. The cell C_i provides $C_i^n(j\Delta t)$ total channels for the new call, and provides $C_i^h(j\Delta t)$ total channels for the handoff call, at time $j\Delta t$. The carried traffic of the cell C_i, $L_i(j\Delta t)$, which is generally a stochastic process, often has a large difference among cells in a cell group. The cell C_i has two states for the new call and the handoff call: the congested state, when the carried traffic reaches the capacity of the current cell; and the non-congested state, when the traffic in the system is less than the capacity of the current cell. The state of the cell C_i for the new call and the handoff call can respectively be represented by the following equations:

$$f_i^n(j\Delta t) = \begin{cases} 1, L_i(j\Delta t) \geq C_i^n(j\Delta t) \\ 0, L_i(j\Delta t) < C_i^n(j\Delta t) \end{cases}$$

and

$$f_i^h(j\Delta t) = \begin{cases} 1, L_i(j\Delta t) \geq C_i^h(j\Delta t) \\ 0, L_i(j\Delta t) < C_i^h(j\Delta t) \end{cases}.$$

System performance metrics, such as the new-call-blocking probability (P_B) and the handoff-call-dropping probability (P_D), are generally used to evaluate the performance of different radio resource-management schemes. These two performance metrics are defined as follows:

New-call-blocking probability (P_B): the ratio of the number of the rejected new-call requests to the number of the total new-call requests in the system.

Handoff-call-dropping probability (P_D): the ratio of the number of the dropped handoff-call requests to the number of total handoff-call requests in the system.

The new-call-blocking probability and the handoff-call-dropping probability of the cell C_i can be calculated by the following equations:

$$P_i^B = \lim_{J \to \infty} \frac{\sum_{j=1}^{J} \lambda_i^n(j\Delta t) f_i^n(j\Delta t)}{\bar{\lambda}_i^n J \Delta t}$$

and

$$P_i^D = \lim_{J \to \infty} \frac{\sum_{j=1}^{J} \lambda_i^h(j\Delta t) f_i^h(j\Delta t)}{\bar{\lambda}_i^h J \Delta t},$$

where

$$\sum_{i=1}^{N} \lambda_i^n(j\Delta t) = 1$$

or

$$\sum_{i=1}^{N} \lambda_i^h(j\Delta t) = 1,$$

and $\bar{\lambda}_i^n$ ($\bar{\lambda}_i^h$) is the average new-call (handoff-call) arrival rate. It is generally assumed that each cell has the same average new-call or handoff-call arrival rate.

The total blocking probability (P_B) and handoff-call-dropping probability (P_D) for a cell-reuse group can be calculated by following equations:

$$P_B = \lim_{J\to\infty} \frac{\sum_{i=1}^{N}\sum_{j=1}^{J} \lambda_i^n(j\Delta t) f_i^n(j\Delta t)}{\sum_{i=1}^{N} \bar{\lambda}_i^n J\Delta t}$$

$$= \lim_{J\to\infty} \frac{\sum_{j=1}^{J}\sum_{i=1}^{N} \lambda_i^n(j\Delta t) f_i^n(j\Delta t)}{\sum_{i=1}^{N} \bar{\lambda}_i^n J\Delta t},$$

$$P_D = \lim_{J\to\infty} \frac{\sum_{i=1}^{N}\sum_{j=1}^{J} \lambda_i^h(j\Delta t) f_i^h(j\Delta t)}{\sum_{i=1}^{N} \bar{\lambda}_i^h J\Delta t}$$

$$= \lim_{J\to\infty} \frac{\sum_{j=1}^{J}\sum_{i=1}^{N} \lambda_i^h(j\Delta t) f_i^h(j\Delta t)}{\sum_{i=1}^{N} \bar{\lambda}_i^h J\Delta t}.$$

We define the new-call (handoff-call) arrival state vector, $\bar{\lambda}^n(j\Delta t) = \left[\lambda_1^n(j\Delta t) \ldots \lambda_N^n(j\Delta t)\right]$ ($\bar{\lambda}^h(j\Delta t) = \left[\lambda_1^h(j\Delta t) \ldots \lambda_N^h(j\Delta t)\right]$) and the cell-state vector for new calls (handoff calls) $\bar{f}^n(j\Delta t) = \left[f_1^n(j\Delta t) \ldots f_N^n(j\Delta t)\right]$ $\bar{f}^h(j\Delta t) = \left[f_1^h(j\Delta t) \ldots f_N^h(j\Delta t)\right]$). Blocking (dropping) happens when $\bar{\lambda}^n(j\Delta t) \bullet \bar{f}^n(j\Delta t) = 1$ ($\bar{\lambda}^h(j\Delta t) \bullet \bar{f}^h(j\Delta t) = 1$). To reduce the new-call-blocking probability (handoff-call-blocking probability), radio resource-management schemes try to orthogonalize the call-arrival vector $\bar{\lambda}^n(j\Delta t)$ ($\bar{\lambda}^h(j\Delta t)$) and the cell-state vector $\bar{f}^n(j\Delta t)$ ($\bar{f}^h(j\Delta t)$) at each time $j\Delta t$. The orthogonalization equations are given as follows: $\bar{\lambda}^n(j\Delta t) \bullet \bar{f}^n(j\Delta t) = 0$ and $\bar{\lambda}^h(j\Delta t) \bullet \bar{f}^h(j\Delta t) = 0$.

In the following section, we provide an explanation of orthogonalization and how it relates to the radio resource-management schemes, such as direct retry [12], queuing, channel borrowing [10], load balancing [14], and cooperative directional handoff [16]:

- Direct retry: When a user in the overlap area tries to access an overloaded cell C_{i0} ($f_{i0}^n(j_0\Delta t) = 1$) at time $j_0\Delta t$, he will try to access another candidate under-loaded cell, C_{i1} ($f_{i1}^n(j_0\Delta t) = 0$). In this way, $\bar{\lambda}^n(j_0\Delta t) \bullet \bar{f}^n(j_0\Delta t) = 0$.

- Queuing: When a user tries to hand off from a cell C_{i1} to an overloaded cell C_{i0} ($f_{i0}^h(j\Delta t) = 1$) at time $j_0\Delta t$ the handoff call request will be queued until a user in the cell C_{i0} leaves the cell at time $j_1\Delta t$. In this way, $\bar{\lambda}^n(j_0\Delta t) \bullet \bar{f}^n(j_0\Delta t) = 0$ and $\bar{\lambda}^n(j_1\Delta t) \bullet \bar{f}^n(j_1\Delta t) = 0$ The handoff-dropping probability is related to the maximum queuing time, which is restricted by the distance between the handoff-initiating boundary and the cell boundary, and the platform's speed. The bigger the maximum queuing time, the more probably one user will leave the cell, and the smaller the handoff-dropping probability that can be achieved.

- Cooperative directional handoff: When a user tries to handoff from a cell C_{i1} to an overloaded cell C_{i0} ($f_{i0}^h(j_0\Delta t) = 1$) at time $j_0\Delta t$, another user, who resides in C_{i0} and is in the overlap area of cell C_{i0} and an under-loaded cell C_{i2}, will try to hand off to cell C_{i2} to free up a channel for the handoff call that is supposed to be dropped. In this way, $f_{i0}^h(j_0\Delta t) = 0$, $f_{i2}^h(j_0\Delta t) = 0$ and accordingly $\bar{\lambda}^n(j_0\Delta t) \bullet \bar{f}^n(j_0\Delta t) = 0$. In this case, the handoff-dropping probability is related to the maximum overlap distance. The bigger the maximum overlap distance, the more probably another user can be found, and the smaller the handoff-dropping probability that can be achieved.

- Load balancing: This scheme tries to reduce the probability that a cell falls into the blocking state, $P\left[f_i^n(j\Delta t) = 1\right]$ ($P\left[f_i^h(j\Delta t) = 1\right]$). Accordingly, this increases the orthogonalization probability $P\left[\bar{\lambda}^n(j_0\Delta t) \bullet \bar{f}^n(j_0\Delta t) = 0\right]$ ($P\left[\bar{\lambda}^h(j_0\Delta t) \bullet \bar{f}^h(j_0\Delta t) = 0\right]$). If each cell has equal channels, the cell state can be redefined as follows:

$$f_i^n(j\Delta t) = f_i^h(j\Delta t) = \begin{cases} 1, C - L_i(j\Delta t) = 0 \\ 0, C - L_i(j\Delta t) > 0 \end{cases}$$

To minimize $P\left[f_i^n(j\Delta t) = 1\right]$, we should maximize $C - L_i(j\Delta t)$ and minimize $L_i(j\Delta t)$.

The directional traffic-aware intra-HAP handoff scheme proposed in the next section extends the cooperative directional handoff scheme by forcing the users in the overlap area to hand off earlier than their optimal handoff boundaries, in order to balance the traffic. The new scheme is also a partial load-balancing scheme, which means that only overloaded cells execute load-balancing actions. Simulation results will show that the new scheme performs better than the other two schemes for some situations.

3. Directional Traffic-Aware Intra-HAP Handoff Scheme

All the users in the HAP communications system have the same direction of movement if they are assumed to be located at fixed positions on the ground, and the platform moves with a specific velocity. This characteristic has already been mentioned and been utilized in [16]. It is

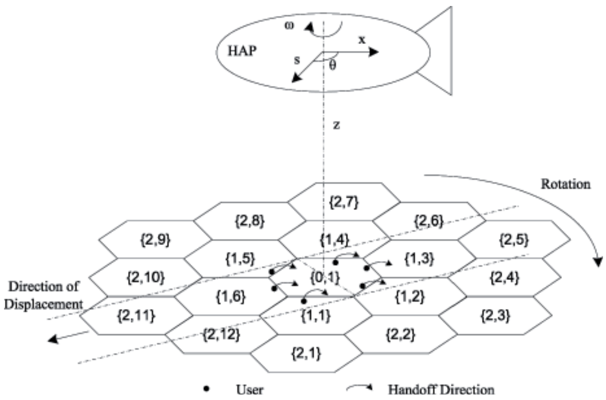

Figure 1. A directional-handoff scenario in HAP communications systems [16].

assumed that the trajectory of the platform can be well traced, the acceleration rate of the platform is small, the velocity of the platform remains fixed in a time Δt, and the horizontal movement can be broken down into the displacement (with velocity (s,θ)) and the rotation (with rotation speed ω) with respect to the z axis (Figure 1). Users generally hand off from the cell in the handoff source cell group ($\{1,5\},\{1,6\},\{1,1\}$) to the observing cell ($\{0,1\}$) and from the observing cell to the cell in the handoff destination cell group ($\{1,2\},\{1,3\},\{1,4\}$).

To simplify the analytical process, a one-dimensional cellular model is adopted (as illustrated in Figures 2 and 3) [16]. In the model, the cells are linearly aligned. It is assumed that the distance between the centers of two adjacent cells is D, and that the overlap distance (determined by the minimum received signal strength (RSS_{min})) is Δx. Considering the direction of movement in the current time Δt, each cell can be divided into three service areas: the overlap service area in the direction of movement (OSA-DM), which is the overlap area between the observing cell and the cell in the direction of movement; the overlap service area opposite to the direction of movement (OSA-ODM), which is the overlap area between the observing cell and the cell opposite to the direction of movement; and the non-overlap service area (NOSA). The optimal handoff boundary in the overlap service area opposite to the direction of movement determines when to start handoff for each ongoing call. In this paper, the optimal handoff boundary resides in the middle of the overlap area, and has the same distances to the centers of two adjacent cells. The fixed channel assignment (FCA) is adopted. Each cell has C channels. All the users are fixed to the ground, and uniformly distributed over the service area. The new-call-arrival process in each cell follows a Poisson process, with an average new-call-arrival rate of λ_n. The call-holding time follows the exponential distribution with an average value of $1/\mu$. The current traffic for the cell n is $L_n(t)$. In a time Δt, users usually hand off from one cell to the neighboring cell opposite to the direction of movement. In the following section, we describe the load-balancing handoff scheme, and the new directional traffic-aware intra-HAP handoff scheme.

3.1 Scheme 1: Load-Balancing Handoff Scheme (LBHS)

A load-balancing algorithm is adopted in IEEE 802.11 networks to minimize the differences in the traffic loads of different access points [14]. In this paper, the load-balancing handoff process is executed according to the criteria that tend to minimize the maximum traffic of the adjacent cells. As illustrated in Figure 2, each cell has eight channels. At time t, Cell$\#n-1$, Cell$\#n$, and Cell$\#n+1$ have 4, 6, and 2 ongoing calls, respectively. According to the criteria for load balancing, two load-balancing operations will be executed. The ongoing call, U_1, in the overlap area between Cell$\#n$ and Cell$\#n-1$, residing in Cell$\#n$, will try to hand off earlier than the optimal handoff boundary to Cell$\#n-1$ (Case I). In the meantime, the ongoing call, U_2, in the overlap area between Cell$\#n+1$ and Cell$\#n$, residing in Cell$\#n+1$, will try to hand off later

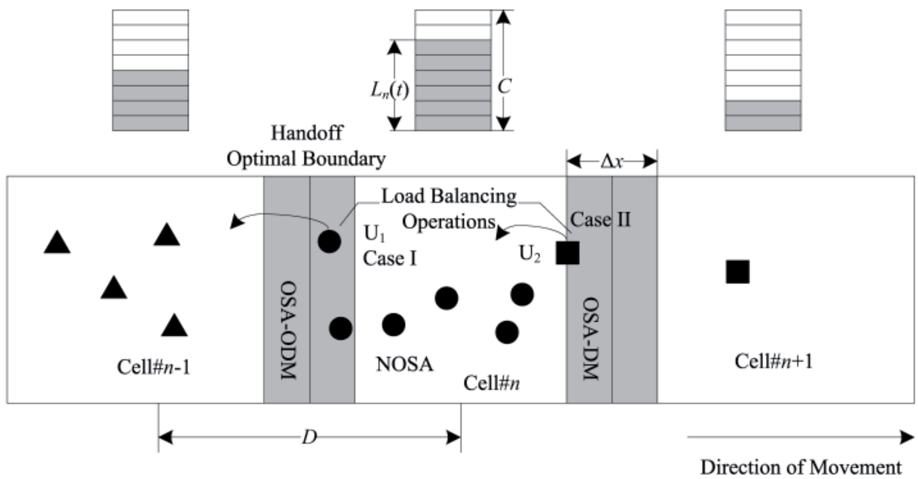

Figure 2. A load-balancing handoff scenario.

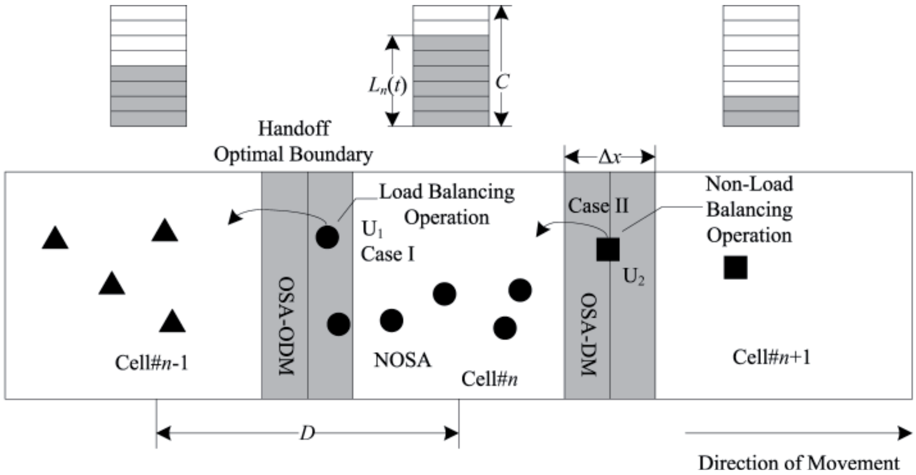

Figure 3. A directional traffic-aware intra-HAP handoff scenario.

than the optimal handoff boundary to Cell$\#n$ (Case II). In this way, the carried traffic of the adjacent cell tends to become balanced. The load-balancing actions are cyclically executed every load-balancing cycle (LBC), as follows:

- The cycle always starts by calculating the carried-traffic (the number of occupied channels) difference between the cell and the cell in the opposite direction of the platform's movement.

- If the carried-traffic difference is less than two or bigger than -2, users in the overlap area start to hand off at the optimal handoff boundaries.

- If the difference is bigger than one, the user that is nearest to the cell boundary in the overlap area will try to hand off earlier than the optimal handoff boundary, to reduce the traffic difference.

- If the difference is less than -1, the user in the overlap area will try to stay in the cell and delay the handoff until that user is going to move out of the cell or the traffic conditions change.

- The cooperative directional intra-HAP handoff scheme process [16] is executed if a handoff is required, and all the channels in the target cell are occupied.

3.2 Scheme II: Directional Traffic-Aware Intra-HAP Handoff Scheme (DTAHS)

The load-balancing handoff scheme can improve the new-call-blocking and handoff-call-dropping performance. However, the improvement of the handoff-call-dropping performance is limited by more ongoing calls introduced to the system. Furthermore, the maximum handoff-queuing time is reduced for most users, which may increase the handoff-call-dropping probability. In the new handoff scheme, only one load-balancing operation is executed to restrict the load-balancing effects and to leave some traffic fluctuation to be exploited by some handoff calls. Concretely, the ongoing call (U_1) in the overlap area will still try to hand off earlier than the optimal handoff boundary to reduce the traffic load difference (Case I). However, the user (U_2) in the overlap area will start to hand off at the optimal handoff boundary according to the maximum SSR criteria if the traffic difference is less than -1 (as illustrated in Figure 3). In this way, we partially balance the carried traffic of adjacent cells, keep the maximum handoff-queuing time, and achieve a tradeoff between the handoff-call-dropping performance and the new-call-blocking performance.

The directional traffic-aware intra-HAP handoff scheme works as follows:

- Similar to the load-balancing handoff scheme, the directional traffic-aware intra-HAP handoff scheme actions are also cyclically executed. The cycle always starts by calculating the carried-traffic difference between the cell and the cell in the opposite direction of the platform's movement.

- If the traffic difference is less than two, users in the overlap area start to hand off at the optimal handoff boundaries.

- If the difference is bigger than one, the user that is nearest to the cell boundary in the overlap area will try to hand off earlier than optimal handoff boundary to reduce the traffic difference.

- The cooperative directional intra-HAP handoff scheme process [8] is executed if a handoff is required and all the channels in the target cell are occupied.

In these handoff schemes, it is assumed that the central resource-management module can trace the velocity

Parameter	Value
Platform mobility model	*Constant linear velocity*
User mobility model	*Fixed to the ground*
Cell structure	*5 cells linearly aligned (Figures 2,3)*
Cell centre distance (D)	*5 km*
Overlap distance (Δx)	*1.0 km*
Call arrival rate per cell (λ_n)	*0.0024 - 0.08 calls/s*
Speed of the platform	*200 km/h, 50 km/h*
Channels per cell	*10*
Average call holding time ($1/\mu$)	*100 s*

Table 1. The simulation parameters.

of the platform and the channel state of the neighboring cells in real time. The decision will be made based on this information. It is assumed that the cell with the maximum SSR is selected as the accessing cell for the new call.

4. Performance Analysis

In the simulation, a five-cell one-dimensional cellular structure was adopted (Figures 2 and 3). The call-arrival and departure processes of different cells in the multi-cell communications system generally had the same statistical properties. The platform moved to the right with a constant speed. The first cell (Cell#1) and the last cell (Cell#5) in the one-dimensional cellular structure were adjacent cells. The new calls were accepted according to the maximum-SSR criteria, and the handoff-call processes were executed according to the load-balancing handoff scheme, the directional traffic-aware intra-HAP handoff scheme, and the cooperative directional intra-HAP handoff scheme, respectively. The handoff queue length was 10. The handoff call requests in the queue were served based on a first-come first-served (FCFS) method. The simulation parameters in Table 1 were adopted.

In this paper, the new-call-blocking probability (P_B) and the handoff-call-dropping probability (P_D) were linearly combined into a new performance metric, named the unified system performance (*P*). This helped us to compare different radio resource-management schemes, considering both new-call and handoff-call performance. This can be represented by the following equation:

$$P = \alpha \frac{P_B}{P_B^{max}} + \left(1-\alpha\right) \frac{P_D}{P_D^{max}} ,$$

where α is the factor associated with new-call blocking, and represents the relative importance of the new-call blocking in the evaluation of the quality of service; P_B^{max} is the maximum-acceptable new-call-blocking probability; and P_D^{max} is the maximum-acceptable handoff-call-dropping probability.

A system-performance comparison of different radio resource-management schemes is illustrated in Figure 4. It is obvious that the load-balancing handoff scheme had a better new-call-blocking probability than the directional traffic-aware intra-HAP handoff scheme, and that the directional traffic-aware intra-HAP handoff scheme had a better new-call-blocking probability than the cooperative directional intra-HAP handoff scheme (Figure 4a). At the same time, the three schemes had a reverse performance order for the handoff-call probability (Figure 4b). It could also be found that the variation of the new-call-blocking probability was lower than that of the handoff-call-dropping probability for different *overlap intervals*, which are equal to the overlap distance divided by the platform's speed. We defined the *key performance metric* as the performance

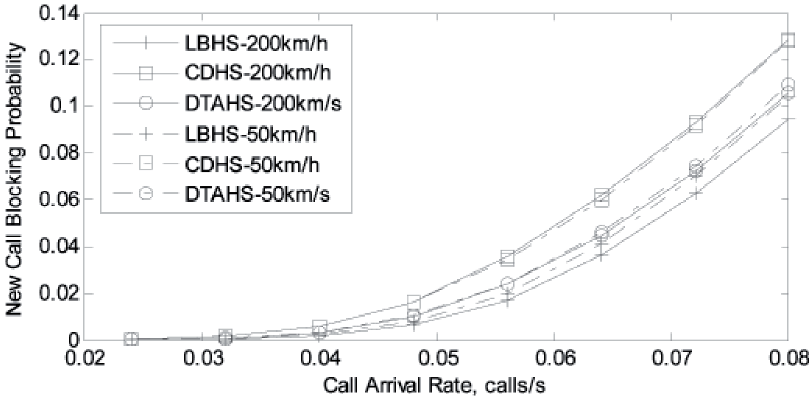

Figure 4a. The system performance of different schemes: The new-call-blocking probability.

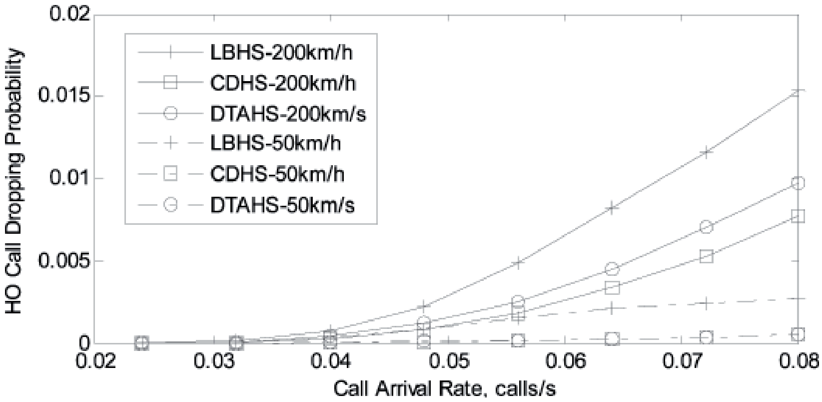

Figure 4b. The system performance of different schemes: The handoff-call-dropping probability.

metric that reached the maximum-acceptable value first as the call-arrival rate increased. When the overlap interval was short (corresponding to a 200 km/h platform speed and a 1.0 km overlap distance), $P_B^{max} = 0.05$, and $P_D^{max} = 0.005$, the new-call-blocking probability was the key performance metric for the cooperative directional intra-HAP handoff scheme, the handoff-call-dropping probability was the key performance metric for the load-balancing handoff scheme, and the call-blocking probability and handoff-call-dropping probabilities reached the maximum acceptable values almost at the same call-arrival rate for the directional traffic-aware intra-HAP handoff scheme. It thus is better to adopt a scheme that sacrifices part of the new-call-blocking performance for the handoff-call-dropping performance. However, when the overlap interval is long (corresponding to a 50 km/h platform speed and a 1.0 km overlap distance), or even when the platform remains stationary, the new-call-blocking probability was the key performance metric for all the three handoff schemes; the handoff-call-dropping performance was good enough for the load-balancing handoff scheme. There was no need to achieve a better handoff-call-dropping performance with a reduction in the new-call-blocking performance. The load-balancing handoff scheme became the best scheme. Hence, the load-balancing handoff scheme and the directional traffic-aware intra-HAP handoff scheme are suitable for long and short overlap intervals, respectively.

The unified system-performance comparison of different schemes for a short overlap interval (corresponding to a 200 km/h platform speed and a 1.0 km overlap distance) is illustrated in Figure 5. It was obvious that the unified system-performance order changed for different factor values associated with new-call blocking. The performance order for the different schemes is illustrated in Table 2. The research results showed that the directional traffic-aware intra-HAP handoff scheme was the best scheme among the three schemes when $0.4 < \alpha < 0.8$, and provided a good compromise between the new-call and handoff-call performance.

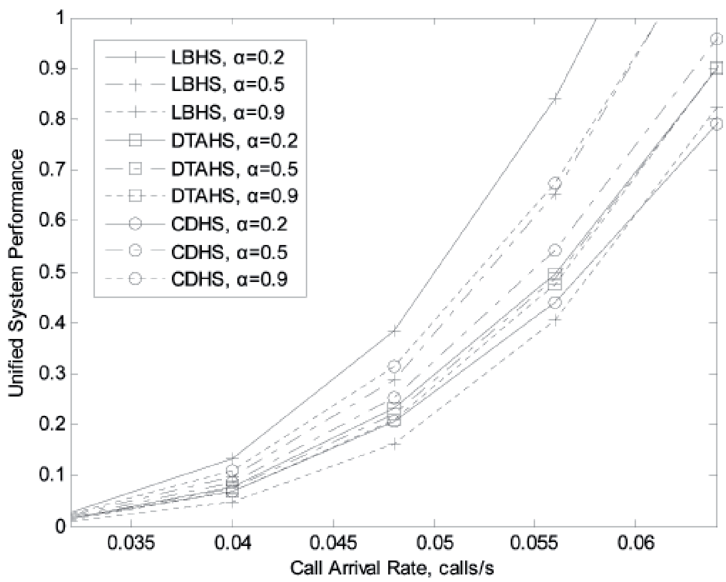

Figure 5. The unified system performance of different schemes.

α	Excellent	Good	Poor
0.2	*CDHS*	*DTAHS*	*LBHS*
0.5	*DTAHS*	*CDHS*	*LBHS*
0.9	*LBHS*	*DTAHS*	*CDHS*

Table 2. The order of the unified system performance for different schemes.

5. Conclusions

This paper has presented a novel directional traffic-aware intra-HAP handoff scheme that partially exploits the traffic fluctuation, and considers the co-located cellular structure and the directional-handoff characteristics of HAP communications systems. Simulation results showed that it is worth it for the new scheme to sacrifice part of the new-call-blocking performance in order to improve the handoff-call-dropping performance when the overlap interval is relatively short. The new scheme outperformed both the load-balancing handoff scheme (LBHS) and the cooperative directional intra-HAP handoff scheme (CDHS) when the factor value associated with call blocking in the equation of unified system performance was smaller than 0.8 and bigger than 0.4 for a relatively short overlap interval. Meanwhile, the variation of new-call-blocking probability for different overlap intervals was lower than that of the handoff-call-dropping probability. The load-balancing handoff scheme is suitable for situations with low platform speed (or even for stationary platforms) and long overlap intervals. The directional traffic-aware intra-HAP handoff scheme performs better for situations with high platform speed and a short overlap interval.

6. Acknowledgments

This work was carried out in the Communications Research Group, Department of Electronics, University of York, supported by China Scholarship Council (2008611011).

7. References

1. B. el-Jabu and R. Steele, "Aerial Platforms: A Promising Means of 3G Communications," IEEE Vehicular Technology Conference, Houston, TX, USA, July 1999, pp. 2104-2108.

2. G. Wu, R. Miura, and Y. Hase, "A Broadband Wireless Access System Using Stratospheric Platforms," IEEE GLOBECOM, San Francisco, CA, USA, November 2000, pp. 225-230.

3. S. Karapantazis and F. Pavlidou, "Broadband Communications via High-Altitude Platforms – A Survey," *IEEE Communications Surveys & Tutorials*, **7**, 1, 2005, pp. 2-31.

4. D. I. Axiotis, M. E. Theologou, and E. D. Sykas, "The Effect of Platform Instability on the System Level Performance on HAPS UMTS," *IEEE Communications Letters*, **8**, 2, February 2004, pp. 111-113.

5. J.-J. Huang, W.-T. Wang, S.-C. Chang, H.-W. Ferng, and D. Shiung, "The Impact of Using Multiple HAPSs to Combat Platform Instability on Uplink CDMA Capacity," IEEE Vehicular Technology Conference, Dublin, Ireland, April 2007, pp. 1365-1369.

6. J. Thornton and D. Grace, "Effect of Lateral Displacement of a High-Altitude Platform on Cellular Interference and Handover," *IEEE Transactions on Wireless Communications*, **4**, 4, July 2005, pp. 1483-1490.

7. K. Katzis, D. A. J. Pearce, and D. Grace, "Impact of High Altitude Platform Movements on Cellular Handover," International Workshop on High Altitude Platform Systems, Athens, Greece, September 2005.

8. S. Liu, Z. Niu, and Y. Wu, "Impact of Platform Motion on Soft Handover in High Altitude Platform IMT-2000 System," IEEE Vehicular Technology Conference, April 2003, pp. 1964-1968.

9. K. Katzis and D. Grace, "Inter-High Altitude Platform Handoff for Communications Systems with Directional Antennas," *URSI Radio Science Bulletin*, 332, March 2010, pp. 29-38.

10. H. Jing and S. Rappaport, "CBWL: A New Channel Assignment and Sharing Method for Cellular Communication Systems," *IEEE Transactions on Vehicular Technology*, **43**, 2, May 1994, pp. 313-322.

11. O. T. W. Yu, and V. C. M. Leung, "Self-tuning Prioritized Call Handling Mechanism with Dynamic Guard Channels for Mobile Cellular Systems," IEEE Vehicular Technology Conference, Atlanta, GA, USA, Aug 1996, pp. 1520-1524.

12. B. Eklundh, "Channel Utilization and Blocking Probability in a Cellular Mobile Telephone System with Directed Retry," *IEEE Transactions on Communications*, **34**, 4, April 1986, pp. 329-337.

13. E. Del Re, R. Fantacci, and G. Giambene, "Handover Queuing Strategies with Dynamic and Fixed Channel Allocation Techniques in Low Earth Orbit Mobile Satellite Systems," *IEEE Transactions on Communications*, **47**, 1, January 1999, pp. 89-102.

14. H. Velayos, V. Aleo, and G. Karlsson, "Load Balancing in Overlapping Wireless LAN Cells," IEEE ICC, June 2004, pp. 3833-3836.

15. O. K. Tonguz and E. Yanmaz, "The Mathematical Theory of Dynamic Load Balancing in Cellular Networks," *IEEE Transactions on Mobile Computing*, **7**, 12, December 2008, pp. 1504-1518.

16. S. Li, D. Grace, J. Wei, and D. Ma, "Cooperative Directional Inter-cell Handoff Scheme in HAP Communications Systems," *IET Communications*, Submitted February 2010 (COM-2010-0110).

On Security Advantages of HAPs Over Satellites

Miroslav Popovic
Ilija Basicevic

Abstract

A significant effort has been put forth by both industry and academia into the research and development of High-Altitude Platforms (HAPs), e.g., in the EU COST action 297. Since a HAP is a mission-critical infrastructure, more research activities are still needed, especially with respect to HAP security. This paper analyzes and compares the security features of network architectures based on HAPs and satellites. The concrete contributions of this paper are twofold. First, this paper proposes a security comparison method of network architectures that are based on airborne infrastructure, e.g., HAPs and satellites. Second, the paper presents the results of the comparison. These showed that network architectures based on HAPs outperform network architectures based on satellites with respect to most of the analyzed security features.

1. Introduction

High-Altitude Platforms (HAPs) [1] are still a very active playground for many researchers, typically organized around scientific projects, one of them being EU COST action 297 (HAPCOS). Many important aspects were successfully analyzed in the last five years or so. However, some aspects remain almost unattached, e.g., security. Of course, since HAPs are mission-critical infrastructure, their security considerations are of the utmost importance. Therefore, this paper tries to make contributions in that area.

The goal of this paper is to analyze and compare security features of network architectures based on HAPs and satellites (see Figures 1 and 2). The concrete contributions of this paper are twofold. First, this paper proposes a security comparison method for network architectures based on airborne infrastructure, e.g., HAPs and satellites. Second, the paper presents the results of the comparison. These showed that network architectures based on HAPs outperform network architectures based on satellites with respect to most of the analyzed security features.

The text of the paper is organized as follows. Section 2 gives the fundamental background for the security analysis conducted in the paper. Section 3 presents a hierarchy of security tactics used to establish the relationship between a given network architecture and its security. Section 4 outlines the applied method. Section 5 presents the results of the applied method. Section 6 contains final remarks and conclusions.

2. Background

This section presents a brief overview of the physical and mathematical background. The *transmission power* of a base station onboard a HAP/satellite that is needed to successfully receive the signal by the receiver (inside the terminal) with a given *receiver sensitivity* and at a given distance is given as

$$P_{TX} = \frac{P_{RX} d^2}{G_{TX} G_{Ref}}, \quad (1)$$

where P_{TX} is the transmission power of a base station onboard the HAP/satellite, P_{RX} is the user-terminal receiver sensitivity, d is the distance between the base station and the terminal, G_{TX} is the base-station antenna's gain, and G_{Ref} is the reference gain. The reference gain is calculated as

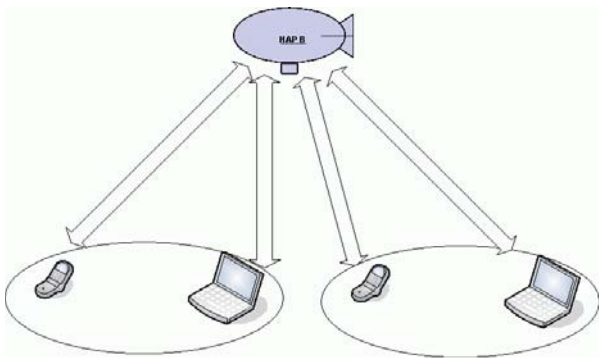

Figure 1. A multi-cell HAP network.

Miroslav Popovic and Ilija Basicevic are with the University of Novi Sad, Faculty of Technical Sciences, Trg Dositeja Obradovica 6, 21000 Novi Sad, Serbia; e-mail: miroslav.popovic@rt-rk.com, ilibas@uns.ac.rs.

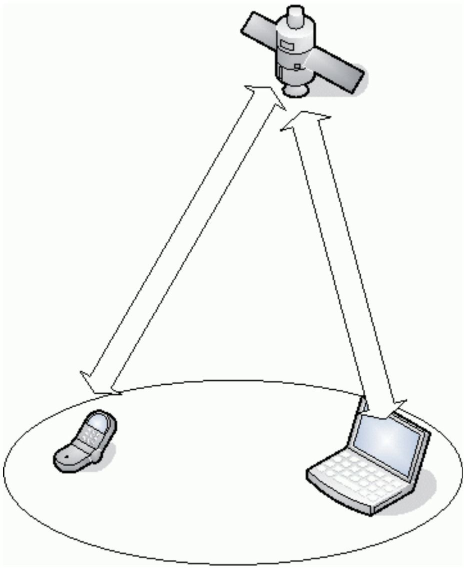

Figure 2. A satellite network.

$$G_{Ref} = \frac{G_{RX}}{(4\pi/\lambda)^2}, \quad (2)$$

where G_{RX} is the terminal's antenna gain, and λ is the electromagnetic wavelength.

The *propagation delay*, τ_p, is defined as the time required for the first bit of information to travel from its source to its destination:

$$\tau_p = t_d - t_s, \quad (3)$$

where t_d is the point in time at which the signal arrives at its destination, and t_s is the point in time at which the signal starts from its source. Obviously, τ_p is directly proportional to the distance between the HAP/satellite and the terminal. The longer the distance *d*, the bigger the propagation delay, τ_p.

The *latency*, τ_l, is given as

$$\tau_l = \tau_p + \frac{D_u}{B}, \quad (4)$$

where D_u is the size of the transmitted *data unit* in bits, and *B* is the *bandwidth* (the number of bits transferred per second). Therefore, besides the propagation delay, τ_p, the bandwidth, *B*, affects the performance of a transmission system, as well. However, for smaller data units or longer distances (which is certainly the case for satellites), the propagation delay, τ_p, represents the major part of the latency, τ_l [2].

Transmission systems use encryption to provide secure communication. The set of characters, *V*, used to used to formulate a plain text is called the plain-text vocabulary. The set of characters, *W*, used to formulate the cipher text, or code text, is called the crypto-text vocabulary. The plain text words, V^*, and the crypto-text words, W^*, are the set of words constructed from *V* and *W*, respectively. ε indicates the empty word. Z^n, a subset of Z^*, is the set of all words of length *n*. V^* is called the plain-text space, and W^* is the crypto-text space. $Z^{(n)}$ denotes a set of all the words the length of which is less than or equal to *n*.

An encryption is defined as a relation $\mathbf{X}: V^* \rightarrow W^*$ The converse relation, $\mathbf{X}^{-1}: V^* \leftarrow W^*$, defined by $\mathrm{x} \leftarrow \mathrm{y}$ if and only if $\mathrm{x} \rightarrow \mathrm{y}$, is called a decryption.

Since the intended recipient of an encrypted message should be able to reconstruct the original message, as a rule, an encryption is injective, and therefore unambiguous from right to left (*left-univalent*):

$$\text{if } (\mathrm{x} \rightarrow \mathrm{z}) \text{ and } (\mathrm{y} \rightarrow \mathrm{z}) \text{ then } (\mathrm{x} = \mathrm{y}). \quad (5)$$

The *encryption system* $M = M\left(V, W, \mathbf{X}^{\sim}\right)$ is the nonempty and as a rule finite set $\mathbf{X}^{\sim}$ of injective relations $x_i: V^{(ni)} \rightarrow W^{(mi)}$. Each x_i is called an encryption step.

A plain-text stream is an infinite sequence of blocks $(t_1, t_2, t_3, ...)$, where t_j is an element of V^n. Similarly, a crypto-text stream is an infinite sequence of blocks $(c_1, c_2, c_3, ...)$, where c_j is an element of W^m. A stream encryption is a block encryption of segments of plain text to segments of crypto text.

Let k_j be the *j*th key used in the sequence. k_j is an element of the key vocabulary, *K*. K^* is referred to as a key space. The following cryptographic equation [3] defines c_j as a function of t_j and k_j:

$$c_j = \mathbf{X}\left(t_j, k_j\right), \quad (6)$$

where $\mathbf{X}$ is a finitely generated block cipher, $\mathbf{X} = [x_1, x_2, x_3 ...]$, $x_j: t_j \rightarrow c_j$; t_j is an element of the plain-text sequence; c_j is an element of the crypto-text sequence; and k_j is an element of the key-text sequence.

Typically, the longer is the key (in bits), the better the security. Therefore, the architectures that support longer keys prove to be more secure than those that support shorter keys. For example, the quality of the encryption system may be characterized by the entropy of the crypto-text sequence. The entropy, *H*, of a discrete random variable *A* with *s* possible different values $\{a_1, a_2, ..., a_s\}$ is

$$H(A) = E\left[I(A)\right], \quad (7)$$

where $E[\ ]$ is an expected-value function, and $I(A)$ is a random variable that represents the information content (self-information) of A. Let p be the probability mass function of A. Entropy can then be calculated in bits as

$$H(A) = \sum_{j=1\ldots s} p(a_j) I(a_j) \quad (8)$$

$$= -\sum_{j=1\ldots s} p(a_j) \log_2 \left[p(a_j) \right] \text{ [bits].}$$

Entropy is a very useful metric. Besides encryption systems, it finds application in detecting network attacks [4]. Essentially, both probability mass functions and entropy (uncertainty) as functions time of monitored network parameters – such as source IP address, destination IP address, destination port address, and flow size – change when a network is attacked. In practice, when these changes are significant, it is assumed that a network attack is taking place. Therefore, network architectures in which probability mass functions and/or entropy of monitored parameters have more significant changes during attacks could be better secured (with respect to anomaly intrusion detection based on entropy) than those for which that is not the case.

3. Security Tactics

A general issue in security is how to assess the security of a given arbitrary architecture, e.g., a network architecture. This problem is hard, because architectural styles address multiple design goals with security goals being just one of the goals, and because architectures are normally customized to solve particular problems. A solution to this problem is to use a hierarchy of *architectural tactics* [5], which establishes a relationship between a recurring architectural structure and its security features.

For the purpose of this paper, we use a rather coarsely grained hierarchy of architectural tactics, shown in Figure 3. Additionally, to enable the comparison, we use this same hierarchy as the first approximation for both networks based on HAPs and on satellites. Our aim in this paper is to show that most of the security tactics in Figure 3 are better accomplished in network architectures based on HAPs than in network architectures based on satellites.

The security tactics in Figure 3 are roughly divided into three groups, each covering a specific aspect of dealing with computer attacks. The first group deals with resistance to attacks. Security techniques that limit the system exposure to attacks are listed. Today's telecommunication networks serve a large number of users in complex scenarios of communication. In such systems, authentication and authorization are of utmost importance. The second group deals with detection of attacks. Support for intrusion-detection techniques is an important aspect of system security. Intrusion detection has been an area of ongoing research for almost three decades. This has resulted in the development of an array of techniques, usually classified into host-based and network-based intrusion detection. The last group deals with recovery from attacks. The importance of audit trails as a basis for forensic activities is underlined.

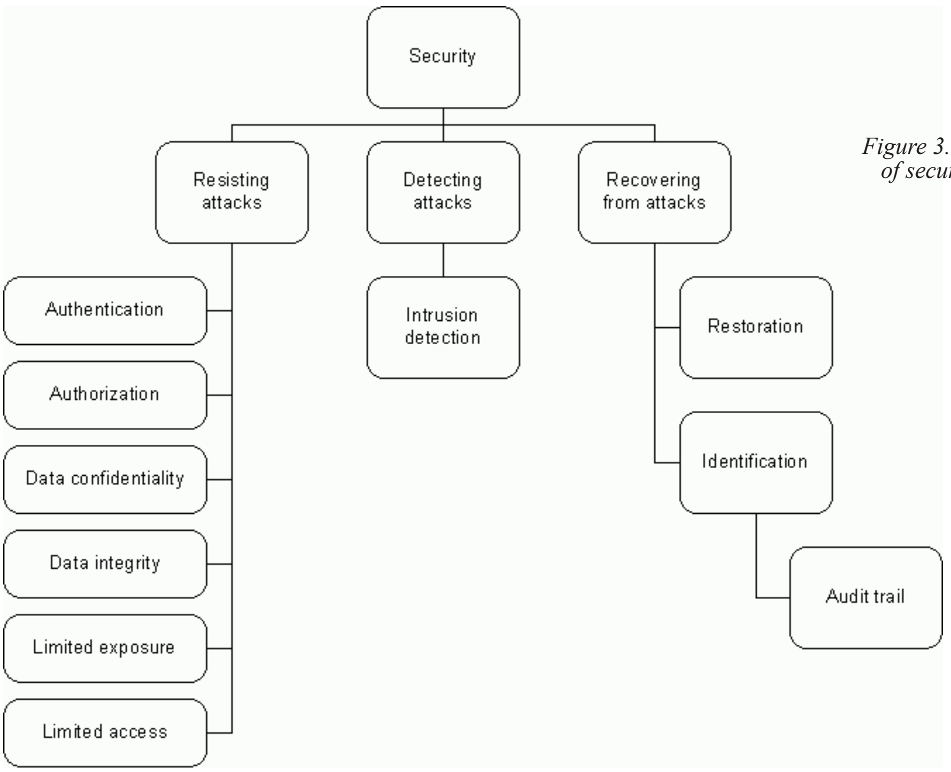

Figure 3. A hierarchy of security tactics.

4. Applied Method of Comparative Analysis

The method of comparative analysis applied is based on the hierarchy of security tactics shown in Figure 3 and on fundamentals outlined in Section 2. The method comprises the following four steps:

- Step 1: Identify security tactics (already done: the result is shown in Figure 3).
- Step 2: Identify features of security tactics that are suitable to assessing and comparing the effectiveness and efficiency of security-tactic implementations in networks based on HAPs and satellites.
- Step 3: Use fundamental knowledge (Section 2) and common sense to evaluate the comparison results for each security feature.
- Step 4: Evaluate the final comparison result (note: this method does not favor any security feature above another).

The results of the comparative analysis are given in the next section.

5. Comparative Analysis of Security of Networks Based on HAPs and Satellites

As already mentioned, the result of Step 1 is shown in Figure 3. The result of Step 2 is a list of security features used to assess and compare security tactics, as summarized in Table 1. The results of Step 3 are summarized in Table 2 and discussed in the text below.

It should be noted that for reasons of clarity, Table 2 contains only the security features for which one of the compared network architectures (based on HAPs or satellites) has an advantage over the other. Other features, for which this is not the case, were omitted from Table 2. For example, both HAPs and satellites enable quantum key distribution (QKD) [11]. Technically, the implementation of quantum key distribution on a HAP is much easier, because if the system fails, the HAP can be brought down and repaired. However, from the application point of view, the footprint is much larger from a satellite. The number of customers one can reach from a satellite is much larger (some thousands) compared to the number from a HAP platform (some hundreds). Therefore, satellites offer higher commercial potential than HAPs. With respect to atmospheric effects resulting in lower bit rates and higher quantum bit-error rates, we don't expect significantly different behavior between the two cases. The most-important atmospheric effects are absorption, multi-scattering with aerosols, and turbulence. Absorption is caused by gases such as CO_2. Turbulence strength depends on air temperature, air pressure, relative humidity, and wind speed. The main atmospheric effects are below the typical altitude of HAPs. However, on the uplink in the case of satellites, the wavefront distortions have more effect, because of the distance. However, with respect to security, both HAPs and satellites provide quantum-key-distribution capability, so neither of them has an advantage over the other. Quantum key distribution thus has not been added to Table 2.

The following is the list of security features for which network architectur Table 2. The order of the unified system performance for different schemes. es based on HAPs have an advantage over the network architectures based on satellites:

1. Better authentication schemes: HAPs cruise at much lower altitudes than satellites. They therefore may exploit much faster and richer connections (as can be seen from Equations (1) and (2)), enabling, among other features, better authentication schemes, because K_j in Equation (6) can be longer.
2. Faster authentication: The time interval needed to conduct authentication and authorization is proportional to the round-trip delay. This time interval is shorter in the case of HAPs, because of a shorter latency (see Equation (4)).

No.	**Security Tactics**	**Feature**	**Attribute in Favor**
1	*Authentication*	*Authentication speed*	*Faster*
		Authentication scheme	*Better*
2	*Data confidentiality*	*Encryption scheme*	*Better*
3	*Data integrity*		
4	*Limited exposure*	*Protection from being physically destroyed*	*Better*
5	*Intrusion detection*	*Security monitoring and reactions*	*Faster*
			Comprehensive
			Distributed attack detection
			Worm detection
6	*Restoration*	*Security disaster recovery*	*Better*
		Security capability over the whole calendar year	*Better*

Table 1. A cross reference of security tactics and associated security features.

No.	*Security Feature*	**Advantage HAP**	**Advantage Satellite**
1	*Better authentication schemes*	*Yes*	*No*
2	*Faster establishment of authorized relation*	*Yes*	*No*
3	*Better encryption schemes*	*Yes*	*No*
4	*Better physical protection*	*No*	*Yes*
5	*Faster security monitoring and reactions*	*Yes*	*No*
6	*Strict enforcement of security policies*	*No*	*Yes*
7	*Better detection of distributed attacks*	*Yes*	*No*
8	*Better use of honeypots for worm detection*	*Yes*	*No*
9	*Better security disaster capability*	*Yes*	*No*
10	*Better security capability over the year*	*No*	*Yes*
11	*Less processing resources required*	*No*	*Yes*
Total score, HAPs versus satellites:		7	4

Table 2. The results of the comparative security analysis.

3. Better encryption schemes: the same as item 1. Faster and richer connections enable allocation of more bits for the transmission of external keys (see Equation (6)). Additionally, the keys may be changed more frequently, as security resynchronizations are much less expensive than in the case of satellites.
4. Faster security monitoring and reactions. The round-trip delays of HAPs are much less than satellites' round-trip delays. Security monitoring reports are provided faster, and therefore both automatic and semiautomatic security-related actions may be performed more rapidly than in the case of satellites.
5. Better detection of distributed attacks. A HAP may host a set of base stations, e.g., a set of UMTS base stations and or a set of WIMAX base stations, etc., which cover a certain region. It may therefore host more networks and more parts of a single network, whereas a satellite covers a much larger area, but is logically viewed as a part of a single network. Therefore, a HAP provides an opportunity to detect (using intrusion-detection systems, IDS [6]) simultaneous attacks from several parts of a single network, and even from different networks.
6. Better use of honeypots for worm detection. The use of honeypots to detect and control the spread of blind-scan and hit-list worms [7] (based on virtual machines and multi-home hosts [8, 9]) is probably of greater value in HAP networks than in their satellite counterparts, for two reasons. One is that HAPs may host several networks, and thus cover a larger address space. The other was already mentioned above.
7. Better security disaster-recovery capability. In a case where all the onboard computers are infected by security viruses, worms, etc., the HAP may be brought down to Earth, where it can be more quickly and easily recovered. Typically, the recovery will include a comprehensive forensic analysis of the attack (disk contents, etc.), and reinstallation of the system.

The following is a list of security features for which network architectures based on satellites have an advantage over the network architectures based on HAPs:

1. Better protection from being physically destroyed: Satellites cruise at much higher altitudes than HAPs, and therefore they are better protected from missiles.
2. Strict enforcement of security policies: In a HAP WIMAX network, there may exist network paths that are not monitored by a base station (direct links between subscriber stations in mesh mode), while in a satellite network, all communication paths traverse the satellite and are therefore subjected to monitoring. With respect to that fact, satellites allow for stricter enforcement of security policies.
3. Better security capability over the whole calendar year. One of the biggest problems with HAPs is battery refill based on solar power during winter. Reduced battery capacity may imply reduced functions, including the more-advanced security functions.
4. Fewer processing resources required. Because of greater bandwidth, the amount of data in the case of HAPs is greater. Thorough data inspection (using techniques such as deep-packet inspection [10]) thus requires more processing resources.

Based on the results shown in the Table 2, we may conclude that network architectures based on HAPs do provide better security features than those based on satellites, and therefore more effective and efficient implementations of security tactics. The total score thus seems to be in favor of networks based on HAPs, and that is the final result of Step 4.

6. Conclusions

Research on HAPs up to today has not systematically covered issues of HAP security. This paper has presented a comparison of the network architectures of HAPs and satellites with respect to security. The comparison used a hierarchy of security tactics. The total score was in favor of networks based on HAPs.

7. References

1. T. C. Tozer and D. Grace, "High-Altitude Platforms for Wireless Communications," *Electronics & Communications Engineering Journal*, June, 2001.

2. J. H. Shaffer and J. M. Smith, "A New Look at Bandwidth Latency Tradeoffs," University of Pennsylvania, CIS TR MS-CIS-96-10; http:// repository.upenn.edu/cgi/viewcontent.cgi?article=1192&context=cis_reports.

3. F. L. Bauer, *Decrypted Secrets: Methods and Maxims of Cryptology, Fourth Edition*, New York, Springer, 2006, ISBN 3-540-24502-2.

4. A. Nucci and S. Bannerman, "Controlled Chaos," *IEEE Spectrum*, December 2007.

5. J. Ryoo, P. Laplante, and R. Kazman, "In Search of Architectural Patterns for Software Security," *Computer*, June 2009.

6. I. Basicevic, M. Popovic, and V. Kovacevic, "The Use of Distributed Network-Based IDS Systems in Detection of Evasion Attacks," AICT 2005, Lisbon, Portugal, July 17-20, 2005.

7. N. Provos, "A Virtual Honeypot Framework," Proceedings of the 13th USENIX Security Symposium, 2004.

8. X. Q. D. Dagon et al., "Honeystat: Local Worm Detection Using Honeypots," Proceedings of the 7th Symposium on Recent Advances in Intrusion Detection, 2004.

9. L. Spitzner, *Honeypot: Tracking Hackers*, Reading, PA, Addison-Wesley, 2002.

10. Po-Ching Lin, Ying-Dar Lin, Tsern-Huei Lee, and Yuan-Cheng Lai, "Using String Matching for Deep Packet Inspection," *Computer*, **41**, 4, April 2008 pp: 23-28.

11. R. Ursin et al., "Space-Quest, Experiments with Quantum Entanglement in Space," *EuroPhysics News*, DOI: 10.1051/epn/2009503.

Microwave Wireless-Power Transmission to High-Altitude-Platform Systems

Jacob Gavan
Saad Tapuchi

Abstract

High-altitude-platform (HAP) systems belong to a new technology that has the potential to become a low-cost and useful alternative or complement to geostationary-Earth-orbit (GEO) and low-Earth-orbit (LEO) radio-relay satellites. The HAP concepts, developments, and applications are also the subject of two special sections in the *Radio Science Bulletin* (March 2010 and September 2010 issues, Nos. 332 and 334), and this paper is included in the second such section. However, the problems of the long sun eclipses and stabilization control of HAPs require significant electrical power and energy, which may delay the realization of long-operation stratospheric HAPs. A possible solution could be the utilization of wireless-power-transmission (WPT) terrestrial systems feeding HAPs. This paper starts with an introduction that defines HAPs, wireless-power transmission, and solar-power satellite (SPS) systems. The concepts of the different wireless-power-transmission systems is followed by a review of the genesis and development of wireless-power-transmission systems. However, the main subject of this paper concentrates on microwave (MW) wireless-power-transmission systems for feeding stratospheric HAP airships. A thorough description of future projects in microwave wireless-power-transmission systems from terrestrial bases to HAPs is therefore presented. In this description, we utilize several research and development results obtained in the evaluation steps of the fascinating solar-power-satellite projects, especially by Japanese and USA scientists and engineers. The solar-power-satellite evaluation results are thus very useful for the future design and implementation of microwave wireless-power-transmission systems, making HAPs much easier to realize. Comparisons between microwave wireless-power-transmission systems for terrestrial links, for stratospheric HAPs, and from solar-power satellites in a geosynchronous orbit are provided. In the Appendix, simple methods for computing the areas of the microwave wireless-power-transmission transmitting-antenna arrays, microwave beams, and rectenna as functions of the required power-transmission efficiency, separation distances, and frequency bands are developed. The results show that the required areas and weights of the microwave wireless-power-transmission systems are significantly less for HAPs than for solar-power satellites. However, the design and realization of microwave wireless-power-transmission systems for HAPs could also be useful for the realization and preliminary tests of solar-power-satellite systems.

1. Introduction

Wireless radio applications have been used extensively from the time of Marconi in the beginning of the 20th century, especially for distant communication. In the beginning, only wireless terrestrial systems were used. From the 1960s, wireless relay geostationary Earth orbit (GEO) and low-Earth orbit (LEO) satellites have been used. Nowadays, more than 400 GEO and some hundreds of LEO satellites are operating. These are dominant for long-distance mobile communication, remote sensing, and many other applications [1, 2]. More recently, a new technology for relaying wireless information using High Altitude Platforms (HAPs) has been expanding. The optimal altitudes for HAPs are from 17 to 24 km, due to lower wind velocities and temperatures [1, 3]. The HAPs have several advantages over GEO and LEO satellites. The heavier-than-air aircraft category is now extensively used, especially for unmanned military UAV and home-security purposes [1, 3]. Lighter-than-air airships using helium gas are also being developed, which are easier to stabilize at a fixed position. However, the main disadvantage of HAPs when compared to satellites is their long eclipse time, which affects their development [3, 4].

Unlike GEO satellites, where the maximum sun eclipse time is 1.2 hours, which occurs only twice each year, and LEO satellites, which suffer only from very short eclipses, HAPs will suffer from very long eclipses. Because of their relative low altitudes, the HAPs Earth shadow results in eclipses around 12 hours per day for locations in proximity

Jacob Gavan and Saad Tapuchi are with Sami Shamoon College of Engineering, Jabotinsky St. 84, Ashdod, Israel; e-mail: jacobg@sce.ac.il; tapuchi@sce.ac.il

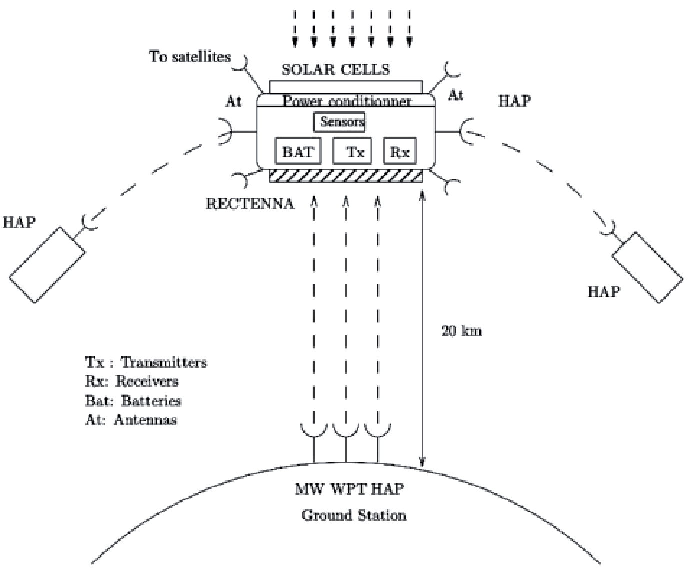

Figure 1. The sandwich microwave wireless-power-transmission system for a terrestrial base transmitter transmitting to a HAP.

of the equator, and up to 24 hours per day in the winter for locations in proximity to the Earth's poles [1, 5]. Therefore, HAPs need significantly bigger and heavier energy-production and storage systems than do satellites. The electrical power required by HAPs is usually in the range of 10 to 200 KW required for payload, stabilization, and fixed positioning [1, 6]. This power can be obtained by efficient photovoltaic (PV) solar cells and, in eclipse periods, by batteries such as NiH_2 , Li Ion, or by fuel cells. These are all very heavy, and are still not sufficient for long eclipse periods and extreme wind velocities, where heavy and polluting fuel engines are required [1, 4].

A possible solution could be the transmission of microwave (MW) energy from a terrestrial base, which is converted at the HAP to direct current (dc) using rectifier antennas (rectennas), as depicted in Figure 1. This is characterized by a high efficiency in energy conversion, which will be detailed in Section 4. The addition of a microwave wireless-power-transmission (WPT) system to limited-capacity and weight photovoltaic solar cells and batteries may enable airships to operate with high-altitude long operation (HALO) for months or even years [3, 5].

The wireless-power-transmission idea is not new. At the beginning of the 20th century, Nikola Tesla performed the first experiments in Colorado Springs, USA [7]. However, the wireless-power-transmission technology was not mature. For many years, no advancements occurred because many problems with efficiency, reliability, human security, and interference to communication systems had to be solved [1, 8]. Following the oil-supply crisis of the Six Days War, several organizations – mainly, the US NASA and the Japanese Aerospace Exploration Agency (JAXA) – invested a lot in the development of wireless-power-transmission systems, especially in the solar-power satellite (SPS) projects. The solar-power satellite concept of supplying large amounts of non-polluting 24-hour-per-day microwave energy from geosynchronous satellites was initiated by Peter Glaser in 1968. At that time, the technological realization of solar-power satellite systems seemed like science fiction. However, the tremendous needs for nonpolluting energy sources resulted in several activities and investments in these programs [8, 9]. Due to the considerable technological challenges in the ambitious solar-power satellite programs – transmitting several GW of microwave power from GEO or LEO satellites to terrestrial stations – the realization may take one or two more decades [10, 11]. The URSI community is also very interested in the solar-power satellite project, and two issues of the *Radio Science Bulletin* were dedicated to this subject, as well as several special sessions at URSI General Assemblies [11-13]. Microwave wireless-power transmission to HAPs is a much-easier technological challenge than are solar-power-satellite projects. The design, realization, and tests with HAPs may contribute to future solar-power-satellite projects. Following a general description of the wireless-power-transmission concept, genesis, and development, in this paper we shall therefore concentrate especially on microwave wireless-power transmission from terrestrial stations to HAPs.

2. The Wireless-Power-Transmission Concept

The most-important issue for wireless-power-transmission systems is the transmission efficiency, which has to be significantly higher than for wireless-communication systems [8]. Short-range wireless-power-transmission systems, up to tens of meters, are used especially in radio-frequency identification devices (RFID) and wireless sensors. Recently, scientists at several organizations, such as Intel and MIT, have been developing wireless-power-transmission devices: energizing electric bulbs, or charging laptops or other devices. A power-transmission efficiency of more than 50% can be obtained by a strong resonance effect between the transmitting and the receiving devices [14, 15]. However, in this paper we shall concentrate on longer-distance wireless-power transmission.

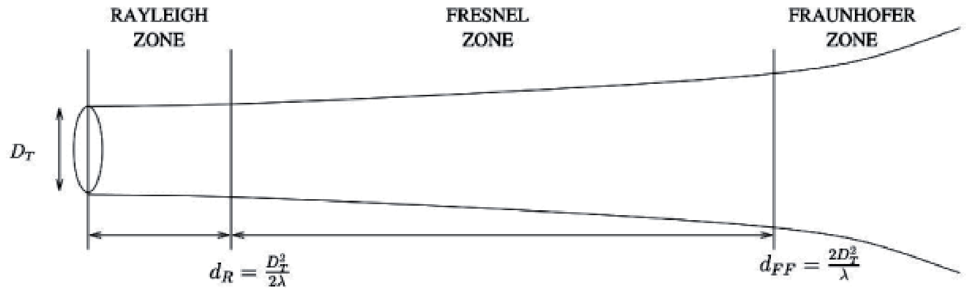

Figure 2. The dispersion effects of the microwave beam transmitted by an aperture antenna of diameter D_T.

For long-distance wireless-power transmission exceeding hundreds of meters, only microwave and laser transmission systems may be efficient, today [8]. The operating principle of microwave wireless-power transmission can be explained from electromagnetic-theory concepts concerning beams of highly directive aperture antennas. The transmitted energy beam from the antenna aperture remains concentrated in a cylindrical volume, the cross section of which is equal to the antenna aperture, and does not disperse in the Raleigh near-field region up to a distance, d_R, of $D^2/2\lambda$. Here, D represents the largest dimension of the antenna aperture – usually, the diameter – and λ is the transmitted wavelength. The beam's power density, S, thus remains constant as a function of the distance, d, from the transmitting antenna in the Raleigh zone, and dispersion of the power density does not occur. Beyond d_R in the Fresnel near-field region, up to the distance, d_F of around $2D^2/\lambda$, the energy dispersion is small, and S decreases slightly as a function of d. Beyond d_F, the far-field Fraunhofer region begins [2], where S decreases as the square of the distance, d, and full dispersion occurs, as depicted in Figure 2. Receiving devices for efficient wireless-power-transmission systems therefore have to be located in the neighborhood of the near-field region of the transmitting antenna. In order to keep the power transmission efficient, the surface apertures of the transmitting antenna and the receiving device have to increase as a function of the distance, d, and decrease as a function of the frequency, f. G. Goubau and W. C. Brown have derived the relations for the wireless-power transmission efficiency as functions of d and other parameters [16]. The relations between the power-transmission efficiency and the different parameters of long-distance microwave wireless-power-transmission systems are derived in the Appendix.

The common receiving device is the rectifier-antenna (rectenna), which converts the received microwave power beam into direct current (dc) to feed the receiver payload [17]. The development of high-power radar transmitter tubes during World War II enabled the realization of remote-distance wireless-power-transmission systems. However, the microwave wireless-power-transmission transmitting antenna has to be in a line-of-site (LOS) position with the rectenna. A simple block diagram of a typical microwave wireless-power-transmission system is presented in Figure 3. A more-detailed analysis of the microwave-wireless-power transmission system is presented in Sections 3 and 4.

The main categories of microwave wireless-power-transmission systems are as follows:

1. The first category is terrestrial-to-terrestrial systems, where atmospheric losses and terrestrial obstacles have influence. A few microwave wireless-power-transmission systems for separation distances up to 1.6 km are operational. Recently, wireless-power-transmission experiments for a separation distance of 148 km have shown disappointing results, as will be explained in Section 3 and in the Appendix [5, 17, 18].

2. The second category is terrestrially-based-to-atmospheric-platforms, including HAPs. Several experiments supplying energy to low-altitude helicopters and other platforms were successful. The terrestrially based microwave wireless-power-transmission technology for feeding HAPs up to distances of 20 km is much easier and nearer to realization than solar-power satellites, but has not yet been tried [8, 18-22]. These wireless-power-transmission systems will be the main subject of this paper.

3. The third category is terrestrially-based-to-remote-terrestrial bases, using as relays elevated platforms up to the altitude of HAPs, to overcome terrestrial obstacles. These wireless-power-transmission systems may be the main subject of a following paper [8, 10].

4. The fourth category is terrestrially based systems to energize orbital-transfer vehicles by microwave wireless-power-transmission beams for positioning or transporting materials from LEO to GEO satellites, up to an altitude of 36000 km. From ground to LEO, the heavy materials required for solar-power satellite construction will be transported by heavy cargo lifters, similar to the Falcon. This nonpolluting future wireless-power-transmission technology for launching rockets using electrical-ion thrusters for propulsion may replace very weighty and expensive fuel propulsion systems [11, 23, 24]. This future technology may be useful for the realization of solar-power-satellite systems, but is still in its preliminary design steps.

5. The fifth category consists of systems based on geostationary satellites transmitting to terrestrial stations for distances up to 39000 km. These solar-power-satellite

systems may be very useful for solving an important part of the future human-energy supply requirements and for reducing pollution. A lot of activities and budgets were therefore invested to develop these wireless power-transmission systems [8, 9, 25], and more will be. In Figure 4, NASA has provided an artist's concept of a future GEO solar-power-satellite system [8, 27]. However, the technological challenges are huge, and the realization of solar-power-satellite projects may take several years.

6. The sixth category involves LEO-, sun-synchronous-, or highly-elliptical-orbit-based solar-power satellites transmitting to terrestrial stations. These future projects may be less complex and costly than GEO satellites, but the supplied wireless-power-transmission electrical energy to the terrestrial station will be available only for short time intervals, in comparison to a permanent electrical supply from geostationary satellites [8, 10, 11]. Several solar-power-satellite units will therefore be required for the operation of ground-located rectenna stations.

7. The seventh category uses space-to-space platforms. These future wireless-power-transmission projects may use millimeter waves or lasers as transmitter sources, since no atmospheric losses occur in space. This will involve more-compact transmitter antennas, and receiving rectennas with smaller dimensions, weight, and cost [8, 10].

8. The eighth category involves supplying wireless-power-transmission electrical energy for future human missions on the moon, planets not too far from the sun, and for Earth-moon Lagrangian-position-located stations. These wireless-power-transmission systems may be useful for future missions. However, some scientists are designing such wireless-power-transmission projects [8, 26].

In the future, microwave beaming may be challenged by lasers for wireless-power-transmission systems. Laser advantages may provide much smaller and more-compact wireless-power-transmission transmitters and receivers. However, the disadvantages of higher atmospheric losses, especially in the case of clouds or rain, and the lower infrared-to-dc conversion efficiencies of less than 0.2 – even for relatively efficient CO_2 lasers – prohibit their use today. In this paper, we shall analyze only microwave wireless-power-transmission systems [8, 11].

3. Genesis of and Developments in Microwave Wireless-Power-Transmission Systems

The first pioneers in the concept and development of wireless-power-transmission systems were N. Tesla, K. Tsiolkowski, G. Goubeau, and W. C. Brown [7-12, 16, 17]. These should be compared to J. C. Maxwell, H. Hertz, Popov, and G. Marconi for wireless communication systems [1-6]. The first experiments for the realization of long-distance microwave wireless-power-transmission systems were done by N. Tesla in the beginning of the 20th century [7, 10]. However, the lack of maturity of the microwave technology, and very low power efficiency, stopped any interest in the development of wireless-power-transmission systems for many years. In the meantime, significant advancements in microwave power tubes, antennas, control tracking systems, and photovoltaic solar cells in the 1950s enabled the development of efficient wireless-power-transmission systems [5, 8, 11]. The most important step was the development of efficient rectennas by W. C. Brown of Raytheon Corp. in 1964. This enhanced the conversion efficiency of microwave-to-direct-current power from 15%, with point-contact diodes, to more than 50%, with silicon Schottky-barrier diodes; the efficiency can reach more than 85% today [11, 17]. In 1968, W. C. Brown and his team succeeded in supplying 200 W of dc power to a low-altitude helicopter, at an altitude of 15 m, using a dish antenna, transmitting at a frequency of 2450 MHz [21]. Later, in 1975, Brown assisted R. M. Dickinson from JPL in building a large terrestrial wireless-power-transmission installation at the Venus Site of the Goldstone Facility in California. The separation distance was 1.54 km between a transmitting parabolic antenna, with a diameter of 26 m, and a rectenna array, with dimensions of 3.4 m × 7.2 m, located on a tower. The transmitting frequency was 2.388 GHz from a klystron tube, and the receiver's output dc power was 30 kW, with 82.5% rectenna power-conversion efficiency [17, 18].

In consideration of the progress achieved in wireless-power-transmission technology and the oil energy crisis, in 1968 P. Glaser proposed the concept of a solar-power satellite in a GEO orbit [9]. This revolutionary concept, similar to A. Clarke's suggestion about GEO satellites in 1945, was even patented in the US in 1973 [24]. Later, the NASA and the US Department of Energy (DOE) initiated a solar-power satellite concept, development, and evaluation program. This lasted from 1979 to 1981, without any concrete results [8, 27].

The Canadian Research Communication Group (CRC) in Ottawa designed, constructed, and tested a microwave wireless-power-transmission system for energizing a prototype HAP aircraft. The one-eighth full-scale model of a future stratospheric high-altitude relay platform (SHARP) was successfully tested at an altitude of 100 m in October 1987. A 4.5 m parabolic antenna transmitted 10 kW of power at 2450 MHz to the 4.5 m-wingspan airship rectenna [19]. However, the SHARP project was discontinued due to financial problems [20].

Latter, the CRC group, which had earned experience in the design of microwave wireless-power-transmission systems, collaborated with Japanese specialists. Japan was involved in the development of wireless-power-transmission systems from the 1940s, especially for shooting down

US bombers. From the 1980s, Japan invested a lot in microwave wireless-power-transmission technologies with the cooperation of North American organizations, especially NASA [8, 11, 27]. H. Matsumoto's team, from the Kyoto University radio science center for space and atmosphere, carried out the first wireless-power-transmission microwave ionospheric nonlinear interaction experiment in space in 1983 [11, 28]. This was followed in the 1990s by initial studies on rocket electronic propulsion, energized by a terrestrial microwave wireless-power-transmission installation, especially for transporting material from LEO to GEO orbits [11, 27]. Several experiments of feeding a helium airship with a 2450 MHz beam from a terrestrial vehicle, providing 3 kW at the output of an efficient rectenna, were performed in 1995. In 2002, Japan's JAXA proposed a GEO solar-power-satellite system to transmit 1 GW of microwave power at a frequency of 5.8 GHz [27, 28].

Several organizations in Europe, especially the European Space Agency (ESA), became interested in wireless-power-transmission and solar-power-satellite issues. This began in 1996 with the development of a microwave wireless-power-transmission project on the French island of Reunion, in the Indian Ocean. The first prototype transmitted power over a distance of 100 m at 2450 MHz. The final microwave wireless-power-transmission product transmitted 10 kW to an isolated village for a distance of 700 m between the transmitting antenna and the receiving rectenna [29, 30]. ESA initiated several studies for the development of solar-power satellites, such as a European sail tower for a future microwave solar-power-satellite proposition in 2001 [31, 32].

The main activities for the development of the future solar-power-satellite projects were led by US organizations. NASA initiated a new solar-power-satellite concept and technology-maturation program starting in 2001 [11, 33]. However, NASA's funding for the solar-power-satellite project was restrained from 2002, but a few private companies and multinational consortiums, mostly located in the US, are still active in solar-power-satellite research and development projects. In 2008, J. Mankins, in collaboration with Japanese scientists, designed a 2.45 GHz microwave wireless-power-transmission test system, operating from a mountaintop in Hawaii to another inland at a distance of 148 km. However, only 20 W was received, instead of a predicted 64% efficiency, because of lack of funding, especially for the required large dimensions of the transmitting antenna and rectenna, as discussed in the Appendix [34]. The Weightless Solar Modules (Welsom) consortium for space power has developed technologies for producing up to 16.8 kW/kg space solar arrays that are significantly lighter, smaller, and of lower cost than existing arrays. In collaboration with ESA and other European organizations, they claim to soon be able to supply wireless-power-transmission systems of 10 to100 kW for HAPs and for space, and to build space solar-sail boom arrays [35]. Welsom is also active with Japanese companies in the Palau beam-down demonstration project, to supply electrical energy to Palau and other islands in the Pacific Ocean from polar-elliptical LEO solar-power satellites [36, 37]. More recently, in April 2009, PG&E, a Californian electricity corporation, entered into a contract with the Solaren Company to supply 1700 GWH of solar energy from a solar-power satellite in orbit, beginning in 2016 [38].

However, the realization of the innovative, complex, and rewarding solar-power-satellite projects will require tremendous future investments in human and financial resources. This will require an international effort at a higher scale than the realization of the international space station. The involvement of more technology-expending countries, such as China, may be useful [11, 27, 33].

The design of the challenging solar-power-satellite projects are only in their preliminary steps. However, the terrestrially based microwave wireless-power transmission to a HAPs system is much easier to realize. In the following section, we shall therefore concentrate on the wireless-power-transmission HAPs issues, where design, realization, and experiments may contribute to the solar-power-satellite efforts.

4. Microwave Wireless-Power Transmission from Terrestrially Based Sites to HAPs: Future Projects

4.1 Frequency Choice

Experiments have been done to employ microwave wireless-power transmission in low-altitude platforms, as described in the previous section. Several patents have been obtained on this subject, following the invention of the rectenna by W. C. Brown [8, 24, 28, 39]. However, no tests or supplying of microwave power to stratospheric HAPs altitudes have been done. Such future implementations may contribute to long-duration operation of HAPs. An important preliminary step to such a realization is the choice of the proper frequency in the microwave bands.

Considering ITU recommendations, the industrial, scientific, and medical (ISM) frequency bands have to be chosen, in order to avoid serious interference to communication systems. The relevant microwave ISM frequency bands are from 2.4-2.5 GHz, 5.725-5.875 GHz, and 24.00-24.25 GHz. In general, communication equipment must accept any interference generated by systems operating at ISM frequencies [2, 3]. The required physical dimensions of the transmitting antenna and receiving rectenna for optimal power-transmission efficiency increase as an inverse function of frequency, as explained in the wireless-power-transmission concept section and in the Appendix. To achieve compactness and lower cost, the use of higher frequencies are therefore preferable. However, microwave

f [GHz]	2.45	5.8	24.5	35	94
D_T [m]	70	45.5	22.1	18.5	11.3
A_T [m^2]	3850	1625	385	270	100
S_T [$\mathrm{W/m}^2$]	52	123	520	740	2000

Table 1. The HAPs microwave wireless-power-transmission antenna aperture parameters D_T, A_T, and S_T as functions of f.

atmospheric and dispersion losses increase with frequency. The 2.45 GHz band is preferable for terrestrial microwave wireless-power transmission, especially for humid and rainy regions, where losses can be neglected even in heavy rains. This lower-frequency microwave band has to be chosen in spite of the huge dimensions and costs of the antennas and rectenna for long-distance operation. The 5.8 GHz band is more favorable for terrestrial-to-HAPs microwave wireless-power transmission, where the atmospheric path is less dense [5, 8].

For HAPs operating in very-dry-climate or desert regions, higher atmospheric-window frequencies in the 35 GHz or 94 GHz bands can be used, which involve more-compact and lower-cost transmitting antennas and rectennas, as depicted in Tables 1 and 2. Another advantage of increasing microwave frequencies is a reduction of interference risk to radio-communication systems, which operate more in the lower microwave-frequency bands. There is also a reduction of biological-hazard threats, because of the skin-depth effect that results in lower penetration of the microwave power into the human head and body with increasing frequency, as treated in Section 4.6. However, there are also a few disadvantages of increasing the microwave frequency, because of the cost increase in components, a higher accuracy required in the construction of antennas, and a slight decrease of the power efficiency [39, 41].

Microwave wireless-power-transmission systems operating in space or on planets without oxygen can use the 60 GHz band, which is the absorption frequency band of oxygen or even infrared lasers [2, 8, 27].

4.2 Block-Diagram Description of Microwave Wireless-Power-Transmission Systems

A simplified block diagram of a typical microwave wireless-power-transmission system is presented in Figure 3. The microwave transmitter (TX) usually has to supply up to 200 kW to the HAPs under maximum wind velocity, where electrical motors and, in extreme cases, a fuel supply or transformation of wind to electrical energy could be useful to keep the airship in a fixed position. However, the required average power is significantly lower, in the 20 kW range [1, 42]. Terrestrially based high-power transmitters are significantly simpler and lower cost than for a solar-power satellite located in orbit, because of the launches, and the special reliability and redundancy requirements for satellite transmitters. The output frequency of the transmitter can be in the ISM bands. In relatively dry climate locations it is suggested to use the 5.8 GHz or higher atmospheric-window-frequency bands, in order to reduce the physical dimensions of the antenna and rectenna, as explained in the Appendix. The diameter of the antenna's aperture and surface have to be large, in order that most of the transmitted power will reach the rectenna, connected at the lower part of the HAP airship [5]. It is recommended to use a phased array, which is better for stabilizing the microwave beam and the HAP than is a huge single antenna element [42, 43]. The rectenna, which transfers the microwave energy to direct-current (dc) energy in the HAP, is located in the lower layers of the stratosphere, contrary to the solar-power-satellite rectenna, located on the Earth [5, 27]. The dc energy at the output of the rectenna is supplied to the power-conditioner unit that energizes the HAP payload, and

Frequency Band	**Terrestrial** $d = 10,000$ **m**		**HAPs** $d = 20,000$ **m**		**SPS** $d = 36,000,000$ **m**	
	$\eta_T = 60\%$	$\eta_T = 95\%$	$\eta_T = 60\%$	$\eta_T = 95\%$	$\eta_T = 60\%$	$\eta_T = 95\%$
2.45 GHz	1224	2203	2448	4406	4.4×10^6	7.9×10^6
5.8 GHz	517	931	1034	1862	1.9×10^6	3.4×10^6
35 GHz	86	155	172	310	0.31×10^6	0.56×10^6
94 GHz	32	58	64	116	0.11×10^6	0.2×10^6

Table 2. The numerical values of the required antenna apertures, microwave-beam areas, and HAP rectenna areas, as functions of the power-transmission efficiency and frequency (all areas in $\mathbf{m^2}$).

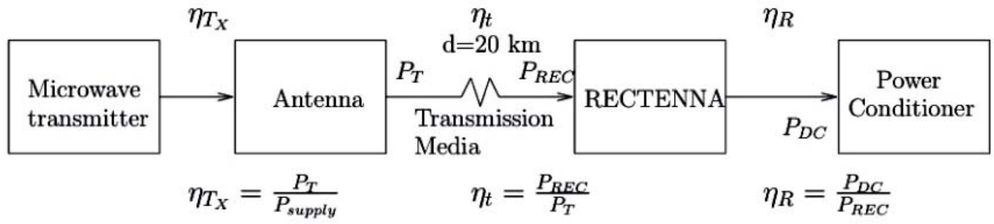

Figure 3. A simple block diagram of a typical microwave wireless power-transmission system.

the electrical motors for stabilizing the platform. A part of the dc energy is supplied to the HAP batteries or fuel cells, which are also fed from the limited photovoltaic solar cells on the top of the HAP airship, as shown in Figures 1 and 3. Figure 5 presents a detailed block diagram of a typical microwave wireless power-transmission system feeding a HAP [11, 39].

4.3 The Microwave Wireless-Power-Transmission Terrestrially Based Subsystem

The main parts of the microwave wireless-power-transmission terrestrially based systems depicted in Figure 5 are the microwave transmitter, TX; the antenna controller; the phased-array antenna; the power supply; and the microwave beam to the HAPs. The main requirements for the microwave transmitter are linearity, efficiency, reliability, low cost, and compactness [5, 42]. Linearity is important in order to reduce harmonics, intermodulation, and spurious products and other interference to radio-communication systems as much as possible. This may partly be achieved by operation in the linear part of the power-amplifier stages' transfer characteristics, far from saturation, which reduces the transmitter's power-conversion efficiency. Selective (sharp) output filters can be applied for reducing spurious emissions, as the transmitted CW power is not modulated [2, 27]. For a terrestrially located transmitter, power-conversion efficiency, reliability, and compactness are less important than for a solar-power satellite. This is because possibilities for power supplies and heat dissipation are available, as well as permanent maintenance on the spot, and no launch requirements for the transmitter and its antenna. The cost of the terrestrial transmitter will therefore be significantly less than for the space-located solar-power-satellite transmitter. The required maximum 200 kW is significantly lower than the GW power levels necessary for the solar-power satellite [11, 43].

Electronic vacuum tubes are preferred over solid-state semiconductors for power levels exceeding 100 W, due to their superior power efficiency and quality factor (selectivity), in spite of their lower reliability and lifetime [11, 27]. However, maintenance and component replacement are very easy for a terrestrially located transmitter. Tubes are recommended even for solar-power-satellite transmitters, due to their significantly lower kg-to-kW ratio, and their better power-dissipation facilities than solid-state oscillators and amplifiers. The best choice for a tube is the phase-controlled magnetron. W. C. Brown used a low-cost, noisy, microwave-oven type of crossed-field magnetron tube in a phased-locked-loop to control phase, as depicted in Figure 6, to achieve stable low-harmonic and low-spurious-emission performance [8, 42]. Later, a group of scientists from Kyoto university succeeded in the development of higher-performance phase-controlled magnetron arrays at 2.45 and 5.8 GHz. These were called space-power radio-transmission systems (SPORTS), or a compact microwave-

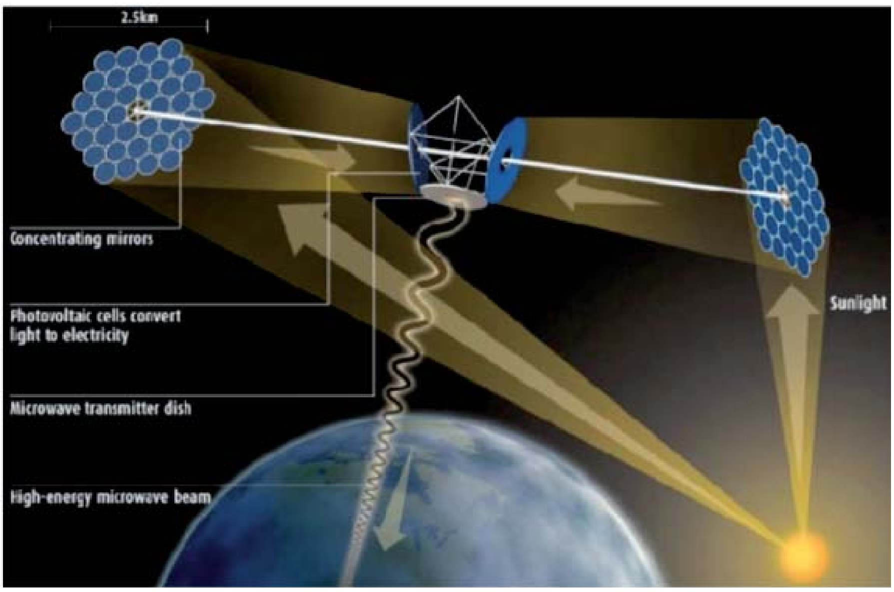

Figure 4. An artist's concept of the NASA solar-power-satellite concept.

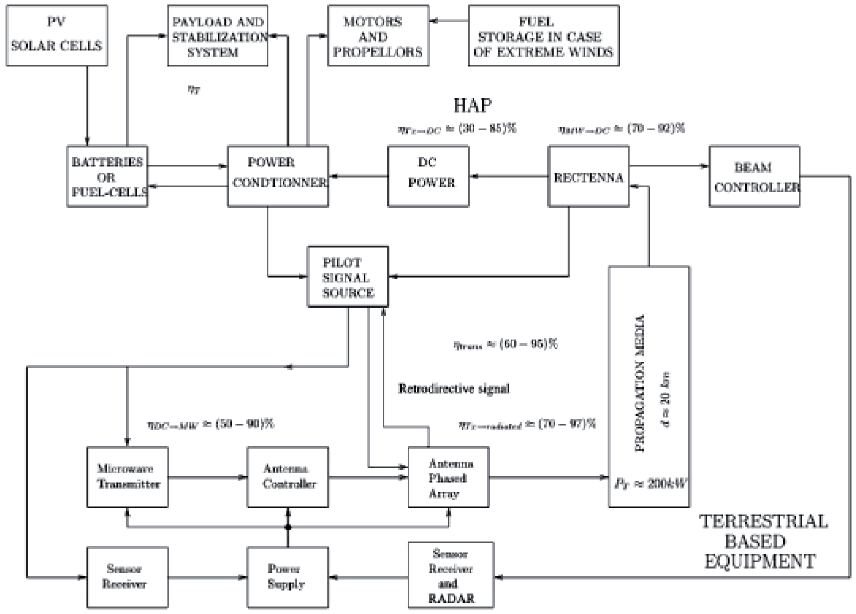

Figure 5. A detailed block diagram of a typical microwave wireless power-transmission-system feeding a HAP.

energy transmitter (COMET), as depicted in Figure 7. These 5.8 GHz SPORTS achieved very low harmonic levels, better than −70 dBc, and a stability better than 10^{-9}. The SPORTS transmitters were very compact, with a weight-to-power ratio below 25gr/W. However, in spite of low-loss phase shifters, the cost was a significant reduction of the efficiency, from around 75% for a magnetron circuit to 60% for a SPORTS unit providing power levels from 1 to 10 kW [27, 44].

Some research groups have preferred recovery-type traveling-wave tubes (TWTs), which have track records in space and on satellites. Microwave-power modules (MPM) were therefore developed, which combined the best aspects of traveling-wave tubes, semiconductor amplifiers, and state-of-the-art power-supply technology into one package. This makes microwave-power modules good candidates for future solar-power-satellite or microwave wireless-power-transmission transmitters, because they have high conversion efficiency, small size, and low weight [27].

Klystron reflex tubes can provide higher power levels, in the hundreds of kW. They have high conversion efficiency, around 70%, and low harmonic emissions, but require a heavy magnet and a bulky power supply. They therefore were used only for microwave wireless-power-transmission systems between two fixed terrestrial stations, such as in the Goldstone project [17, 18].

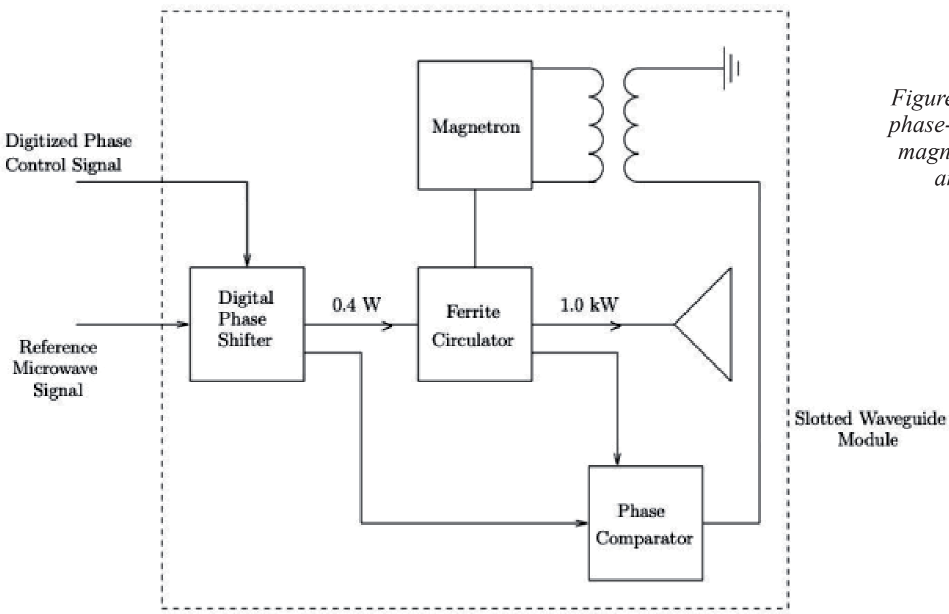

Figure 6. A circuit for a phase-locked, high-gain magnetron directional amplifier [42].

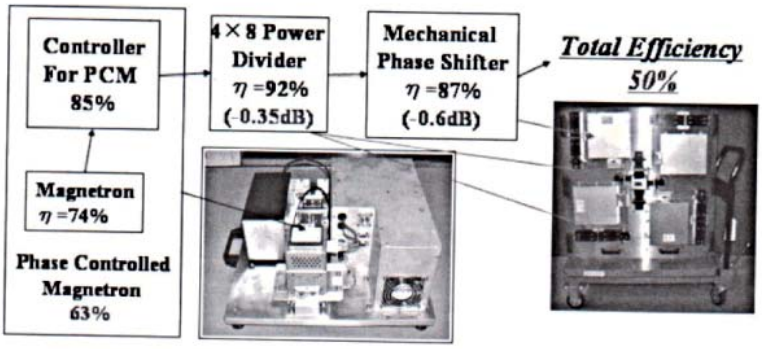

Figure 7. A block diagram and the computation of the efficiency of the space power radio-transmission system [44].

The power-conversion efficiency and performance of the phased-controlled magnetrons and traveling-wave tubes decline for the millimeter-wave atmospheric windows at the 35 GHz and, especially, 94 GHz or even 140 GHz frequency bands, where gyrotron tubes become efficient. Gyrotron sources are capable of generating hundreds of kW of millimeter-wave CW power in a circularly polarized beam format [39, 41]. High-power gyrotrons have been under development for nuclear-fusion programs over the past decade, and are now commercially available. A typical gyrotron includes a supply voltage of 80 kV, a current of 35 A, a water cooling system, and a magnetic field of 14,000 Gauss [45, 46].

Semiconductors, such as SiC or GaN high-electron-mobility transistors (HEMT), can be used for low power levels, up to100 W [27, 47].

The best solution for a microwave terrestrially based transmitter to date is to use some tens or hundreds of hybrid semiconductors and phase-controlled magnetron units, as depicted in Figures 7 and 8 [27, 44]. Each magnetron unit is connected via the antenna controller to an antenna element of a phased-array antenna. All the elements of the phased array are included in a very highly directive aperture-antenna beam shape, which can be controlled with high speed and accuracy to transmit optimum power to the stabilized airship's HAP rectenna [42, 47]. The power efficiency of the phased-array transmitter is slightly reduced in comparison to the single-element antenna's transmitter, due to the limited losses of the transmission lines and the phase shifters. However, the cooling requirements are reduced, due to better power-dissipation conditions, and the breakdown of a few magnetrons will not stop the system's operation, due to a graceful deterioration process [5, 8]. In the case of extremely large arrays of several thousand elements, it is even possible to use semiconductors instead of phase-controlled magnetrons.

The antenna elements may be waveguide cavity-backed slots, horns, microstrip patches, or dipoles. For smaller numbers of array elements, even dishes or Cassegrain antennas could be used [42, 44].

A 10 dB Gaussian-taper amplitude distribution can reduce the transmitter antenna's array-grating lobes and sidelobes, and concentrate the power density in the center of the transmitted beam, both at the transmitting antenna and at the rectenna. The power level of the active microwave amplifiers and the power density are decreased at least by 10 dB at the beam's perimeter limit [27, 42]. The external environmental threats of radio interference and biological effects are thus significantly reduced. The microwave-power-transmission efficiency from the terrestrial transmitter-antenna array to the rectenna can approach 100% if their physical dimensions are sufficiently large as a function of the transmitted frequency, as shown in the Appendix.

The terrestrial power supply can be supplied by the local electrical-company grid, by a polluting diesel generator, or, in the future, by photovoltaic solar cells, or

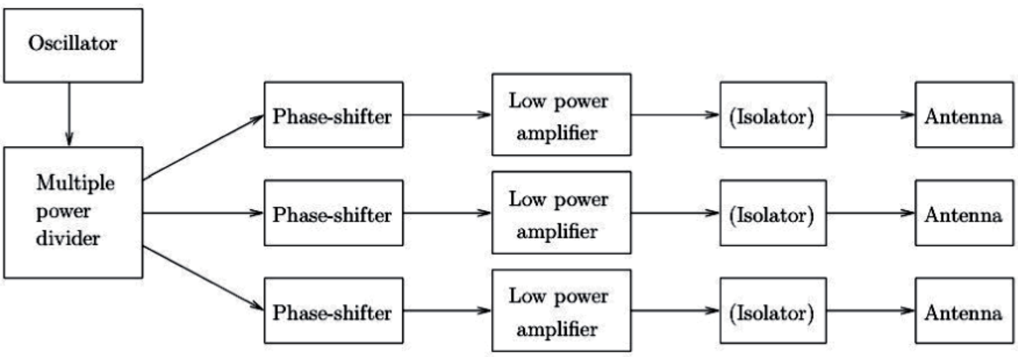

Figure 8. A block diagram of a terrestrial phase-controlled array.

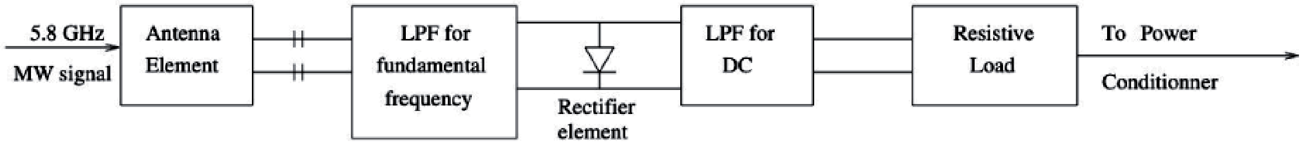

Figure 9. A block diagram of a typical 5.8 GHz rectenna connected to the HAP power supply.

even by a small part of the power obtained from a solar-power-satellite rectenna [8, 42].

4.4 The Microwave Wireless-Power-Transmission HAP-Based Subsystem

The microwave wireless-power transmission from the terrestrial phased-array antenna has to be captured by the rectenna's receiver, located at the bottom (lower) part of the HAP. As mentioned in Section 3, the rectenna is composed of an array of antennas and rectifier units, operating as a transducer converting microwave power to direct current (dc) [5, 8]. Starting with the development of rectennas by W. C. Brown 45 years ago, a lot of resources were invested in improvements, which were followed by numerous patents [17, 46, 48-50]. Nowadays, power-conversion efficiencies of 70% to 92% can be achieved [27, 42]. The rectenna antenna can be a monopole, a dipole, a Yagi, a microstrip, a spiral, or even a parabolic dish and, in some cases, have a reflector. The rectenna's rectifying circuit can be a shunt half-wave silicon Schottky barrier diode and GaAs for the higher-frequency bands or a full-wave rectifier for higher power levels. Even active FETs or HEMTs have been recently tested [27, 51]. A block diagram of a typical rectenna element is presented in Figure 9. The input low-pass filter (LPF) at the fundamental frequency serves for impedance matching, and for reducing re-radiation of harmonics and other spurious frequencies from the rectenna's antennas. The rectifier is connected to a second low-pass-filter circuit for receiving dc power at the resistive load connected, with other resistive loads, to the power-conditioner unit on the HAP [5, 52]. The large-surface rectenna is composed of an array of numerous elements, as shown in Figure 10. It was proven that maximum power-conversion efficiency and lower spurious re-radiation are obtained for a larger number of shunt elements than of series elements, for high-peak-inverse-voltage and for low-internal-resistance rectifying diodes [27, 33].

The rectenna array can be included in a very light thin-film format, providing more than 2 kW per kg. This is very important, considering the weight constraints for HAPs and other airborne platforms [27, 50]. The power dissipation of the HAP's rectenna and the transmission-line losses are lower, and the elements are significantly simpler to design, than for the terrestrial case. This is because the ambient temperature at the altitude of the HAP altitude is around −65° C, the humidity is very low, and the microwave

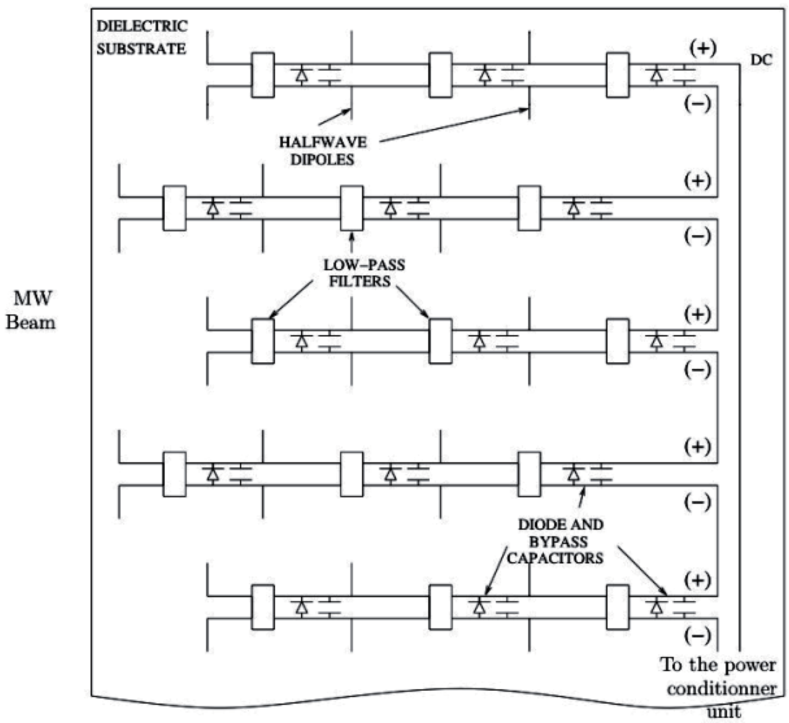

Figure 10. A thin film rectenna array for HAPs [5].

power is limited to 200 kW [1, 49]. The rectenna can be protected from UV radiation and ozone present at HAP altitudes by shielding and Kapton coating with Teflon [33, 43]. The surfaces of current rectennas can reach approximately tenths of a square meter, compared to the few thousands of square meters required for efficient power-conversion HAPs, which need still to be developed. However, the design of terrestrial solar-power-satellite rectennas will be much more complex, because they will require millions of square meters [18, 27, 46].

The dc energy from the rectenna is connected to the power-conditioner unit, which provides the required electrical energy to the HAP payload and station-keeping functions. The power-conditioner unit also controls the HAP batteries, which are fed from the photovoltaic solar cells, supplying limited power (of the order of 15 kW), and from the rectenna during the long periods when the solar cells are not energized. However, most of the HAP's required energy is supplied by the rectenna, and not by the batteries. The batteries can be NiH_2 or, even better, Li Ion, Li S, or fuel cells, the performance of which decreases with altitude [27, 55]. Utilization of a terrestrial microwave wireless-power-transmission system with a rectenna connected to the HAP would significantly reduce the mass penalty for energy storage using much-lighter and compact batteries and photovoltaic solar-cell arrays. This will afford HAPs long-term operation of months or even years [8, 35].

Figure 1 depicts the sandwich concept, with the rectenna connected to the lower part of the HAP airship, and an ultra-thin solar-cell array. This can be rolled into long cylindrical packages, and covered with a thin metal shell made of light material, with the upper part in the direction of the sun. Currently, the weight burden is around 1 kW per kg. Typical silicon space-qualified photovoltaic solar-cell arrays can provide a power-conversion efficiency around 25% at the beginning of life (BOL), and around 15% at the end of life (EOL), after several years [27, 37]. An actual larger space solar-cell array, of 65 kW, is located in the International Space Station (ISS). Recently, state-of the-art triple-junction GaAs solar cells with a maximum efficiency of 40.7% were developed, but they may not yet be feasible [54, 56].

4.5 HAP Microwave Wireless-Power Transmission Beam-Guidance and Station-Keeping Control Functions

Precise control of the microwave wireless-power-transmission beam direction and intensity is crucial for the system's operation. The guidance of the microwave beam can be achieved by a beacon generating a pilot signal from the center of the rectenna. This beam is transmitted to the terrestrial phased-array antenna. At the center of the phased-array antenna, a sensitive interferometer can establish the direction of the beacon. This directional information feeds a microprocessor unit, which sends two signals: one is sent to the rows and the other to the columns of the phased-array antenna's radiation-module matrix. Using these signals as a reference, each radiation module multiplies the signals by a term corresponding to its position in the row and column matrix to establish its phase relative to the center of the array. There is also a phase reference sent to each module, which is connected to a low-power phase shifter with up to 360° variation. Utilization of the phased-array antenna with a pilot signal eliminates the need for mechanical beamforming and tracking [8, 42]. The control loop is closed by placing sensors on the periphery of the rectenna, which generate an error signal if not evenly illuminated. The error signal is transmitted to the terrestrial microprocessor, which modifies the signal sent out to the radiation modules to change their phase relationships to re-center the beam on the rectenna [39, 42].

Research and development centers in Japan and the USA have developed advanced techniques for increasing the accuracy, reliability, and efficiency of microwave-beam guidance for solar-power-satellite systems, where the implementation is much more complex than for HAPs [27, 33]. Retrodirective systems with phase-conjugating circuits can enhance the accuracy and conversion efficiency of the microwave beam reaching the rectenna, without the necessity of expensive phase shifters [57, 58]. In typical retrodirective units, the pilot operates at the half of the microwave wireless-power-transmission frequency. This would be 2.9 GHz for our choice of 5.8 GHz, because of an interference threat to the pilot signal from the much higher-power-level microwave-transmitter beam. The retrodirective system unifies target detection with beamforming by the phase-conjugating circuits, and eliminates the possibility of beam-pointing error due to Doppler shift. The beaming accuracy also depends on the stability of the frequency of the pilot and the retrodirective-receiver's local-oscillator (LO) signals [59, 60].

A novel technique uses a direct-sequence spread-spectrum (DSSS) multiplexed pilot signal. This is applied to the retrodirective array, and a precise beam-arrival value is obtained from the difference between two channels, after de-spreading the direct-sequence spread-spectrum signal. The big advantages of the direct-sequence spread-spectrum technique is an enhancement of the microwave beam's guidance precision and reliability. This is achieved by significantly reducing the effects of interfering signals, spurious emissions, and the required power level of the rectenna's pilot signal. The direct-sequence spread-spectrum technique enables the use of a single frequency for both the microwave monochromatic power transmission and the carrier of the pilot signals, which share the same antenna-array elements [27, 61]. The beam-guidance complexity can be decreased because the tolerances on construction and power-collection efficiency for the rectenna are relatively insensitive to small variations of the incoming beam angles. Even having the incoming microwave beam at 30° from normal incidence to the solar-power satellite's rectenna will result in less than a 5% reduction in the received power-collection efficiency, which is also relatively insensitive to load and power-level variations [27, 42]. Systematic measurements and calibration of the phased-array elements can improve the beam-direction precision and power-collection efficiency. The new techniques developed for future solar-power-satellite systems can also be applied to enhancing the precision and reliability of the much-simpler proposed HAP microwave wireless-power-transmission systems.

The airship (blimp) HAP is more relevant than a heavier-than-air aircraft for the installation of a microwave wireless-power-transmission system. This is because it is easier to stabilize the airship in a fixed position compared to the aircraft, which has to constantly move in a circle [1, 43]. Nowadays, several companies are involved in the construction of blimps for HAP purposes. These can reach a length, L, of 75 m and a diameter, D, of 22 m [62, 63]. Future models, such as the Lockheed Martin HAP, which was cancelled because of budgetary constraints, or the new Northrop Grumman joint project with Hybrid Air Vehicles Corp., claim $L = 150$ m and $D = 44$ m [64, 65]. Thus, these big cylindrical airships can enable the large surface photovoltaic solar cells and rectenna arrays required to achieve a high microwave-power-transmission efficiency [5, 66]. The control system for stabilizing the airship HAP includes retrodirective beam control, with a precise control unit connected to a differential-GPS (DGPS) unit linked to the terrestrial transmitter. The energy from the terrestrial microwave wireless-power-transmission transmitter, the solar cells, and the storage batteries will activate the electric propulsion motors and propellers to keep the HAP positioned in space [27, 63]. In the case of extreme winds, an additional limited amount of stored fuel in a gasoline tank could save the situation [64].

4.6 RFI and Biological-Hazard Considerations

The radio-frequency interference (RFI) effects and biological-hazard considerations from microwave wireless-power-transmission to HAPs and from solar-power satellites have several similarities, but are significantly reduced for HAPs. The main reasons are the lower power levels involved, kW instead of GW, and the reduced nonlinear effects generating harmonics, spurious and intermodulation products, which increase with power levels [27, 42]. In addition, the microwave-beam length is only around 20 km, instead of 36,000 km. This also requires significantly smaller surfaces of the beam, the phased-array antenna, and the rectenna, and no interaction with the layers of the ionosphere and the Van Allen belts, for the HAPs [1, 27]. The design of the HAPs' microwave wireless-power-transmission systems requires good collaboration with the ITU-R and the radio-astronomy associations, in order not to return to the mistakes of the GLONASS or other wireless systems, which have not sufficiently respected the radio regulations [2, 11]. The design of the terrestrial transmitter requires maximum linearity of the amplifiers and perfect shielding – even at the expense of power-conversion efficiency from dc to microwave – minimum noise levels, and minimum spurious and out-of-band emissions, as stated in Section 4.3. An antenna array using a 10 dB Gaussian taper has to diminish the grating and sidelobes as much as possible. They are potential sources of interference to other radio systems, and reduce the power-collection efficiency. Satisfactory separation distances are required between the microwave-transmitter antenna array and the locations of radio systems to reduce mutual interference, mainly from the high-power wireless-power-transmission systems [39, 67].

Mitigation techniques have to be applied, especially to the HAP's rectennas, in order to avoid harmonics, and passive and active intermodulation products [67, 68]. Frequency-selective surfaces can be installed in front of the rectenna to attenuate the harmonics, without affecting the beam's fundamental frequency. Absorbers could also be positioned around the perimeter of the rectenna, to reduce interference to other radio systems [27, 33].

However, the radio-frequency interference risks are reduced, due to the advantages of the CW microwave wireless power transmission over typical modulated radio systems. Most radio systems that are potential victims to interference from the microwave wireless-power-transmission systems are located in the far-field zone, where the offending power density decreases at least as the square of the separation distances [2, 8] .

The choice of higher frequency bands reduces the probability of radio-frequency interference, as explained in Section 4.1. The lower 2.45 GHz ISM frequency band can interfere with numerous terrestrial and satellite radio systems. For instance, the second harmonic may disturb the protected 4.9-5.0 GHz radio-astronomy band. The 5.8 GHz band is therefore preferred for HAPs, in spite of the bigger atmospheric losses in case of rain, as shown in Figure 11. For dry climates and elevated locations, even the 35 GHz

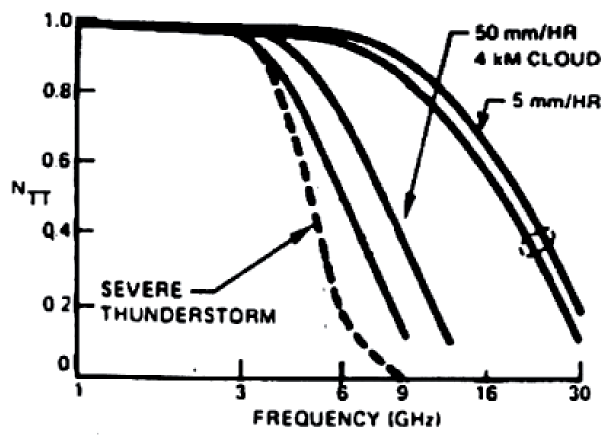

Figure 11. Atmospheric weather losses as a function of frequency [8, 40].

Parameters	Terrestrial Links	Stratospheric HAPs	Geostationary SPS
Technology	*Mature*	*Near maturity*	*Preliminary Design*
MW power needs	*0.01–100 kW*	*200–500 kW*	*0.1–6 GW*
Link length	*0.01–10 km*	*18–21 km*	*36000–39000 km*
Time delay	*0.3–30 μsec*	*60–70 μsec*	*120–130 msec*
Typical frequency bands	*2.45, 5.8 GHz*	*5.8, 35, 94 GHz*	*5.8, 35, 94 GHz*
Space launch issues	*Not required*	*Low cost and easy*	*High cost and complex*
Maintenance conditions	*Easy, on the spot*	*Easy, human access*	*Impossible to say**
PV solar-cell efficiency	*Very Small*	*Small*	*Maximum***
TX + Phased array antenna	*Terrestrial*	*Terrestrial*	*Geostationary orbit*
Rectenna	*Terrestrial*	*Stratospheric altitude*	*Terrestrial*
Temperature	*Variable: –20° to 40°C*	*Constant around –65°C*	*Extremes, Dynamic*
Wind velocity	*Variable*	*Minimal*	*Only Solar Wind Effects*
RFI to other radio systems	*Maximum due to the 2.45 GHz band*	*Minimum due to location and the5.8GHz band*	*Important due to the high power levels*
Environmental conditions	*Atmosphere losses*	*Less atmosphere losses*	*Ionosphere, Van Allen Belt*
Nonlinear interactions	*Minimal*	*Small, low power levels*	*Big, high power levels*
MW beam control	*Ground obstacles*	*Easy, small time delays*	*Difficult, long time delays*
Area required for the TX antenna and rectenna	*Small****	*Moderate****	*Very large****
Benefits to human society	*Moderate*	*Great*	*Very great*

Table 3. Comparisons of microwave wireless-power-transmission systems for terrestrial links, stratospheric HAPs, and solar-power satellites in a geostationary orbit.

* *In the future may be robotics access*

** *Maximum, as the solar cells located on a GEO satellite will collect on average about 10 times as much energy per day than if in a terrestrial location, due to atmospheric conditions and Earth-sun shadow.*

*** *The numerical values of the required areas as functions of power-transmission efficiency and frequency are provided in Table 2.*

and 94 GHz atmospheric radio millimeter-wave bands can be advantageous, due to the significant reductions in the physical dimensions of the antenna and rectenna arrays, as well as in the transmitted microwave-beam cross section. Many fewer radio systems operate at these frequencies, which further reduces the probability of radio-frequency interference. For the case of rain, important percentages of the 35 GHz power beam, and more of the 94 GHz power beam, are attenuated and dispersed, as depicted in Figure 11 [8, 69]. The transmission of power therefore has to be stopped for the limited intervals of rain, using special sensors that switch off or reduce the transmitted power of the transmitter, wherein the HAP will operate only from photovoltaic solar cells and battery energy. Microwave wireless-power-transmission systems can permit significant time intervals of stopping the supply of power to the rectenna, which is not possible for most radio systems [39].

The biological-hazard dangers from the non-ionizing thermal effects of microwave radiation are much reduced compared to the ultraviolet and shorter ionizing wavelengths [2, 70]. However, the power density in the center of the microwave wireless-power-transmission beam from the transmitter to the rectenna is higher than the standardized maximum-permissible exposure (MPE), especially for the millimeter-wave choice. The main maximum-permissible-exposure standards are those of ANSI/IEEE and IRPA/WHO, which have some similarities [71, 72]. The time averaging of exposure is also important, and a factor of safety of five is added, to distinguish between the general public and occupational radiation-exposure conditions for controlled locations [73, 74].

RF radiation absorption that endangers health increases significantly near the resonance frequencies of the human body or head, which were measured from 10 MHz to 300 MHz. Stricter maximum-permissible exposure power-density limits are therefore attributed to this frequency range. The microwave health risks and penetration depths decrease with increasing frequency. The penetration depth is 120 mm at 2.45 GHz, in comparison to only 0.4 mm at 94 GHz. At millimeter-wave frequencies, RF radiation does not reach vital organs, but only the external parts of the human skin [2, 8]. The average maximum-permissible exposure for microwave wireless-power-transmission systems is around 100 W/m^2 [67, 69]. This maximum-permissible exposure is set a factor of 10 to 100 below a threshold of undesirable effects, which can be the causes of concrete damages. However, the extreme HAP microwave wireless-power-transmission power-density magnitudes do not approach the damage values and the 1500 W/m^2 of sunlight power at the ground, even in the center of the microwave beam [39, 42]. The microwave power density increases as a function of frequency, especially for the 35 GHz and 94 GHz wireless-power-transmission systems, as shown in the Appendix. The transmitting antenna's phased array and extended microwave-beam areas, including a buffer zone, therefore have to be controlled and restricted to only authorized and protected maintenance staff . Air traffic should be forbidden in a suitable security zone around the transmitter's beam. In addition, the transmitter has to be switched off and the microwave beam power defocused to significantly reduce it when aircraft, large birds, or other obstacles penetrate the microwave wireless-power-transmission beam's perimeter [11]. This can be achieved by installing an acquisition radar and a monitoring video camera, connected to the transmitter's power-control loop, close to the transmitter site [39].

5. Comparisons of Microwave Wireless-Power-Transmission Systems for Terrestrial Links, Stratospheric HAPs, and Solar-Power Satellites in a Geostationary Orbit

These comparisons are presented in Table 3.

6. Conclusions

Microwave wireless-power-transmission systems for stratospheric HAPs, at an altitude around 20 km, could enable continuous operation for months or even years as radio relays. This airship-sandwich concept, depicted in Figure 1, includes limited photovoltaic solar-cell arrays, batteries, and a rectenna to provide the required energy for the stabilization and payload of the HAP. These HAPs could be a low-cost and useful alternative or complement to geosynchronous and low-Earth-orbit satellites, as presented in the recent special *Radio Science Bulletin* sections on HAPs. However, only a few microwave wireless-power-transmission projects have been realized and successfully tested on terrestrial and low-altitude airborne platforms, for distances of a few kilometers only, not including HAPs. By comparison, a lot of technological effort and investment has been done for the solar-power-satellite issue, as reflected in two special *Radio Science Bulletin* issues and an URSI white paper on solar-power-satellite systems, dedicated to this fascinating subject. A solar-power satellite could provide nonpolluting electrical energy as an alternative to oil, crucial for human society. However, the realization of a geostationary-orbit solar-power satellite is now at the limit of science fiction, very complex, and with a lot of environmental obstacles to overcome. Nevertheless, in 2009, Japan made solar-power satellites a national priority, and indicated that the country may spend US$21B to build an operational solar-power-satellite project over the next 30 years. The US has invested US$80M on solar-power-satellite evaluation since the 1960s, and the European union and some other countries have shown interest in participating in the solar-power-satellite efforts [76, 77].

This paper has presented a short introduction to the definition of HAPs, wireless-power transmission, and solar-power-satellite systems. This was followed by a discussion of the concept of the different categories of wireless-power-transmission systems, and a review of the genesis of and developments in microwave wireless-power-transmission systems. However, the main subject of this paper was microwave wireless-power-transmission systems for feeding stratospheric HAP airships. In a thorough description of future projects for microwave wireless-power transmission from terrestrial bases to HAPs, we utilized several research and development results obtained in the evaluation steps of the solar-power-satellite projects, especially by Japanese and USA scientists and engineers. The results have shown that the cost, technology efforts, environmental radio-frequency interference, and biological threats are significantly less for HAPs. The solar-power-satellite evaluation results are thus very useful for the future design and realization of microwave wireless-power-transmission systems for feeding HAPs, which are much easier to realize.

Comparisons of microwave wireless-power-transmission systems for terrestrial links, for stratospheric HAPs, and for solar-power satellites in a geostationary orbit were provided. A simple method for computing the areas of the microwave wireless-power-transmission transmitting antenna arrays, microwave beams, and rectennas as functions of the required power-transmission efficiency, separation distances, and frequency bands have been given in an Appendix. The results showed that the required areas and weight are significantly less for HAPs than for solar-power satellites. However, the design and realization of microwave wireless-power-transmission systems for HAPs could also be very useful for the realization and preliminary tests of solar-power-satellite systems. The first step could be the realization of a 200 kW, 5.8 GHz wireless-power-transmission system for HAPs, as used in this paper, located in latitudes where wind velocities are minimal. New wireless-power-transmission systems at 35 GHz and 94 GHz for dry regions, and at 2.45 GHz for humid regions, could later be realized. It would also be possible to increase the microwave wireless-power-transmission power level to several hundreds of kW, in order to operate in windy latitudes without requiring fuel tanks for precise stabilization of the HAPs and microwave beams.

7. Acknowledgment

Many thanks to Dr. Thomas Trigano from SCE, and to my beloved daughter, Dr. Michal Yackobovitch- Gavan, who have given me a lot of dedicated assistance and help in the preparation of the text and the figures.

8. Appendix

Analysis of the Microwave Wireless-Power-Transmission System Efficiency

8.1 Approximate Computation of the Required Transmitting (TX) Antenna's Aperture, D_T

This section presents an approximate computation of the required transmitter antenna aperture, D_T, as a function of the frequency, *f*, and the distance, d_R, from the limit of the Rayleigh region. D_T is the largest dimension of the transmitting antenna's aperture, or the diameter of the antenna, in the case of a parabolic dish antenna. Non-dispersion of the microwave wireless-power-transmission beam occurs in the near field, until the Rayleigh-region limit, d_R, from the center of the transmitting antenna's aperture, as explained in Section 2 and Figure 2.

$$d_R = D_T^2 / 2\lambda , \quad (1)$$

where λ is the transmission wavelength, $\lambda = v/f$, where v is the propagation velocity in the atmosphere: $v \approx c = 3\times10^8$ m/sec. Thus,

$$d_R \approx D_T^2 \frac{10 f_{[\mathrm{GHz}]}}{6} , \quad (2)$$

or

$$D_{T[\mathrm{m}]} \approx \left[\frac{0.6 d_{[\mathrm{m}]}}{f_{[\mathrm{GHz}]}} \right]^{1/2} . \quad (3)$$

The most-appropriate frequency bands for power transmission are the ISM bands around 2.45 GHz, 5.8 GHz, and 24.5 GHz, in addition to the millimeter-wavelength atmospheric-window frequencies around 35 GHz and 94 GHz for very dry climates or space conditions, as shown in Section 4.1. At typical rectenna HAPs distances of d = 20 km from the transmitting antenna's aperture, the required D_R for maximum power-transmission efficiency without dispersion as a function of frequency is presented in Table 1. Therefore,

$$D_{T[\mathrm{m}]} = \left[\frac{12000}{f_{[\mathrm{GHz}]}} \right]^{1/2} . \quad (4)$$

In these cases, the rectenna's diameter, D_r, or its area,

$$A_r = \frac{\pi D_r^2}{4} , \quad (5)$$

have to at least be equal to the dimensions of the transmitting antenna's array aperture, $A_r \geq A_T$, due to the microwave-beam dispersion. The beam power density is

$$S_T = \frac{P_T}{A_T} \ [\mathrm{W/m^2}], \quad (6)$$

where $P_T = 200$ kW is the first choice.

The conventional 10 dB Gaussian taper on the transmitting antenna's array aperture will significantly reduce the power density at the edge of the perimeter of the microwave beam. This will enhance the power-transmission efficiency of the beam, which approaches 100% for this approximate computation.

8.2 Computation of the Microwave Wireless-Power-Transmission Beam Power-Transmission Efficiency

This section computes the microwave wireless-power-transmission beam power-transmission efficiency when the HAP's position is at the limit of the far field (FF) of the Fraunhofer zone. In the Fraunhofer zone, the distance, d_{FF} to the rectenna exceeds $2D_T^2/\lambda$. In the far-field zone, the transmitter antenna's aperture is observed as a single spot, concentrated at the center of the transmitting antenna array, due to the high separation distance, $d > d_{FF}$. The classical line-of-sight Friss equation can therefore be applied for computing the main-bean power-transmission efficiency, η_T. From the Friss equation,

$$P_R = P_T G_T \left(\frac{\lambda}{4\pi d} \right)^2 G_R . \quad (7)$$

Therefore,

$$\eta_T = \frac{P_R}{P_T} = \frac{4\pi A_T \eta_t}{\lambda^2} \frac{4\pi A_R \eta_r}{\lambda^2} \left(\frac{\lambda}{4\pi d} \right)^2 , \quad (8)$$

where η_t and η_r are respectively the efficiency of the transmitting and the rectenna antennas. A_T and A_R are respectively the areas of the transmitting and the rectenna antennas.

For instance, the antenna gain of the transmitting antenna (G_T) is

$$G_T = \frac{4\pi A_T \eta_t}{\lambda^2} . \quad (9)$$

Therefore, if we choose $\eta_t \approx \eta_r \approx 0.7$, $d = 20,000$ m, and $f = 5.8$ GHz, we obtain

$$\eta_T = \frac{A_T A_R \eta_t \eta_r f^2}{c^2 d^2} , \quad (10)$$

or

$$\eta_T = 0.46\times10^{-6} A_T A_R . \quad (11)$$

If the required $\eta_T = 0.6$ and we choose $A_R = 2A_T$ because of dispersion effects, we obtain $A_T = 805\ \mathrm{m}^2$ and $A_R = 1610\ \mathrm{m}^2$, which are realistic values for big HAP

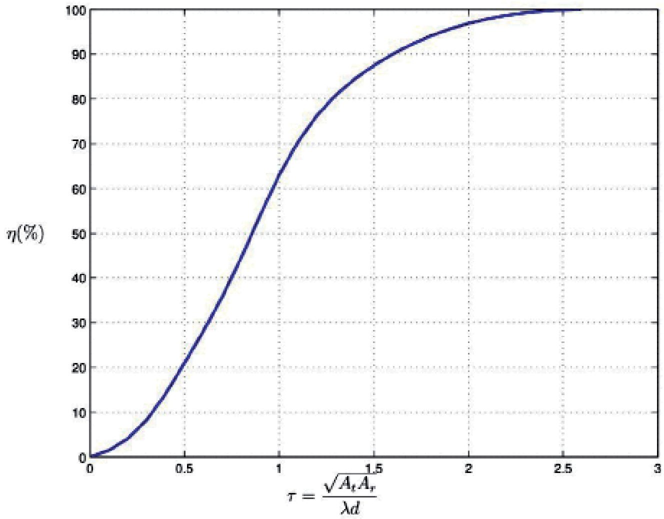

Figure 12. The transmission efficiency as a function of the parameter τ for optimum power-density distribution across the transmitting antenna's aperture [16, 42].

aircraft (blimps). Even if we require a high $\eta_T = 0.95$, we obtain $A_T = 1013\ \mathrm{m}^2$ and $A_R = 2025\ \mathrm{m}^2$, which are still feasible for the case of big blimps. For a transmitter with a circular-aperture antenna, for $\eta_T = 0.6$ we obtain $D_T = \left(\frac{4A_T}{\pi}\right)^{1/2} = 32\ \mathrm{m}$, and $\eta_T = 0.95$ we obtain $D_T = 36\ \mathrm{m}$. Such diameters are used for large satellite-communication antennas.

8.3 More Precise Expressions

This section presents more precise expressions for computing η_T, A_T, and A_R as functions of *d* and *f*.

From the theoretical development of Goubau [16], Brown [42] developed optimized relationships among the data for microwave wireless-power-transmission systems using a power-efficiency transmission parameter, τ:

$$\tau = \frac{\left(A_T A_R\right)^{1/2}}{\lambda d}. \qquad (12)$$

An experimental graph (depicted in Figure 12) shows τ as a function of η_T in percentage values. Consider, for instance, the J. Mankins' project described in Section 3 for Hawaii terrestrial microwave wireless-power transmission. It is easy to compute the transmitter array antenna's area and the rectenna area required to obtain a 60% power-transmission efficiency for a separation distance of 148 km and an ISM frequency of $f = 2.45$ GHz. Using Figure 12, we obtain $\tau = 1$ for $\eta_T = 0.6$. Therefore, if we choose $A_R = 2A_T$, from Equation (12) we obtain $A_R = 25,300\ \mathrm{m}^2$, and $A_T = 12,650\ \mathrm{m}^2$. For the case of a transmitting circular-aperture antenna, this gives $D_T = 127$ m, which is a colossal task to achieve.

It is much easier and less costly to design and realize microwave wireless-power-transmission systems for a HAP at a distance of 20 km for the ISM frequency of 5.8 GHz. The relatively modest required transmitter antennas and rectennas areas are presented in Table 2.

9. References

1. J. Gavan, S. Tapuchi and D. Grace, "Concepts and Main Applications of High-Altitude-Platforms Radio Relays," *The Radio Science Bulletin*, **No. 330**, September 2009, pp. 20-31.

2. J. Gavan and R. Perez (eds.), *Handbook of Electromagnetic Compatibility*, New York, Academic Press, 1995, Chapters 19, 20.

3. R. Stuzak, "Mobile Telecommunications Via Stratosphere," Intercomms. International Communication Project, 2003.

4. T. C. Tozer and D. Grace, "High Altitude Platforms for Wireless Communication," *Electronics & Communication Engineering Journal*, June 2001, pp. 127-137.

5. J. Gavan and M. Haridim, "Stratospheric Quasi-Stationary Platforms (SQSP): Can they Replace Communication Satellite Systems?," *Telecommunications and Space Journal*, April 1997, pp. 275-288.

6. J. Gavan, "Radio Relay Systems Using Stratospheric Quasi-Stationary Platforms. Are they Competitive to Satellite Systems?," Proceedings of the 19th Convention of IEEE in Israel, June 1996, pp. 283-286.

7. N. Tesla, *Experiments with Alternating Currents of High potential and high Frequency*, New York, McGraw Hill, 1905.

8. M. Shigehara (ed.), *Space Solar Power Program*, International Space University, 1992.

9. P. F. Glaser, "Power from the Sun: Its Future," *Science*, **162**, 1968, pp. 857-861.

10. D. Budimir and A. Marincic, "Research Activities and Future trends of Microwave Wireless Power Transmission," 6th International Symposium Tesla, Belgrade, October 2006, pp. 1-5.

11. URSI Working Group on SPS, "URSI White Paper on Solar Power Satellite (SPS) Systems," *Radio Science Bulletin*, **No. 321**, June 2007, pp. 13-27.

12. S. Sasaki et al., "Conceptual Study of SSPS Demonstration Experiment," *Radio Science Bulletin*, **No. 310**, September 2004, pp. 9-14.

13. M. B. Steer et al., "Architecture and Prototyping Laboratory for the development of Space-based Microwave Power Transmission Systems," *Radio Science Bulletin*, **No. 311**, December 2004, pp. 9-15.

14. D. Schneider, "A Critical Look at Wireless Power," *IEEE Spectrum*, May 2010, pp. 3-8.

15. A. Karalis, J. A. Joannopoulis and M. Solijacic, "Efficient Wireless Non Radiative Mid-Range Energy Transfer," *Annals of Physics*, January 2008, pp. 34-48.

16. G. Goubau and F. Schwering, "On the Guided Propagation of Electromagnetic Wave Beams," *IRE Transactions on Antennas and Propagation*, **AP-9**, May 1961, pp. 248-256.

17. W. C. Brown, "The History of Power Transmission by Radio Waves," *IEEE Transactions on Microwave Theory and Techniques*, **MTT-32**, September 1984, pp. 1230-1242.

18. R. M. Dickinson, "Microwave Transmission System for Space Power," *Raumfahrforschung Heft 5*, September 1976, pp. 236-242.

19. J. Schlesak, J. A. Alden and T. Ohno, "A Microwave Powered High Altitude Platform," IEEE MTT-S International Symposium Digest, 1988, pp. 283-286.

20. http://friendsofcrc ca/SHARP/sharp.

21. W. C. Brown, "Experiments Involving a Microwave Beam to Power and Position a Helicopter," *IEEE Transactions on Aerospace Electronic Systems*, **AES-5**, 1969, pp. 692-702.

22. E. M. Onda, "A Ground to Airship Microwave Power Transmission Experiment for Stationary Aerial Platform," AIAA Conference, Florida, May 1995, pp. 15-18.

23. W. C. Brown "All Electronic Propulsion – Key to Future Spaceship Design," AIAA Paper 24th Joint Propulsion Conference, Boston, July 1988, pp. 1-11.

24. P. E. Glaser, "An Overview of the Power Satellite Option," *IEEE Transactions on Microwave Theory and Techniques*, June 1992, pp. 1230-1238.

25. J. O. McSpadden, A. M. Brown, K. Chang and N. Kaya," Microwave Energy Transmission in Space, ISY-METS Rocket Experiment," *IEEE Aerospace and Electronic Systems Magazine*, November 1994, pp. 36-40.

26. Z. Popovic et al., "Lunar Wireless Power Transfer Feasibility Study," March 2008.

27. N. Shinohara, "Wireless Power Transmission for Solar Power Satellites," Supporting Documents for the URSI White Paper on SPS, 2007, pp. 1-43.

28. H. Matsumoto, "Research on Solar Power Station and Microwave Power Transmission in Japan: Review and Perspectives," *IEEE Microwave Magazine*, December 2002, pp. 36-45.

29. A. Celeste, J-D. L. S. Luk, J. P. Chabriat, and G. Pignolet, "The Grand-Bassin Case Study: Technical Aspects," Proceedings of SPS' 97, 1997, pp. 255-258.

30. A. Celeste, A. P. Jeanty, and G Pignolet, "Case Study in Reunion island," *Acta Astronautica*, **54**, 2004, pp. 253-258.

31. L Summerer, "Solar Power Satellites – European Approach," ESA-ESTEC Advanced Concepts Team, Preliminary Study, 2002.

32. W Seboldt and M Klimke, "European Sail Tower SPS Concept," *Acta Astronautica*, **48**, 2001, pp. 785-792.

33. J. O. McSpadden and J. C. Mankins, "Space Solar Power Programs and Microwave Wireless Power Transmission Technology," *IEEE Microwave Magazine*, December 2002, pp. 44-57.

34. N. Kaya, M. Iwashita and J. C. Mankins, "Hawaii Project for Microwave Power Transmission," 54th International Astronautic Congress, Bremen, Germany IAC-03-R3, 2005.

35. A. K. Reed and H. J. Willenberg, "Early Commercial Demonstration of Space Solar Power Using Ultra-Lightweight Arrays," IAC-07-C3, February 2004.

36. A. K. Reed and H. J. Willenberg, "Hyperblimp for Solar Power Transmission," 58th IAC Conference, Hyderabad, India, September 2007.

37. N. Wyrsch, D. Dominé, F. Freitas, L. Feitknectht, J. Bailat, C. Ballif, G. Poe, K. Bates, and K. Reed, " Ultra-Light Amorphous Silicon Cell for Space Applications," 4th World Conference on Photovoltaic Energy Conversion, Waikoloa, HI, May 2006.

38. A. Boyle, "PG&E Makes Deal for Space Solar Power Utility to Buy Orbit Generated Electricity from Solaren in 2016," *Technology & Science/Space*, April 2009.

39. C. Malcolm and H. W. Friedman, *System Using a Megawatt Class Millimeter Wave Source and a High-Power Rectenna to Beam Power to a Suspended Platform*, US Patent 6919847, July 2005.

40. R. K. Crane, "Fundamental Limitations Caused by Propagation," *Proceedings of the IEEE*, **69**, 2, February 1981, pp. 196-208.

41. P. Koert and J. T. Cha, "Millimeter Wave Technology for Space Power Beaming," *IEEE Transactions on Microwave Theory and Techniques*, June 1992, pp. 1251-1258.

42. W. C. Brown and E. E. Eves, "Beamed Microwave Power Transmission and its Application to Space," *IEEE Transactions On Microwave Theory and Techniques*, June 1992, pp. 1239-1250.

43. A. Colozza and J. L. Dolce, "High Altitude, Long Endurance Airships for Coastal Surveillance" NASA/TM, February 2005, 2005-213427.

44. N. Shinohara, H. Matsumoto and K. Hashimoto, "Phase Controlled Magnetron Development for SPORTS Space Power Radio Transmission System," *Radio Science Bulletin*, **No. 310**, September 2004, pp. 29-35.

45. L. J. Dressman, D. B. McDermolt, and N. C Luhmann, "Design and Test of a 34 GHz Peniotron," 7th Workshop on High Energy Density and High Power RF, 2006, pp. 252-256.

46. Alden, et al., *Mobile and Tactical Applications of a 35 GHz Rectenna*, US Patent 6919847, 2003.

47. K. M. K. H. Leong et al., "Active Antenna Approach for Power Transmission," *Radio Science Bulletin*, **No. 311**, December 2004, pp. 21-30.

48. Koert et al., *A Power Beaming System*, US Patent 5068669, November 1991.

49. Foote, *Microwave Powered Aircraft*, US Patent 5503350, April 1996.

50. McSpadden, *Rectenna Cover for a Wireless Power Receptor*, Patent 20100026603, August 2008.

51. A. Douyere, J. A. Lan Sun Luk and F. Alicalope, "High Efficiency Microwave Rectenna Circuit: Modeling and Design," *Electronics Letters*, **44**, November 2008, pp. 1409-1410.

52. J. McSpadden, L. Fan and K. Chang, "Design and Experiments of a High Conversion Efficiency 5.8 GHz Rectenna," *IEEE Transactions on Microwave Theory and Techniques*, December 1998, pp. 2053-2060.

53. L. Miura, N. Shinohara and H. Matsumoto, "Experimental Study of Rectenna Connection for Microwave Power Transmission," *Electronics and Communications in Japan*, **84**, 2001, pp. 27-36.

54. F. Geyer, D. Caswell and C. Signorini, "Powering the Future," *ESA Bulletin*, **131**, August 2007, pp. 46-49.

55. http://www.prospace.com; http:// www.nanotube.com.

56. http://www.spectrolab.com; http:// www.fullspectrum.eu.org; http://www.iis.fraunhofer.de/ EN.

57. R. Y. Miyamoto, Y. Qian, and T. Itoh, "An Active Integrated Retro-Directive Transponder for Remote Information Retrieval-on-Demand," *IEEE Transactions on Microwave Theory and Techniques*, **49**, September 2001, pp. 1658-1662.

58. K. M. K. H. Leong, Y. Wang, and T. Itoh, "A Full Duplex Capable Retro-Directive Array System for High-Speed Beam Tracking and Pointing Applications," *IEEE Transactions on Microwave Theory and Techniques*, **52**, 5, May 2004, pp. 1479-1489.

59. R. Miyamoto and T. Itoh, "Retrodirective Arrays for Wireless Communications," *IEEE Microwave Magazine*, March 2002, pp. 71-79.

60. F. E. Little et al., "Development of a Retro-Directive Control Transmitter for Wireless Power Transmission," *Radio Science Bulletin*, **No. 311**, December 2004, pp. 38-45.

61. K. Hashimoto, K. Tsutsumi, H. Matsumoto and N. Shinohara, "Space Solar Power System Beam Control with Spread Spectrum Pilot Signals," *Radio Science Bulletin*, **No. 311**, December 2004, pp. 31-37.

62.http://www.sanswire-tao.com; http://www.rosaerosystemsstratospheric.pbo.ru; http://www.spacedata.net.

63. E. Herlik, "Persistent UAS in the Stratosphere will Revolutionize Commercial and Defense Markets," *Homeland Security Research Corp*, 2008, pp. 1-217.

64. A. Colozza, "High Altitude Long Endurance Airship," *NASA 2003*, pp. 105.

65. http://www.lockheedmartin.com; http://www.hybridairvehicles.com.

66. L. Jamison, G. S. Sommer and I. R. Porche, "High Altitude Airships for the Future Force Army" Technical Report, RAND Arroyo center, 2005, pp. 9.

67. ITU-R, "Applications and Characteristics of Wireless Power Transmission" Question 210/1, September 2000.

68. J. Gavan, "Collocated Passive and Active Intermodulation Effects," Proceedings of the ESA Workshop on Passive Intermodulation, Estec, Nl, September 2000, pp. 91-103.

69. MIL-STD-461C, Parts 2, 3.

70. J. M. Osepchuk, "Microwave Power Applications," *IEEE Transactions on Microwave Technology Theory*, **50**, 3, March 2002, pp. 975-985.

71. J. C. Lin, "The New IEEE Standard for Human Exposure to Radio frequency Radiation and the Current ICNIRP Guide Lines," *Radio Science Bulletin*, **No. 317**, 2006, pp. 61-63.

72. ANSI\IEEE, *Standard for Safety Levels with Respect to Human Exposure Radio Frequency Electromagnetic Fields 3 kHz to 300 GHz*, New York, IEEE, 1999.

73. http://www.grouper.ieee.org/groups/scc28; http://www.homepage.seas.upenn.edu/kfoster/comar.

74 J. Gavan, "Comments on URSI White Paper on SPS Systems," *Radio Science Bulletin*, **No. 323**, December 2007, p 4.

75. J. C. Lin, "Wireless Transmission of Space Solar Power and its Biological Implications," *Radio Science Bulletin*, **No. 301**, June 2002, pp. 31-34.

76. S. Sato and Y. Okada, "Mitsubishi, IHI to Join $21B in Space Solar Project," August 31, 2009, http://www.Bloomberg.com.

77. http://www.bloomberg.com/apps/news.

SAVNET: A Ground-Based Facility for Studying Ionospheric, Atmospheric, and Natural Phenomena

F.C.P. Bertoni
J.-P. Raulin
H. Rivero Gavilan
W. Guevara Day
R. Rodrigues
G. Fernandez

Abstract

We present recent results obtained by the observatory stations from the South America VLF NETwork (SAVNET), an international project coordinated by Brazil in cooperation with Peru and Argentina. In this paper, we first give an overview of the research activities being undertaken using the SAVNET array. We then describe in more detail specific observations of phase and amplitude changes during solar flares. We present a new lower limit for the ionospheric sensitivity using the VLF phase-detection technique. We finally discuss recent and genuine observations of magnetar X-ray and γ-ray bursts detected by SAVNET on January 22, 2009.

1. Introduction

The very-low-frequency (VLF) wave-tracking technique has been demonstrated to be a powerful tool for several scientific applications in ionospheric research. Due to its relative simplicity from both the conceptual and instrumental standpoints, it has been recognized as an important source of data and information during the last decades.

The natural waveguide cavity formed by the Earth and the ionosphere – the Earth-ionosphere waveguide (EIW) – permits the propagation of electromagnetic VLF signals emitted by powerful transmitters located around the globe (USA, Australia, Germany, and Japan, among other countries). These waves propagate within the Earth-ionosphere waveguide and travel over long distances of thousands of kilometers, without significant attenuation. Their amplitudes and phases are measured and recorded at the receiver stations.

The Earth-ionosphere waveguide's upper boundary is the lowermost portion of the ionosphere, the D region, at approximately 70 km altitude during daytime. It is a weakly ionized and cold plasma, produced mainly by the solar Lyman-α spectral line photo-ionization processes [1]. The D region has a very complex chemistry [2], which will not be discussed here. However, its dynamics behave in a simple periodic way through which it is formed at sunrise and vanishes at sunset.

In this paper, we present the South America VLF NETwork (SAVNET), its functionalities, first results, and future plans.

2. Overview of Results Obtained with SAVNET

We now summarize the current scientific activities performed using the SAVNET instrumental facilities, an international project coordinated by Brazil in cooperation with Peru and Argentina [3, 4]. VLF data are used to investigate solar quiescent and transient phenomena, i.e., the monitoring of long-term solar activity, and faster phenomena related to flares [5]. Impulsive energy releases from magnetars are also under investigation and characterization. SAVNET is well suited to study low-ionosphere (C- and D-region) phenomena, such as the use

F. C. P. Bertoni, J.-P. Raulin, and H. Rivero Gavilan are with Centro de Radio Astronomia e Astrofísica Mackenzie (CRAAM), Universidade Presbiteriana Mackenzie, Av. da Consolação, 896, Ed. Prof. Modesto Carvalhosa, 6º andar, s. 603, São Paulo, SP, CEP 01302-907, Brazil; Tel: +55 11 2114-8734, Fax: +55 11 3214-2300; E-mail: fbertoni@craam.mackenzie.br. W. Guevara Day is with Comisión Nacional de Investigación y Desarrollo Espacial (CONIDA), Luis Felipe Villaran, 1069, San Isidro Lima, Lima, Perú; Tel: +51 1 4429973, Fax: +51 1 4429973; E-mail: walter@conida.gob.pe. R. Rodrigues is with Universidad de Piura (UDEP), Av. Ramón Mugica 131, Urb. San Eduardo, Piura, Perú; Tel: +51 (073) 28 4500, Fax: +51 (073) 28 4510. G. Fernandez is with Complejo Astronómico El Leoncito (CASLEO), Av. España 1512 sur - Casilla de correo 467, J5402DSP, San Juan, Argentina, Tel: +54-264-4213653/+54-264-4273653; E-mail: gfernandez@casleo.gov.ar.

Prefix	Latitude	Longitude	Location
ATI	23°11'S	46°36'W	Atibaia, Brazil
SMS	29°43'S	53°43'W	Santa Maria, Brazil
EACF	62°05'S	58°24'W	Estação Antártica Comandante Ferraz
PAL	10°10'S	49°20'W	Palmas, Brazil
PIU	05°12'S	80°38'W	Piura, Peru
PLO	12°30'S	76°48'W	Punta Lobos, Peru
ICA	14°01'S	75°44'W	Ica, Peru
CAS	31°32'S	68°31'W	CASLEO, Argentina

Table 1. The locations of the SAVNET stations.

of C-region characteristics as a solar-activity proxy [6], or the determination of recombination coefficients in the D region. Atmospheric-temperature-variability measurements by spacecraft have shown good correspondence with the presence of the "winter anomaly," as revealed by the SAVNET data [6]. Due to the localization of several SAVNET receiver bases nearby seismically active regions, a systematic search for possible seismo-electromagnetic effects is under way. Finally, modeling using the *Long Wave Propagation Capability* (*LWPC*) code and the Finite-Domain Time-Difference (FDTD) method is being performed, in order to simulate sub-ionospheric propagation anomalies caused by solar/geomagnetic phenomena or by natural sources.

In the next section, we describe the SAVNET instrumental facilities. In the remaining Sections 4 and 5, we will describe in more detail two of the above-mentioned subjects: the detection of solar flares by SAVNET, and the low-ionospheric effects during the magnetar event of January 22, 2009.

3. Instrumental Setup

Currently, SAVNET has eight receiver stations operating at the geographic coordinates presented in Table 1. The VLF signals come from radio transmitters that have been used for marine and submarine communication/navigation. Some of them were formerly known as the Omega system network for radio navigation, which was shut down in 1997. The transmitters with signals that are currently received by SAVNET stations are listed in Table 2, along with the respective geographical coordinates, operating frequencies, and transmitted powers.

Figure 1 shows a map indicating some VLF propagation paths between SAVNET stations (diamond symbols) and MSK-modulated transmitters (triangle symbols). We note that SAVNET VLF paths, which are part of the great-circle paths (GCP), offer a large range of path lengths between 3 and 13 Mm, as well as many orientations between paths oriented north-south and east-west.

Each SAVNET station is composed of three antennas (one electric dipole and two square loops), pre-amplifiers, an audio analog-to-digital converter card, a GPS clock, a power supply, and a microcomputer for data processing and storage. Currently, SAVNET uses the Software Phase and Amplitude Logger (SoftPal) (see, e.g., [7]) to measure and perform spectrum analysis of the received signals. Due to the audio card's crystal-clock signal, locked to the GPS internal clock (1 PPS), the resulting signal phase presents a precision of approximately 0.05 to 0.07 μs. Depending on the frequency of the incoming VLF wave, this corresponds to less than about 1°. SAVNET therefore has the capability of providing high-stability long-term phase measurements, without any drift.

4. SAVNET Measurements: Uses for Solar-Activity Prognostics

Lyman-α radiation is responsible for the formation of the quiescent D region, and for maintaining it during daytime [1]. However, during solar flares, soft X-ray enhancements overcome the ionization produced by the Lyman-α emission. At this time, the electrical conductivity of the Earth-ionosphere waveguide's upper boundary is changed. This results in the well-known sudden phase anomalies (SPAs), detected in the VLF signals.

Prefix	Frequency (kHz)	Latitude	Longitude	Power (kW)	Location
NDK	25.2	46°22'N	98°20'W	10	La Moure, ND, EUA
NAA	24.0	44°38'N	67°17'W	1000	Cutler, MA, EUA
NLK	24.8	48°12'N	121°55'W	130	Jim Creek, WA, EUA
NPM	21.4	21°25'N	158°09'W	630	Lualualei, HI, EUA
NAU	40.7	18°36'N	67°11'W	100	Aguada, Porto Rico
NWC	19.8	–21°48'S	114°09'E	1000	H. E. Holt, Australia

Table 2. The locations of the transmitter stations used by SAVNET.

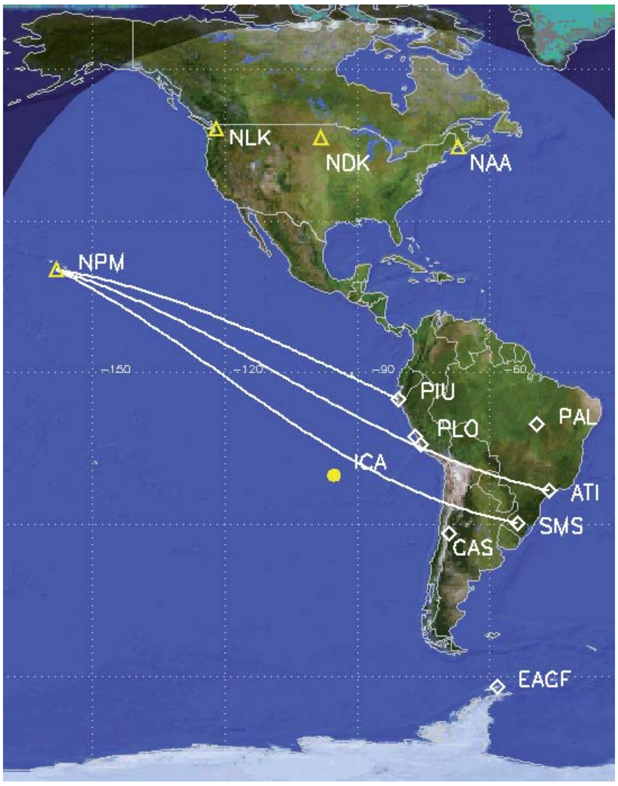

Figure 1. SAVNET stations (diamonds) and some of the transmitters used in our studies (triangles), along with some VLF propagation paths.

References [15, 16] have studied the dependency of the ionospheric response to solar flares as a function of the solar-activity level. They found that the low ionosphere is more sensitive to small solar flares for periods of reduced solar activity. At the same time, the detection of larger flares was found to be independent of the solar-activity level. The authors concluded that this was an indication of the low-ionospheric sensitivity dependence on the solar activity.

Recently, using SAVNET data, we have confirmed and quantified this relationship. We found for the time period of very low solar activity between 2007 and 2009 that the minimum soft X-ray flux (P_{min}) needed to produce an ionospheric perturbation was about 2.7×10^{-7} W/m^2 [5]. This corresponds to a very small solar flare, classified as a GOES B-Class event. An example of such a sudden-phase-anomaly event is represented with a one-minute time integration in Figure 2, along with the simultaneously observed soft X-ray flux. This small sudden phase anomaly event therefore represents a new lower limit for the ionospheric sensitivity using the VLF phase-detection technique.

We combined this finding with similar P_{min} values inferred from earlier work [5, 8-14] as a function of the solar-activity level, represented by the solar Lyman-α photon flux. The resulting relationship is illustrated in Figure 3, which indicates a clear trend between increasing P_{min} and solar Lyman-α photon flux. The interpretation of Figure 3 is straightforward: the minimum energy deposit in the low ionosphere needed to produce a detectable change in its electrical conductivity is higher when the solar Lyman-α flux is higher.

This result is therefore in agreement with the earlier findings of [15, 16]. In addition, it reinforces the idea that the solar Lyman-α radiation is at the origin of the quiescent ionospheric D region. Finally, we mention that such a

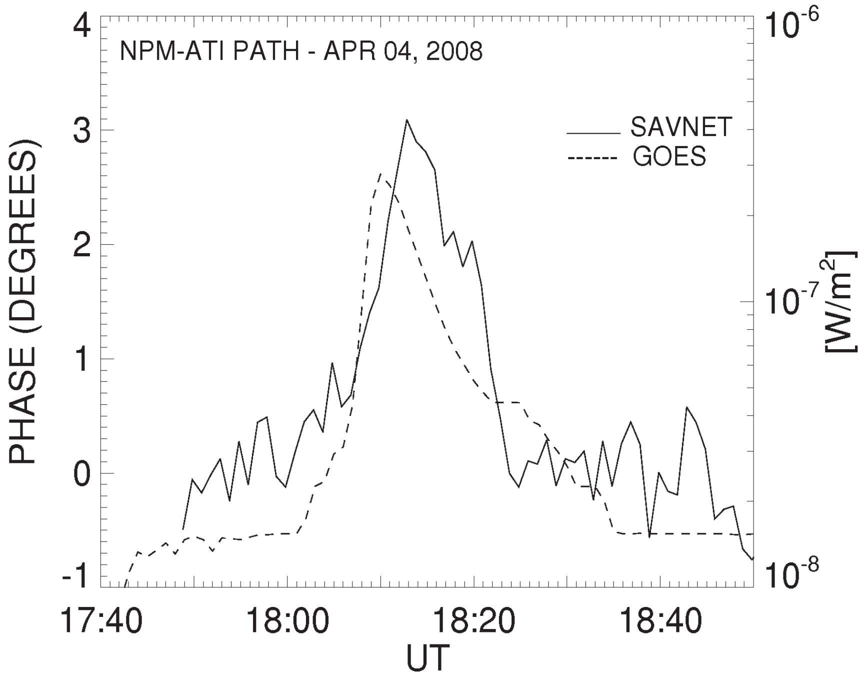

Figure 2. A sudden phase anomaly detected in the SAVNET propagation path NPM-PLO, along with the solar X-ray flux measured by a GOES satellite sensor: a small GOES class B solar X-ray flare.

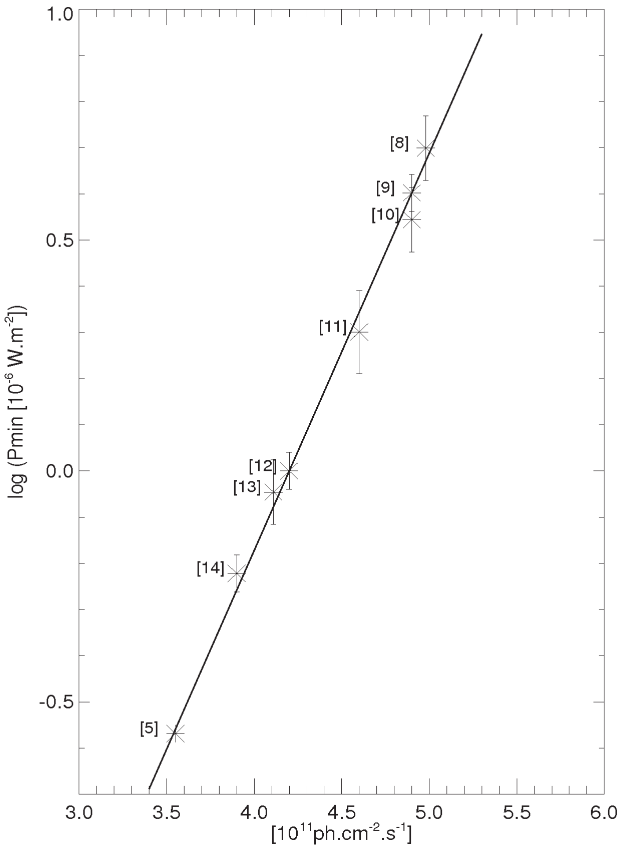

Figure 3. The soft X-ray peak flux P_{min} values inferred from earlier work as a function of the solar-activity level, represented by the solar Lyman- α photon flux. The minimum energy deposite d in the low ionosphere needed to produce a detectable change in its electrical conductivity is higher when the solar Lyman-α flux is higher (adapted from [5]).

result suggests the possibility of indirectly monitoring the solar Lyman-α radiation through its signature in the low ionosphere.

5. SAVNET Detection of Magnetars

Magnetars constitute a peculiar class of neutron stars that have extremely intense magnetic fields, approximately 10 to 100 billion times stronger than the Sun's magnetic field. Magnetars can suddenly release huge amounts of energy, up to ten orders of magnitude higher than that observed during large solar events. At these times, energetic particles are accelerated, and copious amount of X and γ-rays are emitted. This radiation travels through the intergalactic medium, and may reach the atmosphere of the Earth. How these stars, with a reduced size, store such an amount of energy, and what are the mechanisms resulting in the sudden release of this energy, are still unsolved questions.

On January 22, 2009, the object AXP 1E1547-5408 presented a hundred sudden releases of energy observed by the INTEGRAL satellite sensor [17, 18]. The effect of the ionization excess caused by the incoming photons was detected by some of the SAVNET propagation paths located in the dark portion of the globe [19, 20]. Other VLF propagation paths around the world were in the Earth's sunlit region, and did not detect the energetic event, most likely because the ionization excess was not enough to produce a significant change of the low ionosphere's electrical conductivity.

Two among the hundreds of bursts emitted by the AXP 1E1547-5408 magnetar are displayed in Figure 4. Solar-illumination conditions are shown, along with signal-amplitude variations detected on three VLF propagation paths, and compared with the INTEGRAL satellite count rates for the bursts at 06:48 UT (top) and at 08:16 UT (bottom). The different solar illumination for the first burst explains why it was not detected by propagation paths ending at PIU, the more-western station, contrary to what occurred during the 08:16 UT burst.

We did notice very good correspondence between these time profiles, even for the finest and faintest time structures as illustrated by the dashed lines. This certainly indicates the high sensitivity of the low-ionosphere plasma to the sudden precipitation of energetic photons from the remote source.

Amplitude variations, caused by changes in the electrical conductivity at ~90 km altitude, showed increasing attenuation during the magnetar burst, in contrast to the generally observed reduced attenuation at the same frequency during solar flares. This may be attributed to the nighttime portion of the Earth-ionosphere waveguide, where several propagation modes are present at a given time. Therefore, further multimode propagation simulations need to be fully compared with the VLF amplitude data. Such observations will allow studying the low-energy emission spectrum for this magnetar, thus providing information on the object's physical conditions.

Another interesting aspect of VLF detection of magnetar outbursts is to get the true low-energy photon spectrum, that is, the energy distribution of the photons that do actually precipitate in the low ionosphere. Sometimes, this is not possible from satellite data, because of a sensor's saturation, or absorption by the shielding material onboard in the direction of the bursting source. For magnetar burst studies, the VLF-tracking-technique diagnostic is then an important complement to satellite measurements.

6. Conclusions

In this work, we have presented the South America VLF NETwork (SAVNET). This is an instrumental facility the main objectives of which are the monitoring of the solar activity on different time scales, and the study of the south-Atlantic magnetic anomaly (SAMA). Due to the VLF technique's versatility itself, and the good spatial coverage of the network, other questions may be addressed, which we have summarized.

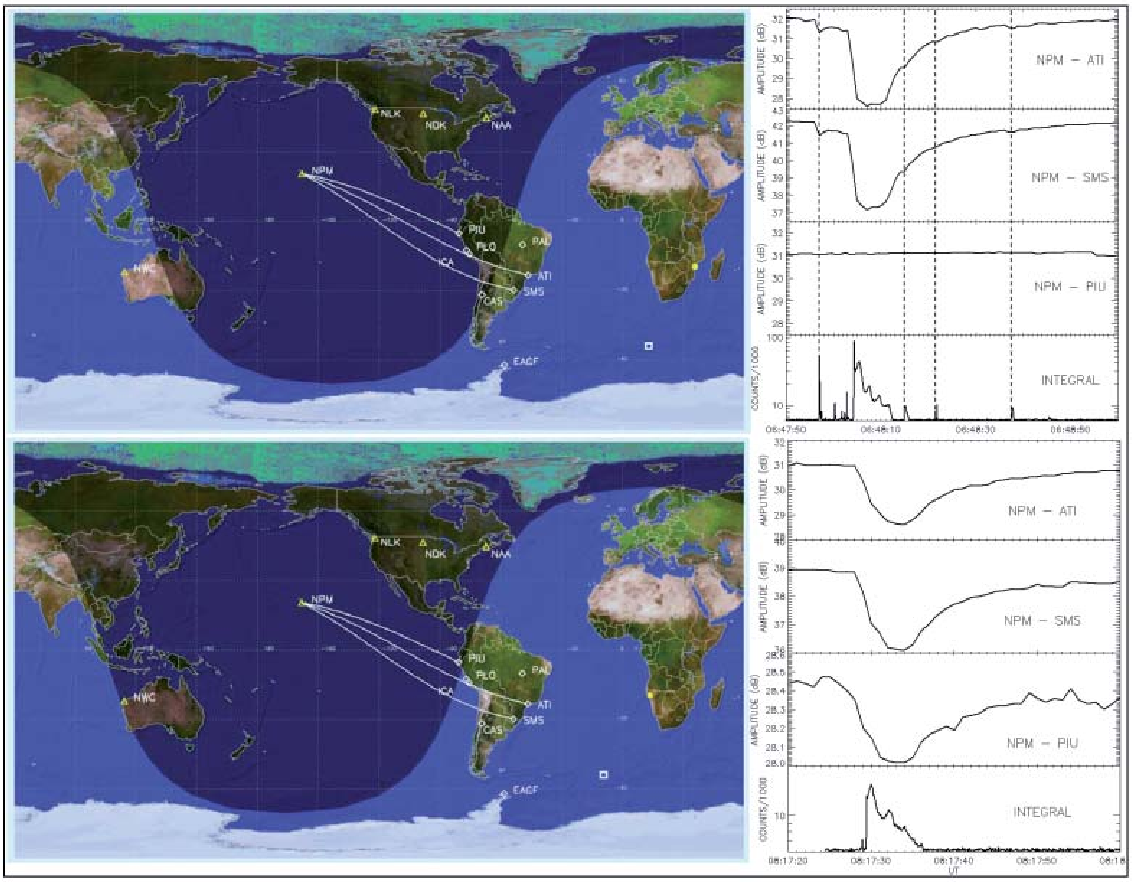

Figure 4. The illumination conditions during a magnetar gamma-ray burst that occurred on January 22, 2009 (left), with the subflare point (square) for two moments at 06:48 UT (top) and 08:16 UT (bottom). In the right-hand panel, amplitude variations for the NPM-ATI, NPM-SMS, NPM-PIU SAVNET propagation paths, along with the photon flux measured by the INTEGRAL satellite sensor, are shown. The dashed lines indicate corresponding structures seen by the instruments (see text for details).

The study of hundreds of solar flares during the current solar-activity minimum led to establishing a soft X-ray-flux lower threshold needed to perturb the low ionosphere. The correlation found between this soft X-ray threshold and the Lyman-α radiation for different solar-activity levels confirmed that the latter is at the origin of the quiescent D-region formation.

We also discussed SAVNET amplitude variations during a rare observation of a series of magnetar-outbursts on January 22, 2009. These were well time-correlated with hard X-rays detected by INTEGRAL. Detailed sub-ionosphere propagation modeling is in progress for a better understanding of such phenomena.

Network integration should be considered as an important decision in allying forces to face the several above-mentioned open questions. Nowadays this is possible, since few of these extended VLF networks are operating simultaneously in different parts around the globe. SAVNET data are available on request via e-mail to savnet@craam.mackenzie.br.

7. Acknowledgments

This work was financed partly by FAPESP (grants 2007/05630-1, 2008/05644-5, and 2006/02979-0). The authors thank MackPesquisa and CNPq through project 304433/2004-7.

8. References

1. M. Nicolet and A. C. Aikin, “The Formation of the D Region of the Ionosphere,” *J. Geophys. Res.*, **65**, 1960, pp. 1469-1483.

2. P. M. Banks and G. Kockarts, *Aeronomy, Part A*, New York, Academic Press, 1973.

3. J.-P. Raulin, P. David, R. Hadano, A. C. V. Saraiva, E. Correia and P. Kaufmann, “The South America VLF NETwork (SAVNET),” *Earth, Moon and Planets*, **104**, 2009, pp. 247-261.

4. J.-P. Raulin, P. David, R. Hadano, A. C. V. Saraiva, E. Correia and P. Kaufmann, “The South America VLF Network

(SAVNET): Development, Installation Status, First Results," *Geofísica Internacional*, **48**, 2009, pp. 185-193.

5. J.-P. Raulin, F. C. P. Bertoni, H. Rivero Gavilan, W. Guevara-Day, R. Rodriguez, G. Fernandez, E. Correia, P. Kaufmann, A. A. Pacini, T. R. C. Stekel, W. L. C. Lima, N. J. Schuch, P. R. Fagundes and R. Hadano, "Solar Flare Detection Sensitivity Using the South America VLF Network (SAVNET), *J. Geophys. Res.*, 2010, doi:10.1029/2009JA015154, in press.

6. H. Rivero Gavilan, *Estudo das Propriedades da Região C Ionosférica Utilizando a Rede SAVNET*, master's thesis, INPE-16613-TDI/1591, 2009, Instituto Nacional de Pesquisas Espaciais, São José dos Campos; available at http://urlib.net/sid.inpe.br/mtc-m19@80/ 2009/11.06.18.11.

7. R. L. Dowden, J. B. Brundell, and M. Hayakawa, "Remote Sensing by VLF Using SoftPAL: Investigation of Short Path Propagation for Possible Earthquake Detection," Proceedings, Mathematical Methods in Electromagnetic Theory, **1**, 1998, 29-34.

8. P. Kaufmann, L. R. Rizzo Piazza, and J. H. Fernandez, *J. Geophys. Res.*, **107**, A8, 2002, SIA30-1.

9. P. Kaufmann and M. H. Paes de Barros, "Some Relationships Between Solar X-Ray Bursts and SPAs Produced on VLF Propagation in Lower Ionosphere," *Solar Phys.*, **9**, 2, 1969, pp. 478-486.

10. J.-M. Comarmond, *Contribution à l'Etude de la Basse Ionosphère par des Mesures de Phase et d'Amplitude d'Ondes Électromagnétiques à Très Basse Fréquence*, Thése de Doctorat d' Etat, Université Pierre et Marie Curie, Paris VI, 1977.

11. P. Pant, "Relation Between VLF Phase Deviations and Solar X-Ray Fluxes During Solar Flares," *Astrophysics and Space Science*, **209**, 1993, pp. 297-306.

12. W. M. McRae and N. R. Thomson, "Solar Flare Induced Ionospheric D-Region Enhancements from VLF Phase and Amplitude Observations," *J. Atmos. Solar-Terr. Phys.*, **66**, 2004, pp. 77-87.

13. V. Zigman, D. Grubor, and D. Sulic, "D-Region Electron Density Evaluated from VLF Amplitude Time Delay During X-Ray Solar Flares," *J. Atmos. Solar-Terr. Phys.*, **69**, 7, 2007, pp. 775-792.

14. A. A. P. S. Marques, *Dependência das Propriedades da Região-D Ionosférica com o Ciclo de Atividade Solar*, master's thesis, INPE-15173-TDI/1290, 2006, São José dos Campos, Instituto Nacional de Pesquisas Espaciais; available at http://urlib.net/sid.inpe.br/MTC-m13@80/2006/10.02.11.55.

15. J.-P. Raulin, P. Kaufmann, E. Correia and M. A. G. Martinez, "On the Detectability of Solar X-Ray Flares Using Very Low Frequency Sudden Phase Anomalies," *J. Atmos. Solar-Terr. Phys.*, **68**, 9, 2006, pp. 1029-1035, doi:10.1016/j.jastp.2005.11.004.

16. A. A. Pacini and J.-P. Raulin, "Solar X-ray Flares and Ionospheric Sudden Phase Anomalies Relationship: A Solar Cycle Phase Dependence," *J. Geophys. Res.*, **111**, A09301, 2006, doi: 10.1029/2006JA011613.

17. V. Savchenko, "Gamma-Ray Bursts Coordinates Network," circular 8837, 2009, available at http:// gcn.gsfc.nasa.gov/gcn3/8837.gcn3.

18. S. Mereghetti, "Gamma-Ray Bursts Coordinates Network," circular 8841, 2009, available at http:// gcn.gsfc.nasa.gov/gcn3/8841.gcn3.

19. J.-P. Raulin, F. C. P. Bertoni, H. Rivero-Gavilan, N. J. Schuch, P. Kaufmann and E. Correia, "Rede SAVNET Detectou Presença de um Magnetar," available at http://www.mackenzie.br/ 13911.html?&tx_ttnews[pointer]=3&tx_ttnews[tt_news]=24&tx_ttnews[backPid]=13896&cHash=dec92178ad. Universidade Presbiteriana Mackenzie, Artigos Acadêmicos, São Paulo, 2009.

20. Y. Tanaka, J.-P. Raulin, F. C. P. Bertoni, N. J. Schuch, T. Terasawa, M. Hayakawa and T. Takahashi, "SAVNET and Japanese VLF Observations of Ionospheric Disturbances Caused by Giant Recurrent Gamma-Ray Flares on January 2009," Eos Trans. AGU, **90**, 52, 2009 Fall Meet., Abstract SA13A-1471.

Man-Made Noise in Our Living Environments

Frank Leferink
F. Silva, J. Catrysse
S. Batterman, V. Beauvois
A. Roc'h

Abstract

The ITU's (International Telecommunication Union's) man-made noise levels are based on measurements performed in the 1970s. Some measurements have been carried out since then, showing that noise caused by automotive ignition systems has been reduced, but man-made noise in business areas and city centers increased, especially due to the widespread use of electronic systems. The interference scenario also changed, from analog communication systems in relatively free-space conditions, to digital systems in living areas, often semi-enclosed such as offices, industrial production plants, and even inside cars and trains. Several measurements have therefore been carried out to estimate the level of man-made noise in these semi-enclosed environments.

1. Introduction

The knowledge of the electromagnetic ambient or radio noise is of particular interest in planning and setting up wireless systems, and for estimating the risk and impact of electromagnetic interference (EMI). Radio noise external to the radio receiving system is derived from either natural sources – such as atmospheric, galactic noise, and lightning – or unintended radiation from electrical and electronic equipment, power lines (including railway systems), and internal-combustion engines. This unintended radiation is called man-made noise (MMN). It is assumed to comprise two dominant and distinct components: white Gaussian noise (WGN) and impulsive noise (IN) [1-4]. The impulsive noise is further classified into Class A and Class B, these two classes respectively being narrowband (with respect to the receiver's bandwidth) and broadband. Class B is typically made up of wideband pulses, often caused by ignition circuits, lightning, and switching elements causing spark gaps. However, it is important to recognize that the distinction between white Gaussian noise and impulsive noise is based on statistical models. The widespread use of all kinds of electronic systems creates noise levels that are often a combination of both white Gaussian noise and impulsive noise.

The levels for radio (including man-made) noise are usually taken from ITU-R 372-8 [5]. The atmospheric-noise figures are taken from CCIR 322 [6]. The levels in these documents are based on measurements made in the 1960s and 1970s in the United States [7, 8], although the update rate of the ITU document suggests including new information ("-8" version). Technology changed considerably in the last decades, as well as the use of wireless systems. An example of the change in utilization of the ether is the widespread use of wireless systems for monitoring data and control in wireless-local-area networks and in industrial environments. Some measurement campaigns have been carried out to update the man-made noise levels as reported in [7], and a short overview of the results is presented in the next section.

It is remarkable that nearly no data is available on the EM ambient levels in semi-enclosed environments. Semi-enclosed environments are industrial sites, such as production plants, offices, houses, and even include cars, trains, or planes. Wireless communication systems are being used in these semi-enclosed environments, while the interference model is based on the conventional assumption that free-space radio-communication systems have to be protected. The interference case will be discussed in Section 3. Measurements have been carried out to characterize the EM ambient levels in industrial environments. The results are presented in Section 4.

Frank Leferink and Anne Roc'h are with the University of Twente & Thales, The Netherlands; e-mail: Frank.Leferink@UTwente.nl. Ferran Silva is with the Universitat Politecnica de Cataluny, Barcelona, Spain. Johan Catrysse is with FMEC/KHBO, Oostende & MICAS/ESAT/KULeuven, Heverlee, Belgium. Sven Battermann is with Leibniz Universität Hannover/WAGO Kontakttechnik, Minden, Germany. Veronique Beauvois is with the University of Liege, Belgium.

This paper is one of the invited *Reviews of Radio Science* from Commission E.

2. Man-Made Noise

The basic document for describing radio noise is ITU-R-P.372 [5]. It gives the external noise figure,

$$F_a = 10 \log f_a \quad \text{[dB]}, \qquad (1)$$

where f_a is the noise factor, defined as

$$f_a = \frac{p_n}{k t_0 b}. \qquad (2)$$

p_n is the available noise power from an equivalent lossless antenna; k is Boltzmann's constant (1.38×10^{-23} J/K); t_0 is the reference temperature (K), taken as 290 K; and b is the noise-power bandwidth of the receiving system (Hz).

In the case of man-made noise, we have to convert measured field strength in a measuring bandwidth to the noise figure, F_a. The power in a matched receiver due to a measured electric field strength, E, is

$$P_r = SA = \frac{1}{2} \frac{\left|\hat{E}\right|^2}{\eta_0} A_e, \qquad (3)$$

with

$$A_e = \frac{\lambda^2}{4\pi} \qquad (4)$$

for an isotropic antenna with unit gain and no losses. The noise power in an equivalent lossless antenna can thus be replaced by the man-made noise as measured. Converted to logarithmic units, the noise figure related to the field strength, E_n, of the noise, measured with a bandwidth b, becomes

$$F_{aM} = E_n + 95 - 20 \log f_{\text{MHz}} - 10 \log b \quad \text{[dB]}. \qquad (5)$$

Probabilistic descriptions of the received noise waveform are required to determine system performance and the amplitude probability distribution (APD) (exceedance probability) of the received envelope that is used. The most important minimum expected median values of F_a are shown in Figure 1. The average of the upper-decile deviation of the man-made noise in business, residential, and rural environments is approximately 10 dB (depending on time and location), measured in the 1970s. Data is available only for the business area between 200 MHz and 900 MHz, which is also shown in Figure 1. In the HF range, the background noise is the ambient noise in the external environment, i.e., the atmospheric noise. In the VHF and UHF ranges, it was assumed to be the receiver noise, but it later appeared to be the galactic noise. This level was exceeded by man-made noise. In 1970s, a significant component of man-made noise in VHF was due to ignition impulses from motor vehicles.

Since the publication of the radio noise levels in CCIR 322 and ITU-R-P.372, several experiments have been carried out [7-32] (listed on publication date). It is not the intention to be complete, but to determine the trends. Measurements performed in business areas of Montreal and Ottawa, and in residential areas of Ottawa, were described in [10, 13]. These showed that there has been no significant increase of the manmade noise, but even a decrease in the noise level, caused in part by the practice of using buried

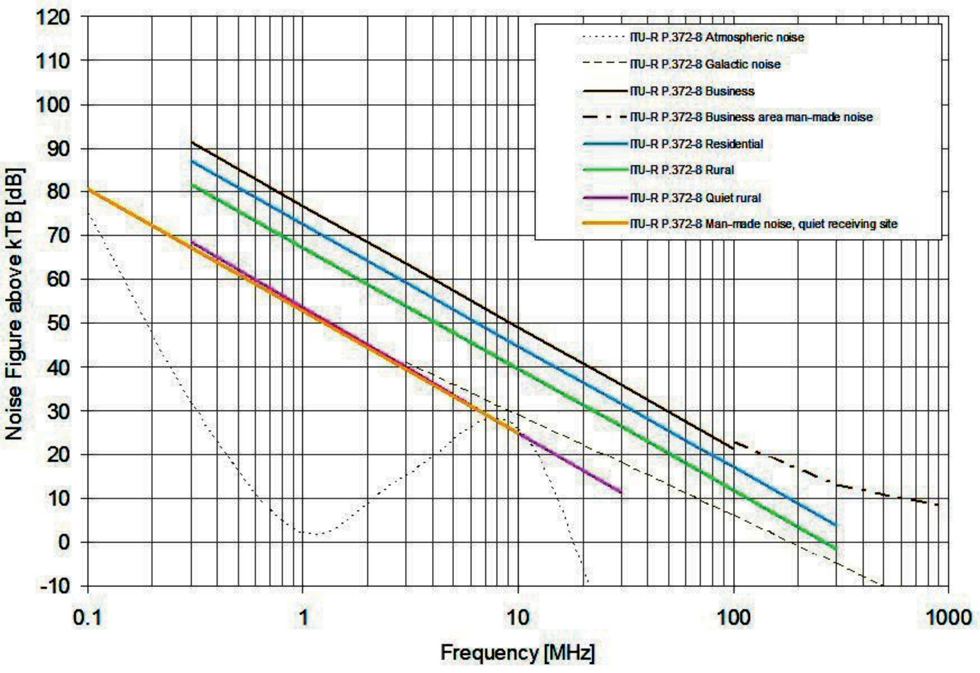

Figure 1. The minimum expected median values of F_a.

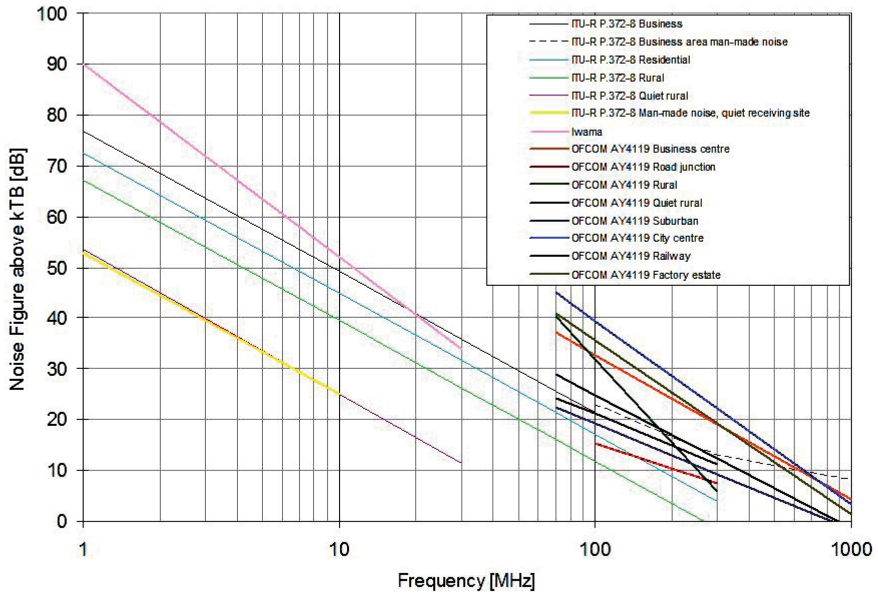

Figure 2. Recent results for the minimum expected median values of F_a.

power lines rather than overhead power lines. In [14], it was stated that the CCIR methods may have been made inaccurate by technological advances. For example, newer automotive ignition systems radiate less noise, but personal computers capable of producing considerable noise have become ubiquitous in business and residential environments. This was confirmed in [15], where measurements showed that automotive noise was no longer a significant VHF noise source, but that computers were found to be capable of generating a significant amount of noise. A follow-up report on man-made noise-power measurements at VHF and UHF frequencies [18] concluded that 402.5 MHz UHF noise levels in business areas were high enough to adversely affect communication-system performance some of the time. This report also remarked that more measurements were needed to determine the extent of these high noise levels.

OFCOM awarded a contract in 2001 for setting up a measurement facility for measuring the man-made noise in various areas [17]. Measurement results were published in 2003 and 2005 [20, 21]. One argument supporting the performance of these measurements was that the ITU measurements were performed in 1974, when digital RF systems were not widely deployed. Figure 2 gives the values for F_a for man-made noise. The decile deviations are approximately the same as stated in [5]. Man-made-noise data was collected in eight locations: a (large) city center, a factory estate, a business center, a town center, a shopping center/mall, a major highway, and suburban and rural locations, at mid-morning, evening, and rush hour (in relevant environments). The study concluded that the decreasing levels as a function of frequency were comparable with the ITU report, but that the overall level was substantially higher. The highest man-made noise levels were found at the city center, the factory estate, and the business center. The road junction showed lower results, which again showed the effectiveness of measures taken via European legislation to reduce the automotive-ignition noise.

Measurements in Sweden [25] showed lower noise levels than the ITU levels. This was true except for urban areas and the city of Stockholm, where the man-made noise was up to 15 dB higher. Iwama [32] showed a much higher man-made noise at lower frequencies in the HF region, decreasing faster in the UHF region. The resulting curve is also shown in Figure 2.

A NATO (North-Atlantic Treaty Organization) study group investigated the impact of widespread use of power-line communication (PLC) and digital data communication (xDSL: various forms of digital subscriber line) on HF communication links. HF communication is the backbone system for safety-critical services, including the armed forces [31]. This group concluded that the ambient noise was not changed in the last decades. To prove this, measurements were performed in rural areas in parts of the spectrum without any man-made noise interference, resulting in the atmospheric-noise levels. Real man-made noise will never be measured in this manner. However, their problem was the various suggestions made that man-made noise has increased. This argument was being used by power-line communication providers in a way that even more man-made noise could be allowed. Power-line communication, as xDSL, will cause unintentional RF emissions, which directly may increase the established noise floor nearby, or by cumulative propagation far away from multiple distributed sources. This type of emission is quite different from that produced by electronic devices and equipment: it is broadband noise, most of the time with a high level, and extending over the HF band. The incidental noise generated even by devices and equipment compliant with EMC standards can greatly exceed the existing noise floor, but due to the statistical nature of the incidental noise, reception of long-haul HF signals is still possible. These HF communication systems are opportunistic. If incidental noise prevents communication at any particular time, the transmission is repeated at a later time, when the interference has ceased. However, this protocol does not

Figure 3. The locations of the house and train track for the measurements in Figure 4.

work with a broadband noise floor increased by power-line communication and/or xDSL.

3. Interference Case

In the 1970s, the man-made noise was mainly due to ignition impulses from motor vehicles. This has changed to man-made noise due to the use of electrical equipment [15]. Especially in the VHF range, computers were found to be capable of generating a significant amount of noise in this band [18].

Most existing radio receivers are designed for the case of additive white Gaussian noise (WGN), and their performance may deteriorate in other scenarios, for example, when subjected to impulsive noise [25]. In rural environments, the man-made noise can be approximated as white Gaussian noise, but in urban and suburban environments, the man-made noise is often impulsive noise (IN). For digital communication systems, white Gaussian noise does not represent a major problem, as long as the mean power of the desired received signal is high enough. The impulsive noise is harmful for digital communications because each pulse may cause bursts of bit errors and possible loss of synchronization. In [19], the use of a root-mean-square was suggested for weighting the effects of disturbances on digital communication systems, instead of the conventional quasi-peak detector, as described in [33].

An extreme example of underestimating the man-made noise was the German toll project [34, 35]. Several billions of Euros were lost due to interference in GPS receivers in industrial areas and city centers, and the system had to be redesigned, causing a long delay without income (from toll).

The conventional detectors in electromagnetic-emission measurements are based on quasi-peak measurements, which is actually a filtering process, reducing the impulsive noise. The quasi-peak detector depicts the reduced noise impression of impulsive noise in analog radio systems. However, impulsive noise due to modern electrical and electronic systems can more easily disturb modern digital systems, as shown in [26, 27]. To confirm this assumption, a test was performed in the digital terrestrial broadcast band (DVB-T), around 850 MHz, in a house in a suburban area in Spain near to a train track, as shown in Figure 3. The received signal is shown in

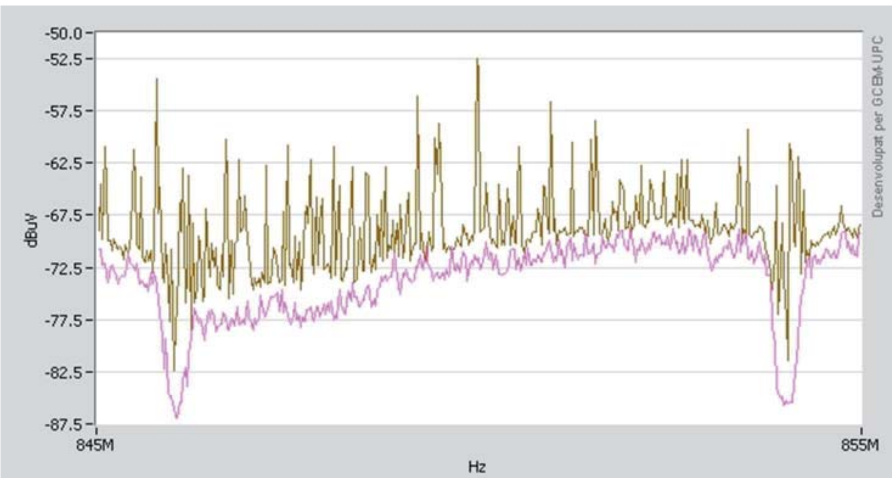

Figure 4. The DVB-T signal received in the house: (lower curve) the correct signal, (higher curve) with interference from the train.

Figure 5. The interference due to man-made impulse noise.

Figure 4. The passing train disturbed the DVB-T reception. The interference was repeated in the lab, and the effect is shown in Figure 5.

Another key issue is the classic interference case. This assumes a source of noise on the road, or from a neighbor, which interacts with the wanted signal received with an antenna placed on the rooftop of a building, as shown in Figures 6 and 7, respectively.

In our modern living environment, many electronic systems are used, including modern wireless communication systems. A huge increase of wireless control systems can be observed, especially in the transport sector, from the wireless bridge-control systems on large cruise liners, to the next-generation passenger planes, where fly-by-wire could be replaced by wireless. However, many wireless systems are already in use in industrial production plants, and many interference problems have had to be solved.

Figure 6. A classic interference case, from a neighbor to your aerial (cartoon by Rupert Besley).

Figure 7. A classic interference case, from the environment (cartoon by Rupert Besley).

Wireless data transmissions – for instance, in the 433 MHz band – are already disturbed, and the coverage of digital video broadcast services (DVB-T) and Tetra (400 MHz) is much lower than predicted in these environments.

A key problem is the limited knowledge of man-made noise in these semi-enclosed problems. In [15], it was stated that further study was needed to determine how narrowband noise power from computers and other electronic devices within a building would impact a receiving antenna mounted on or near an office building. In [18], the conclusion was that more measurements were needed, especially to make future measurements inside of buildings and vehicles.

An additional issue is the multiple reflections inside semi-enclosed environments at VHF and UHF, where the wavelength of the noise is smaller than the dimension of the semi-enclosed environment. These multiple reflections erratically scatter man-made noise and radio waves, and interfere with or block wireless transmissions.

4. Ambient EM Survey in Semi-Enclosed Environments

IEC 61000-2-5 [36] provided some guidance for the characterization of the ambient electromagnetic levels under different circumstances. However, the electromagnetic environments inside transportation equipment, vehicles, trains, ships, and aircraft, are not described. The procedure to establish the ambient EM levels was described in [37]. However, there is almost no data available on the ambient EM levels in industrial environments. This is the

Figure 8. Some of the semi-enclosed, industrial environments where EM ambient surveys were performed.

case for both conducted and radiated ambient levels. The knowledge of the ambient noise is of particular interest in planning and setting up wireless data communication in industrial applications, and to estimate the risk and impact of electromagnetic interference.

Based on press reports, NIST (National Institute of Science and Technology, Boulder, USA) performed tests in manufacturing plants crowded with stationary and mobile metal structures, such as fabrication and testing machinery, platforms, fences, beams, conveyors, mobile

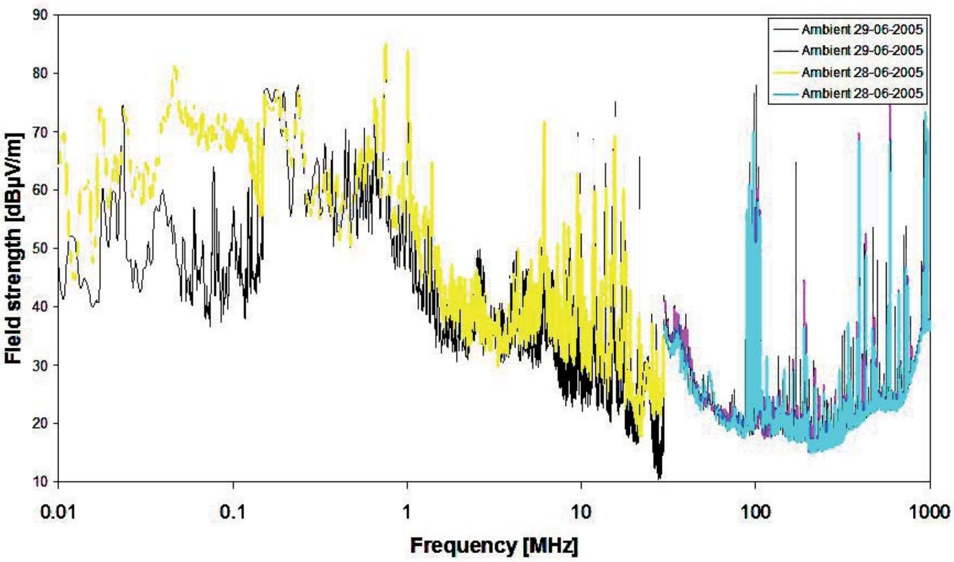

Figure 9. Some scans in semi-enclosed industrial environments.

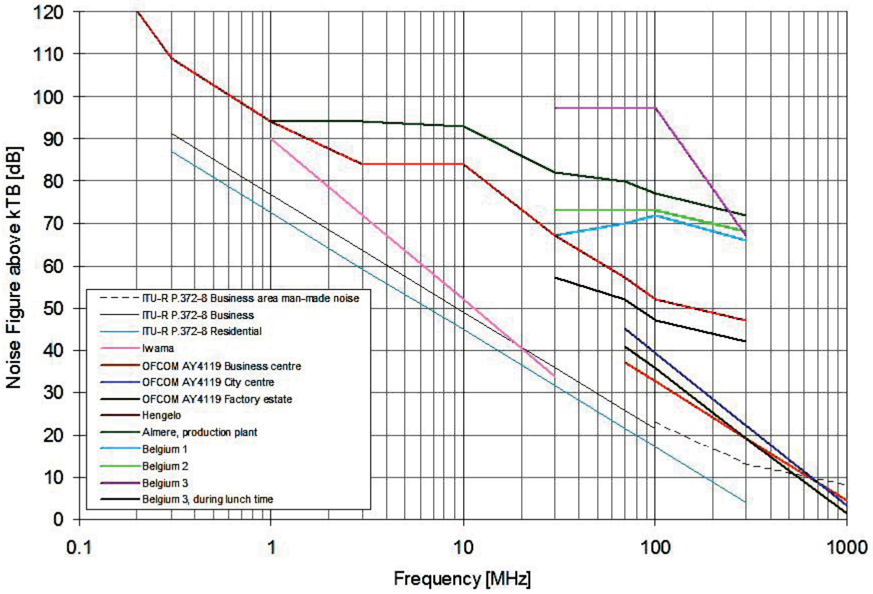

Figure 10. The noise levels in semi-enclosed industrial environments. The lines within the ellipsoid are the noise levels outside the buildings.

forklifts, maintenance vehicles, and automobiles in various stages of production. The survey showed that interference from heavy equipment could impair signals for wireless-data-transmission applications, such as those used in some controllers on the production floor.

Within the framework of COST 286, several institutes performed site surveys following [36, 37] in industrial environments, including KHBO Brugge-Oostende, Belgium; University of Liege, Belgium; University of Catalunya, Spain; University of Hannover, Germany; University of Twente, The Netherlands [23, 24, 26, 27, 28, 30, 38, 39]. These site surveys were not complete measurement sessions, and so had limited long-term monitoring and statistical evaluation of data. Measurements were performed in the HF, VHF, and UHF bands, using equipment and bandwidths as described in [33]. At microwave frequencies, electromagnetic interference due to man-made noise is often less than the interference caused by improper frequency management or the scattering of radio waves. These scatterings and/or multiple reflections cause multipath interference, where radio signals travel in multiple complicated paths from the transmitter to the receiver, arriving at slightly different times [40]. Pictures of some of the environments are shown in Figure 8. Hundreds of measurements were performed. Some scans are shown in Figure 9. Some noise-figure curves have been added based on the surveys, as shown in Figure 10. Some measurements have even been carried out inside machines [30]. Maximum field-strength levels have been measured but no noise figures, as shown in Table 1.

The difference in man-made noise levels looks enormous, and it is. The large increase is due to the high emission levels of machinery controlled by computers, frequency converters, and valves. These machines have to fulfill rather relaxed and high radiated-emission levels at distances of 10 m to 30 m. In the survey, we investigated the emission levels around these machines with measuring distances sometimes less than 2 m. One measurement was performed during lunchtime. Comparing the results, on average the man-made noise has decreased by 40 dB.

5. Conclusion

Man-made noise has changed in the last decades. Noise from automotive ignition has been reduced, but the man-made noise caused by electrical and electronic equipment increased in the conventional outside areas.

Type of Machinery	*Frequency Band [MHz]*	*Maximum Emission Level [dBμV/m]*
Frequency converter	*1-200*	*170*
Punch press	*1-1600*	*169*
CNC center	*1-400*	*169*
Laser cutting machine	*1-1700*	*162*
Weaving machine	*1-2000*	*156*
Welding machine	*1-50*	*140*
Computer	*1-150*	*138*

Table 1. Measurements made inside machines.

Most modern man-made noise is impulse noise, which causes more interference in digital systems than in the old analog systems.

Based on the survey and limited measurement data, we observed that inside semi-enclosed living environments, the man-made noise is much higher – 20 dB to sometimes more than 40 dB – than the baseline noise levels described in ITU-R P.372.

If new services are introduced in these environments, assuming the old man-made noise levels, then serious link problems will occur: many examples of EMI after the introduction of new services have been reported. The main cause of the high man-made-noise level is the conventional-interference case founded on the current electromagnetic-compatibility standards, which do not consider wireless communication systems operated in semi-enclosed environments.

The conclusions are based on the limited measurement data available. More research and measurements are needed to build up a statistically significant set of measurement data. The impacts of different bandwidths than the CISPR bandwidths, and other detectors (such as rms instead of quasi-peak), on interference in digital communication systems should also be investigated.

6. Acknowledgement

This paper resulted from Joint Technical Action 3, within COST 286, which is supported by the European Science Foundation – European Union.

7. References

1. D. Middleton, "Statistical-Physical Models of Man-Made and Natural Radio-Noise Environments – Part I: First-Order Probability Models of the Instantaneous Amplitude," Office of Telecommunications Report OT 74-36, April 1975.

2. D. Middleton, "Statistical-Physical Models of Man-Noise and Natural Radio-Noise Environment – Part II: First-Order Probability Models of the Envelope and Phase," Office of Telecommunications Report OT 76-86, April 1976.

3. D. Middleton, "Statistical-Physical Models of Man-Made and Natural Radio-Noise Environments – Part III: First-Order Probability Models of the Instantaneous Amplitude of Class B Interference," NTIA Contractor Report 78-1, June 194. D. Middleton, Statistical-Physical Models of Man-Made and Natural Radio-Noise Environments – Part IV: Determination of the First-Order Parameters of Class A and Class B Interference," NTIA Contractor Report 78-2, September 1978.

5. ITU Report ITU-R P.372-8, "Radio Noise," International Telecommunications Union, 2003.

6. CCIR Report 322, "World Distribution and Characteristics of Atmospheric Radio Noise," International Radio Consultative Committee, International Telecommunications Union, Geneva, Switzerland, 1964.

7. A. D. Spaulding and R. T. Disney, "Man-Made Noise: Estimates for Business, Residential and Rural Areas," NTIA 74-38, 1974.

8. CCIR Report 258-5, "Man-Made Radio Noise," International Radio Consultive Committee, International Telecommunication Union, 1990.

9. R. Struzak, "Urban Electromagnetic Environment: Facts, Models, Trends," Proceedings of the International Symposium on Electromagnetic Compatibility, Montreux, May, 20-22, 1975, pp. 88-92.

10. W. R. Lauber, J. M. Bertrand, and P. R. Bouliane, "An Update of CCIR Business and Residential Noise Levels," IEEE International Symposium on Electromagnetic Compatibility, 1994, pp. 348-353.

11. N. G. Riley and K. Docherty, "Modeling and Measurement of Man-Made Radio Noise in the VHF-UHF Band," Proceedings of the Ninth International Conference on Antennas and Propagation 1995, **2**, pp. 313-316.

12. F. H. Sanders and V. S. Lawrence, "Broadband Spectrum Survey at Denver, Colorado," NTIA Report 95-321, September 1995.

13. S. N. Murthy and G. Krishnamraju, "Interference to Low Earth Orbit Satellite (LEOS) Services in VHF Band from Ground-Based Emissions," *IETE Technical Review*, **12**, 1995, pp. 325-329.

14. A. D. Spaulding, "The Natural and Man-Made Noise Environment in Personal Communications Services Bands," NTIA Report 96-330, May 1996.

15. Robert Achatz, Yeh Lo, Peter Papazian, Roger Dalke, and George Hufford, "Man-Made Noise in the 136-138 MHz VHF Meteorological Satellite Band," NTIA Report 98-355, 1998.

16. DSTO-TR-0855, "A Comparison of DSTO and DERA HF Background Noise Measuring System with the International Radio Consultative Committee (CCIR) Model Data," DSTO Australia, 2000.

17. RA(OfCom) AY 3952: "Feasibility Study into the Measurement of Man-Made Noise," 2001.

18. R. J. Achatz and R. A. Dalke, NTIA Report 02-390, "Man-Made Noise Power Measurements at VHF and UHF Frequencies," 2001.

19. P. F. Stenumgaard, "Using the Root-Mean-Square Detector for Weighting of Disturbances According to its Effect on Digital Communication Services," *IEEE Transactions on Electromagnetic Compatibility*, **42**, November 2000, pp. 368-375.

20. RA(OfCom) AY4119, "Man-Made Noise Measurement Programme," 2003.

21. A. Sugiura, "Radio Noise Measurements and Related Standards," presented at an FCC tutorial, 2003.

22. A. Wagstaff and N. Merricks, "Man-Made Noise Measurement Programme," *IEE Proceedings on Communication*, **152**, 3, 2005.

23. J. Catrysse, "Study and Simulation of the Ambient Noise of an Industrial Environment for Wireless Communication Applications," Mechatronics and Robotics 2004, Aachen, September 13-15, 2004.

24. A. Vidal, S. Verdaguer, and F. Silva, Medida de Transitorios RF de Baja Potencia, XIX Simposio Nacional de la Unión Científica Internacional de Radio (URSI), Barcelona Spain, 2004.

25. J. Rantakko, E. Lofsved, and M. Alexandersson, :Measurements of Man-Made Noise at VHF," EMC Europe Workshop, 2005.

26. S. Verdaguer, A. Vidal, A. Atienza, and F. Silva, "Time-Domain Measurement System for Impulse Noise Characterization in Digital Communication Environments," EMC Europe Workshop on Wireless Systems, Proceedings 73-76, Roma, Italy, 2005.

27. S. Verdaguer and F. Silva, "Time-Domain Measurement System for Impulse Noise Characterization," Barcelona Spain, 2005.

28. S. Battermann and H. Garbe, "Sensitivity of a Short-Wave Receiving Station Regarding PLC Transmission Session 1: Broadband Powerline Communications [BPC]," 16th International Zurich Symposium on EMC, Zürich, 2005.

29. P. Torıo and M. Sanchez, "Novel Procedure to Determine Statistical Functions of Impulsive Noise," *IEEE Transactions on Electromagnetic Compatibility*, **47**, 3, August 2005, p. 559.

30. J. Catrysse, J. Rayée, and D. Degrendele, "Study and Simulation of the Ambient Noise of an Industrial Environment for Wireless Communication Applications," EMC Europe Workshop, Rome, 2006.

31. NATO Research and Technology Organization, "HF Interference, Procedures and Tools," RTO Technical Report TR-IST-050, June 2007.

32. M. Iwama, "Estimation of Background Noise in HF-Band," 2008 Asia-Pacific Symposium on Electromagnetic Compatibility and 19th International Zurich Symposium on Electromagnetic Compatibility, May 2008, Singapore, pp. 478-481.

33. Specification of Radio Disturbance and Immunity Measuring Apparatus and Methods. Part 1-1: Radio Disturbance and Immunity Measuring Apparatus – Measuring Apparatus," IEC CISPR 16-1-1, Edition 2.2 2007-10.

34. "Volpe GPS Vulnerability Report, Recommendations and FAA Response," September 10, 2001.

35. "Die Maut, die Macht und die Manager, Der grosse Flop von Toll Collect, ZDF, January 30, 2004.

36. "Classification of Electromagnetic Environments, Basic EMC Publication, IEC 61000-2-5, Technical Report, Part 2 – Environment, Section 5, 1995.

37. "Guide for In Situ Measurements – In Situ Measurement of Disturbance Emission," CENELEC CLC/TS 50217 (2004-04).

38. S. Battermann, et al., "Electromagnetic Compatibility Analysis of Unstructured Mains Networks for High-Speed Data Transmission: Part 1," *IET Science Measurement and Technology*, **2**, 3, May 2008, pp. 146-153.

39. S. Battermann et al., "Electromagnetic Compatibility Analysis of Unstructured Mains Networks for High-Speed Data Transmission: Part 2," *IET Science Measurement and Technology*, **2**, 3, May 2008, pp. 154-159.

40. F. Leferink and W. van der Wurff, "Wireless Communication Systems: The Impact on Throughput in Highly Reflecting Environments," EMC Europe 2004, Eindhoven, pp. 211-215.

Classifying EM Sensors According to the Frequency of Operation

Ben-Zion Kaplan
Uri Suissa
David Yardeny
Arie Sheinker

Abstract

The present discussion suggests a non-conventional viewpoint in considering the method of operation of certain electromagnetic sensors. They are dealt with here mainly according to their frequency range. Most of the attention is paid to sensors associated with electric fields. Nevertheless, the treatment is also relevant to magnetic-field sensors, and some magnetic sensors are even directly mentioned. The present mode of approach to the classification of sensors is mainly through the variability that results from the frequency of the measured field. The main lesson is that sensors, which measure radiated fields – namely, sensors for VHF and HF – rely on radio receivers. Sensors at somewhat lower frequencies can rely on direct capacitive coupling (or direct inductive coupling, in the magnetic case). On the other hand, sensors for ULF and dc rely on the mechanical movement of the sensor, or on the movement of some of its parts. Hence, when the field becomes static, the sensor is the dynamic entity in the system.

1. Introduction

The present discussion attempts at suggesting a relatively unusual viewpoint in considering the performance of various electric, magnetic, and electromagnetic sensors. The main detailed discussion is due to sensors that are associated with electric field-strength measurements. However, it may also be of value for other types of sensors. The present discussion is mainly a review, and possesses an educational benefit. Nevertheless, it enables deep understanding of the various sensors, and is expected to contribute to their improved design. It is shown that the electromagnetic sensors can be divided into several classes, according to their sensing-frequency range. It is demonstrated that the measured field frequency influences the operating principle of the sensors. As a result, it also affects the various devices' structural design. It appears relatively obvious that at the higher-frequency ranges, the sensors rely on collection of radiated power, which is impossible at the lower frequencies, where the sensors respond directly to the field intensities. The latter is impossible at ULF and dc, where the operation is assisted by the mechanical movement of the electrodes.

Some applications of the treated sensors are mentioned throughout the paper's sections, in association with the particular sensors under consideration. The applications issue is additionally expanded and explained in Section 7, which precedes the conclusions section.

2. VHF Electric-Field Sensors

There exist sensors that operate at relatively high frequencies. For example, regular VHF field-strength meters employ calibrated receivers with conventional antennas of adjustable size to match the operating frequency. A well-known sensor of the latter type used to be supplied by the German firm of Rhode and Schwarz [1]. It employed a calibrated VHF receiver. The receiver operated in the frequency range of 47 to 225 MHz (see the photograph in Figure 1). The receiver was integrated with and coupled to a built-in antenna. The antenna was a half-wavelength dipole of adjustable size. The operator was responsible for manually and symmetrically varying the length of the antenna's arms. The operator was responsible for adjusting the antenna's length to be $\lambda/2$ at the frequency of concern. This resulted in a similar calibration for measurements all over the system's frequency range. The receiver box acted as a mechanical support for the antenna. The height of the antenna (namely, its distance from the top of the receiver box) could also be adjusted [1].

Ben-Zion Kaplan is with the Department of Electrical and Computer Engineering, Ben-Gurion University of the Negev, PO Box 653, Beer-Sheva 84105, Israel; Tel: 972-8-6461506; Fax: 972-8-6472949; E-mail: kaplan@ee.bgu.ac.il. Uri Suissa is with the Department of Electrical and Electronic Engineering, Sami Shamoon College of Engineering, PO Box 45, Beer- Sheva 84100, Israel; Tel: 972-8-8475738; Fax: 972-8-6475703; E-mail: uris@sce.ac.il.

David Yardeny is with ELTA Systems Ltd. Group & Subsidiary of Israel Aircraft Industries Ltd., PO Box 330, Ashdod, 77102, Israel; Tel: 972-8-8575874, Fax: 972-8-8564568; E-mail: dyardeny@elta.co.il. Arie Sheinker is with R&D Integrated Systems Section, Propulsion Division, Soreq NRC, Yavne 81800, Israel; Tel: 972-8-943-4855; Fax: 972-8-943-4227; E-mail: sheinker@ee.bgu.ac.il.

Figure 1. A photograph of the Rohde and Schwartz VHF field-strength indicator.

3. HF Electric-Field Sensors

Similar means are also employed at lower radio frequencies, however with less-convenient additional hardware. The usual procedure is to employ an improvised dipole constructed at the measurement site. The size of the mobile antennas is a fraction of a wavelength, and is usually smaller than $\lambda/2$. The dipole is made of conducting wires, and is mounted between two temporary poles. The related measurements and calibration become more cumbersome at the lower-HF frequency ranges. The situation is such that virtually each frequency requires a separate calibration procedure. This is due mainly to the fact that the wavelengths are large, and do not enable the use of portable, relatively small antennas with a size that is conveniently related to a wavelength. This leads to the employment of improvised antennas, and the system calibration is carried out separately for each of the frequencies of concern. The main item that should be calibrated is a multi-frequency receiver of several frequency bands, where virtually each choice of a new frequency of measurement leads to a new calibration of the system. The tuning needed is that of the receiver, together with the antenna at the particular frequency of concern. The related procedure employs a well-calibrated signal generator, connected to a transmitting antenna with known transfer characteristics (namely, the field strengths at various distances and orientations that are known for the particular output voltage and frequency). There is usually no specific equipment manufactured especially for the task. Regular receivers together with wire antennas are employed in this case [2]. The related measurement procedure is usually lengthy and cumbersome, and employs several sessions of trials until a satisfactory result appears to be reached.

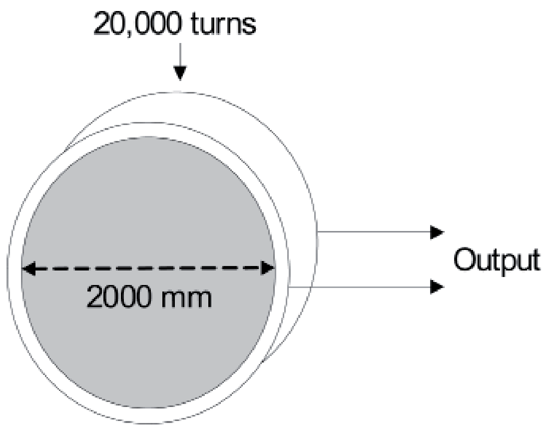

Figure 2. A stationary search coil, employed for monitoring magnetic fields in major geophysical monitoring stations.

4. Sensing of Non-Radiating Dynamic Fields

Some sensors operate at even lower frequencies. (We refer here to frequencies that do not enable sufficient radiation power. This means that the wavelength is much larger than the system's typical dimensions.) These sensors employ what we may regard as an ordinary reactive coupling. It is furnished in the magnetic case by mutual-inductance coupling, similar to that employed in circuits and transformers. The employment of static search coils for low-frequency magnetic-field measurements is a manifestation of this principle. Such sensors have a typical diameter of two meters, and typically consist of ten thousand turns. They are usually mounted in major geophysical research observatories [3] (see Figure 2). One may perhaps argue that large diameters and the related bulkiness can be avoided by employing ferromagnetic cores for the coils. However, the employment of such cores is not recommended in major observatories because of the associated core nonlinearity, which may generate erroneous frequency products. However, ferromagnetic cores are nevertheless employed for less-precise applications. (On the other hand, the sensing of strictly dc magnetic fields may be furnished by rotating coils [4], and this is discussed in the next section.) There also exist electric devices that may be viewed as members of the class. They can be regarded as being analogous to regular capacitive coupling in electric circuits. Their counterparts among geophysical electric-field measuring devices are some stationary capacitive probes, which are known in the remote-sensing of clouds from Earth [5] (see Figure 3). Their sensing ability is enabled by the movement of the clouds, which causes the related electric field to vary in time. The cloud capacitive probes are sometimes mounted above the roofs of meteorological stations [5]. Figure 3 shows a conductive probe mounted on such a roof. A separate wooden hut is usually devoted for the latter monitoring of clouds in such stations [5],

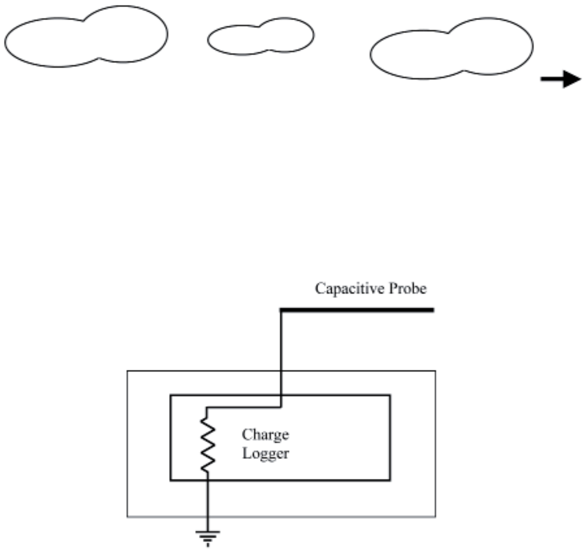

Figure 3. A capacitive probe for sensing moving clouds (see [5])

which is actually the arrangement sketched in Figure 3. The conductive probe senses the variable electric field, which is due to the movement of the clouds. Through its connection to the ground, the probe tends to accumulate charge, the polarity of which opposes that of the cloud. The probe is connected to ground through a low-input-resistance monitor, which counts the number of the latter charging events, and records their variation in time.

5. Electric ULF and dc sensors

The third class of devices consists of sensors that are related to ULF and dc. The ordinary magnetic coupling of the second group cannot be established in this case, since the reactance associated with the sensing coil becomes much too small at such low frequencies. It effectively causes the transferred signal to be short circuited. Of course, the transferred signal itself becomes smaller for smaller frequencies, and disappears at dc. The capacitive-coupling reactance in this frequency range becomes too large, and does not enable effective transfer of signal. The coupling in the latter cases is therefore recovered by employing mechanical movement of the sensor's members. Such sensors were known in the thirties, and relied on rotating coils [4]. More-modern magnetic sensors replace the mechanical movement by periodically driving parts of the sensor's ferromagnetic core, which stays stationary in its location, into saturation and back [6]. Magnetic sensors of this kind are usually known as fluxgate magnetometers. There is probably no closely similar effect in use in the electric case, where one periodically modulates the permittivity associated with a coupling capacitance. Nevertheless, in the electric case, there exist various sensors of vibrating or rotating electrodes that maintain a sufficiently large reactive coupling through mechanical movement. The rotating-covering field-mill is

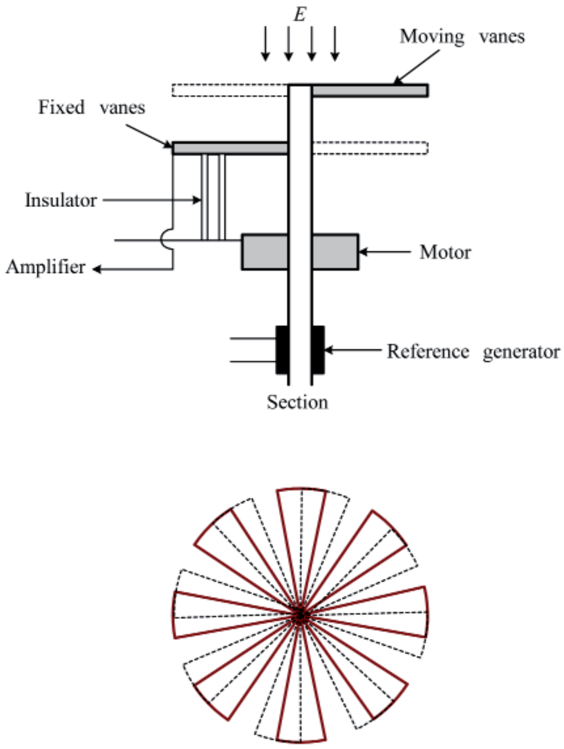

Figure 4. A rotating-covering-field-mill system.

an example of the latter [7]. It is shown in Figure 4. It is regarded as the most common amongst the mechanically achieved electric-field-strength measuring devices. The performance of the sensor becomes understandable by resorting to its circuit diagram, in Figure 5. A superficial approach may suggest that the sensor's performance is due to a sort of chopper-like operation. This would mean that the electric-displacement-vector flux is periodically chopped. It thus results when detected in an ac signal, the size of which is proportional to the measured nearly-dc field. The conversion to ac appears to allow a relatively easier treatment of the measured quantity.

The final argument of the previous paragraph represents a helpful feature of the presently discussed sensors. Nevertheless, it does not tell the full story. The movement of the sensor's electrodes creates in addition a sort of "dynamic" reactance, which is similar to the dynamic-reactance features obtained when the measured field frequency is increased and an ac sensor is dealt with [7]. This is explained in the sequel. The argument related to the dynamic reactance could perhaps be better appreciated by resorting to the rotating cylindrical field mill, which is shown in Figure 6 [7]. The latter figure may suggest that each pair of opposite electrodes of the rotating cylindrical field mill experiences a field similar to that of a pair of stationary electrodes submerged in an ac field, as is shown in Figure 7. Hence, the association of the rotating cylindrical field mill's electrodes with measurements similar to those of stationary electrodes in an ac field is relatively obvious.

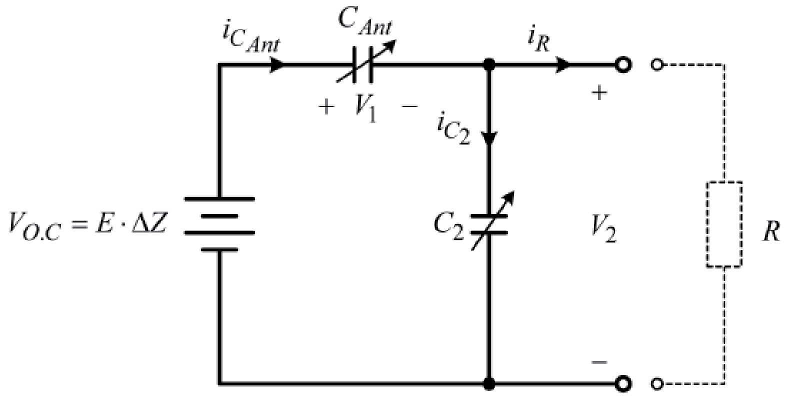

Figure 5. A circuit model related to the rotating covering field mill.

The qualitative approach of the previous paragraph suggests that the electric field sensed by the rotating cylindrical field mill's electrodes is similar to that of a pair of stationary electrodes submerged in an ac field. The frequency of the apparent ac field is the *RPS* (rotations per second) times the number of electrode pairs in the rotating cylindrical field mill. However, it appears that the rotating covering field mill is applied more frequently than the rotating cylindrical field mill. The detailed analysis in the sequel is therefore related to the rotating covering field mill.

6. A Contribution to the Detailed Analysis

The aim of the present section is to deal with the covering field mill analysis in a somewhat simplified manner. A comprehensive analysis was given in [7]; refer also to the present Figures 4 and 5. One is tempted to start such an analysis by setting up a differential equation that balances the various contributions of the capacitors and resistor to the sensor's output voltage [7]. An initial difficulty is related to the capacitances, which are due mainly to the interaction between the rotary and the stationary vanes of the sensor. Nevertheless, the latter periodically varying capacitor does not complicate the analysis, since it is in most practical cases virtually short circuited by the loading of R. It is also observed that the main contributors to the sensing ability of the sensor are the external surfaces of the rotating vanes. As a result, a relatively simple expression is obtained for the sensor's output voltage:

$$V_2 = 8\omega \Delta Z R E \alpha C_{oAnt} ,$$

where E is the measured field strength, ΔZ is the vertical distance between the rotating and stationary electrodes, and C_{oAnt} is the external capacitance of the electrode structure. It therefore represents the coupling between the electrodes and the field sources. It is somewhat similar to the entity known as antenna capacitance in the theory of antennas. ω is the angular velocity of the structure. A factor of eight is added, since the structure consists of eight electrode pairs. V_2 is the amplitude of the sensor voltage at the terminals. α is a factor slightly smaller than unity. It results from the fact that the waveform of the periodically changing capacitance is not triangular with an amplitude of one. Its form is more likely to be nearly sinusoidal. The amplitude of the latter is slightly smaller than unity. Hence, the time-varying capacitance oscillates between a lower value, which is slightly above the zero floor, and it rises to a maximum value of almost two amplitudes.

The value of V_2 in Figure 5 is a simple indicator for deriving the sought electric-field strength.

7. Further Remarks on the Applications of EM Sensors

The main attention in the previous sections was paid to reviewing the principles of operation of various EM sensors. Some of their applications have also been briefly treated. However, the aim of the present section is to deal mainly with the applications, and to further emphasize some practical issues, which are related to the mentioned sensors. The main primary use of most of the EM sensors is measurement of field intensities. An example is the VHF field-strength meter (that of Rohde and Schwarz, which was mentioned in Section 2). The rest of the mentioned sensors also possess a main application related to monitoring the intensity of the sensed fields. In addition, there exist applications that could be regarded as secondary. For example, the Rohde and Schwartz field-strength meter is employed for antenna measurements. One can apply the related sensor, which consists of a portable receiver fed by an adjustable half-wavelength antenna, in order to collect the field-strength readings needed to draw the radiation pattern of an investigated aerial. However, when treating lower frequencies, one becomes increasingly interested with natural phenomena [8, 9]. The electric and magnetic field sensors for the lower frequencies are usually associated with geophysical and atmospheric phenomena. The related magnetic-field sensors (large search coils and fluxgate magnetometers) are employed for monitoring the magnetic field of the Earth. They are used to investigate magnetic geophysical phenomena. Some of them are also associated

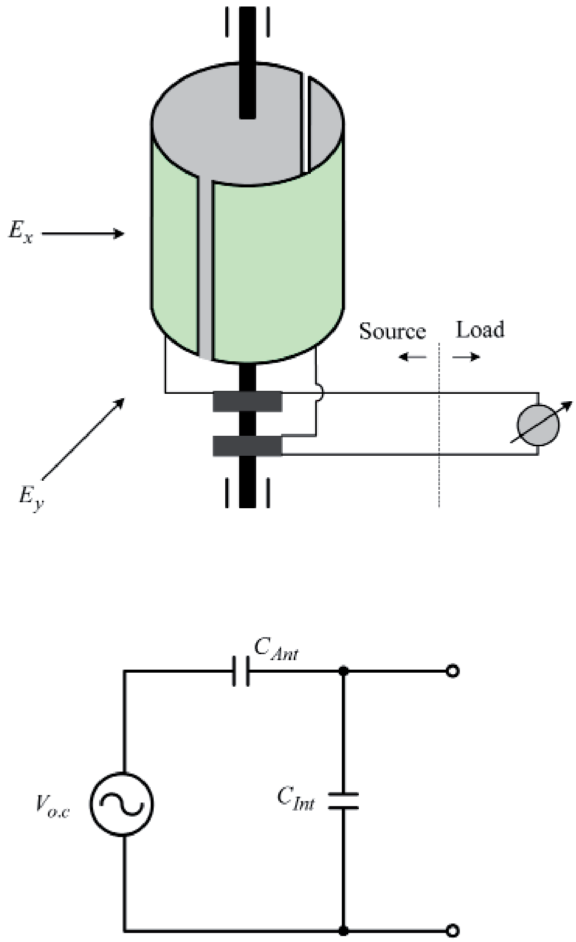

Figure 6. A rotating cylindrical field mill.

with effects related to the ionosphere, and the way it interacts with the Earth's magnetic field. It is interesting that magnetic sensors are installed aboard many of the scientific spacecraft [9], and assist in investigating the features of other planets' structure and of their environment. They are installed aboard the probes orbiting around Earth, and also on NASA's space shuttles. Magnetometers have even been sent to the moon and to Mars. The main objective of the latter sensors is scientific, and is due to the fact that through the investigation of the various fields – and especially through monitoring of the magnetic fields –one learns about the geology of the Earth. The structural details of other stars are also deducted in a similar way by measuring their magnetic fields. It is even believed that certain magneto-metric signals may serve as precursors to earthquakes. A related account on the electromagnetic environment between the ionosphere and the Earth's surface was given in [10]. Some sensing techniques were also mentioned there. One can even learn about the Schumann resonances, which are due to the modes associated with the natural resonator created between the Earth's surface and the lower surface of the ionosphere [10].

8. Conclusions

The present work described the main sensors that are employed for measuring electric fields in the various frequency bands. The sensors employed at VHF and HF are obtained by utilizing radio receivers. The sensors at somewhat lower frequencies are based on regular capacitive coupling between the sensor's members and the field sources. The sensors employed for dc and ULF cannot rely on ordinary capacitive coupling, since the reactance of the coupling becomes much too large at such low frequencies. The problem is overcome by the mechanical movement of the relevant electrodes, which effectively replaces the field frequency by an electromechanical effect of the electrodes' movement.

9. References

1. Rhode and Schwarz Technical Personnel, *Instruction Book for VHF Field-Strength Indicator 47 to 225 MHz HUZ*, Edition R 20818.

2. W. L. Weeks, *Antenna Engineering*, New York, McGraw-Hill, 1968, pp. 323-325.

3. Sensors of this type are known in geophysical monitoring stations: for example, see http:// www.wdc.rl.ac.uk/cgi-bin/gbdc/summary.pl.

4. H. R. Nettleson and F. H. Llewellyn, "A Sensitive Rotating Coil Magnetometer," *Proceedings of the Physical Society*, **42**, 5, 1930, pp. 501-520.

5. W. W. Lewis, *The Protection of Transmission Systems Against Lightning*, New York, Dover Publications, Inc. 1965, pp. 7-21.

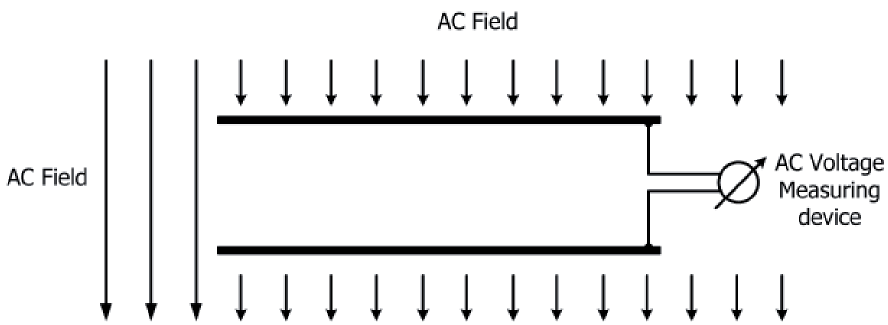

Figure 7. Sensing the ac field by a pair of stationary electrodes.

6. P. Ripka, "Advances in Fluxgate Sensors," *Sensors and Actuators A*, **106**, 3, June 2003, pp. 8-14.

7. B. Z. Kaplan and U. Suissa, "Dynamic Models of Certain DC and Low Frequency Electric Field Sensors," *IEE Proc. Sci. Meas. Technol.,* **144**, 6, November 1997, pp. 247-251.

8. A. D. Watt, *VLF Radio Engineering*, Oxford, Pergamon Press 1967, pp. 399-415.

9. J. E. Lenz, "A Review of Magnetic Sensors," *Proceedings of the IEEE*, **78**, 6, June 1990, pp. 973-989.

10. J. R. Herman, "Electromagnetic Ambients and Man-Made Noise," in Don White (ed.), *Multi-Volume EMC Encyclopedia Series Volume III*, Gainesville, VA, Don White Consultants, Inc., (Gainesville, VA 22065), 1979.

Radio-Frequency Radiation Safety and Health

James C. Lin

Mobile-Phone Use and Brain-Tumor Research

There is a general consensus among researchers that people who use a cellular mobile telephone for ten years or less are not more likely to develop a brain tumor than those who do not regularly use it. This has been the emerging trend for several years. It recently has been confirmed by publication of the summary report of a large international epidemiological study: the INTERPHONE project [1]. However, the challenge is what happens after ten or more years of regular use, since brain tumors are known to have latencies longer than ten years, and maybe as long as 30 years.

The finding that mobile-phone radiofrequency (RF) exposure for less than ten years showed no overall association between mobile phones and increased risk of malignant brain tumors with duration of use, years since first use, cumulative number of calls, or cumulative hours of use is comforting. Even so, the report is not as reassuring for long-term use. The same study showed odds ratios of 2.18, 1.82, or 1.49 for developing a glioma associated with 10 years or more regular use, 1640 or more hours of cumulative call time, or 128,000 or greater cumulative number of calls, respectively. This was when the analyses were performed using the lowest category of users (ever regular user) as the reference category for risk estimates in higher categories, and excluding use of hands-free devices (from Appendix 2 of [1], available online). An odds ratio of 1.0 corresponds to normal incidence. The increased risk was statistically significant for all three measures of RF exposure.

The INTERPHONE project was scheduled to be completed in 2005, at a cost of approximately $30 million. It was coordinated by the International Agency for Research on Cancer (IARC) in Lyon, France, a specialized research agency of the World Health Organization (WHO). It is a complex study, not only because of the large number of investigators from 13 different countries and the enormous effort of data collection (through 2004), but also because of the methodologies involved.

For example, the study observed an overall reduction in risk of glioma with any regular use of a mobile phone. This apparent but suspect downward shift in the risk estimate for cell-phone use suggests possible methodological weaknesses in the study design, resulting from a participation (or selection) bias: the reliability of subject's recall over time, and variations in subject's motivation and willingness to participate in the study. Likewise, possible methodological limitations may have contributed to investigators' disagreement on how to analyze or interpret the findings of an increased incidence of tumors among long-term users (10 years or more regular and heavy user) of mobile phones.

Observations of an increased odds ratio of glioma among long-term and heavy users of mobile phones, and of gliomas in the temporal lobe on the same side of the user's head under direct RF exposure, are causes for concern. Nevertheless, it is important to note that contrary to some popular notions, however desirable, no scientific investigation is complete or perfect. The suggestion from the INTERPHONE summary paper's authors that "The possible effects of long-term heavy use of mobile phones require further investigation," is thus as appropriate and relevant today as it was before launch of the INTERPHONE project, from a public-health perspective.

In fact, there are two ongoing research projects investigating risks associated with cellular mobile telephones: COSMOS and CEFALO. Both of these projects originated from Europe and are being conducted in Europe, well ahead of the recent call to action of the INTERPHONE summary paper.

COSMOS is an international cohort study, examining the possible long-term health effects of cellular mobile telephone use (http:// www.ukcosmos.org/faqs_1.html#1). The study is in its very early stages. The cohort study will follow the health of approximately 250,000 European mobile-phone users (18 or more years of age) in Denmark,

James C. Lin is with the University of Illinois-Chicago, 851 South Morgan Street, M/C 154, Chicago, IL 60607-7053 USA; Tel: +1 (312) 413-1052 (direct); +1 (312) 996-3423 (main office); Fax: +1 (312) 996-6465; E-mail: lin@ece.uic.edu.

[A version of this appeared in *IEEE Antennas and Propagation Magazine*, **52**, 4, August 2010; Copyright ©2010 IEEE; used with permission.]

Finland, Sweden, Netherlands, and the United Kingdom, for 20 to 30 years. Its aim is to follow changes in the frequency of diseases and symptoms over an extended period of time, especially cancers, benign tumors, neurological and cerebrovascular diseases, as well as headaches and sleep disorders.

CEFALO is an international case-control epidemiological study on brain tumors in children and adolescents (http://www.kinderkrebsregister.ch/ index.php?id=2010). Cases are identified through a combination of cancer registry and information obtained from pediatric patient wards through December 2008. All incident cases of brain tumor in the age group of 7-19 year olds, diagnosed between 2004 and 2008, are invited to participate. The CEFALO project is expected to include a total of 550 cases of brain tumors from four participating countries: Denmark, Norway, Sweden, and Switzerland. For each case, two control persons are randomly selected from the general population, matched by age, sex, and geographic regions of residence of the cases.

The objective of CEFALO is to investigate whether use of cellular mobile telephones by children or adolescents increases the risk of developing brain tumors. In addition, the study aims to provide a comprehensive data base to help investigate other potential risk factors for childhood brain tumors, specifically, potential gene-environment interactions. Accordingly, DNA from saliva samples is extracted and analyzed for DNA stability and repair. Polymorphisms in genes that affect oxidative metabolism, detoxification of carcinogens, or immune responses are examined as candidates that might reveal genetic susceptibility to brain tumors.

A very important aspect of this and of all epidemiological studies is RF-exposure assessment. Objective information on the frequency and duration of cell-phone use is obtained from cell-phone operators, and from the information stored in the mobile phone currently in use, as surrogates. Information on the extent of exposure to RF fields from mobile phones and on other known and suspected risk factors for childhood brain tumors is obtained by means of computer-assisted personal interviews. Specifically trained interviewers conducted the interviews, either in the hospital or at the participant's residence.

As of the date of this article, the project, under the leadership of **Martin Röösli** from the Institute of Social and Preventive Medicine, University of Basel, Switzerland, is near completion.

Reference

1. E. Cardis and **the INTERPHONE Study Group.** "Brain Tumour Risk in Relation to Mobile Telephone Use: Results of the INTERPHONE International Case-Control Study," International Journal of Epidemiology, 39, 3, 2010, pp. 675-694.

Conferences

CONFERENCE REPORTS

OCOSS-2010 : Ocean & Coastal Observation: Sensors and Observing Systems

Brest, France, June 21 -23, 2010

The OCOSS conferences are organized every three years by SEE (Société des Electriciens et Electroniciens). OCOSS-2010 took place in Brest in the "Le Quartz" congress hall, from June 21-23, 2010 (Figure 1). There were 130 participants from 18 countries (Figure 2). An additional day (June 24) was entirely dedicated to passive sensors, and was organized by Prof. René Garello (Telecom-Bretagne).

This year, OCOSS took place in the framework of the Seatechweek (June 21-25), organized every two years by "Brest Métropole Océane" (BMO). This is mainly an exhibition of firms (over 30, this year), the activities of which are closely linked to the sea. The main advantage of this type of association is to simultaneously gather all competencies of the same domain. Both the topics of OCOSS

Figure 1. The poster announcing OCOSS-2010.

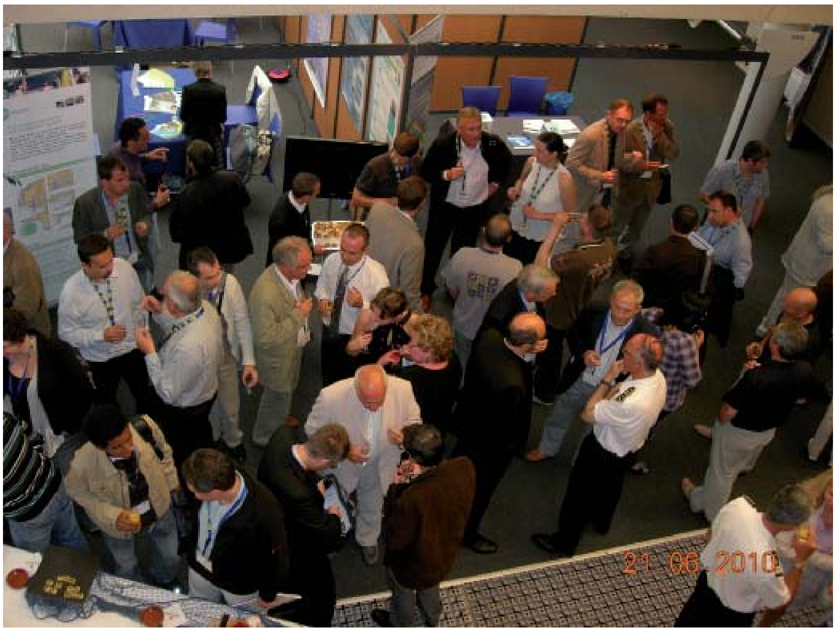

Figure 2. A coffee break at OCOSS-2010.

and the industrial activities displayed a rare diversity, as well as a complementarity of competencies, which are at the basis of any successful project.

After the words of welcome of the Mayor of Brest, François Cuillandre, Chair of BMO, the three speeches of the opening plenary session illustrated this diversity. Mathieu Belbéoch, from the Intergovernmental Oceanographic Commission of UNESCO, presented the achievements, perspectives, and challenges of the Global Ocean Observations System (GOOS). In particular, he explained the role of the Joint WMO/IOC Technical Commission for Oceanography and Marine Meteorology (JCOMM), coordinating all marine meteorology and oceanography observations, services, and data systems, worldwide. He then presented the main elements of the GOOS, including the Argo program, a major achievement in global observations of the last decade, with 3000 subsurface autonomous robots operating worldwide. For the first time ever, this network allows a continuous measurement of temperature, salinity, and the flow of water down to 2000 meters, and data collected are freely available all over the world. In conclusion, he reminded the audience that it was urgent to make the critical importance of observing the oceans more widely understood, to complete and sustain funding for the implementation, data management, and coordination of the core elements. He remarked that the potential of outreach and educational initiatives was enormous and under exploited. The collaboration with developing (and developed) countries will be crucial for the future, in particular with the African continent, a priority for IOC/UNESCO.

In the remote-sensing area, Prof. Hugh Griffiths, University College of London, outlined advantages and limitations of so-called passive systems, also called non-cooperative systems, using transmitters of other services (Broadcasting, radio communications,...). There is no doubt that the operational implementation of such systems would simplify the task of frequency allocation. This statement largely benefited from Prof. Griffiths' knowledge of the development of radar over time.

Fabrice Cohéléach (European Defense Agency – EDA) gave an account of the numerous activities of the agency, in particular of the network of maritime surveillance (MARSUR), as well as the program of unmanned aerial systems (UAS).

Twelve sessions, one specialized session, "Pôle-mer," and one posted session, were necessary to cover the entirety of the 50 selected subjects. The Chair of the Scientific Committee was Frédéric Barbaresco.

Jean-Yves Guyomard, Agence Nationale des FRéquences (ANFR, France), in his presentation, "Overview of Frequency Management," explained the work of the bodies in charge of managing the frequency spectrum, and the evolution of access conditions to this spectrum. He underlined the role of the World Radiocommunication Conferences (WRC), the next taking place in Geneva (January 17 - February 23, 2012). Item 8.1.1.c of its agenda deals precisely with possible means to improve the recognition of the essential role and global importance of Earth observation radio-communication applications. Indeed, several international bodies, such as the Group on Earth Observation (GEO), the World Meteorological Organization (WMO), and the Intergovernmental Panel on Climate Change (IPCC), are working on the matter. A collaboration of ITU-R with these bodies could be important. GEO is leading a worldwide effort to build up a Global Earth Observation System of Systems (GEOSS), to provide comprehensive and coordinated Earth observations from thousands of instruments worldwide.

Figure 3. (l-r) Co-chair of the Organizing Committee, Roland Person (IFREMER); Chair of URSI Commission F, Madhu Chandra (Chemnitz University); and Co-chair of the Organizing Committee, René Garello (Telecom-Bretagne).

The Soil Moisture Ocean Salinity satellite (SMOS) was launched on November 2, 2009, from the site of Plesetsk. This satellite carries a unique instrument, measuring the brightness temperature of Earth surfaces. It is an interferometric radiometer in the L band. Elena Dagonzo-Eusebio (ESA-ESTEC, Noordwijk, The Netherlands) et al. presented "Characterisation of SMOS RF Interferences in the 1400-1427 MHz Band as Detected During the Commissioning Phase." They very well illustrated that even for frequency bands recognized as exclusive for passive sensors, interference does happen. Coordinated support by national-frequency agencies is therefore essential. In this context, one also notes the need to correlate spatial and in-situ measurements.

These difficulties in encountering frequency bands well adapted to both passive and active sensors have led to prospective investigation, mainly for frequency allocations to radars. An example is the FARADAYS project, presented by Alex Mc Namara (Thales Air Systems), in "Frequency Allocation for Radars in the Coming Years – FARADAYS EDA Project."

It goes without saying that many studies on sea-clutter modeling were presented, mainly focusing on determining performance of passive and active sensors. For example, Yvonick Hurtaud (DGA, France) et al., in their presentation, "Characterisation of the Maritime Environment for Systems Performance Assessments and for Decision Aid Tools in RF and EO Wavebands," not only covered this matter, but also proposed decision-making aids.

As the representative of UNESCO had underlined, the building and maintenance of databases accessible to all researchers necessitates important efforts. The presentations of Kim Juniper (University of Victoria, Canada) on "Update on the Neptune and Venus Cabled Ocean Observatories," and of J. Kosakowski et al. (University of Warmia and Mazury, Poland) on "An Attempt to Vistula Lagoon Water Ecosystem Management and Modeling" constituted good examples, although in very different frameworks.

It is impossible to quote all speakers and their interesting and inventive contributions. However, we want to thank the co-Chairs of the OCOSS-2010 organizing Committee, René Garello (Telecom-Bretagne) and Roland Person (IFREMER) (Figure 3), for having communicated their common passion for the matter to this event. The traditional gala dinner on Wednesday evening in the Brest Castle was a rare success from all points of view, benefiting of a beautiful late sunset.

The next OCOSS meeting will take place in 2013, either in Germany or in Great Britain, depending on the outcome of the current discussions.

Jean Isnard
URSI-France, Commission F
E-mail: jisnard-isti@club-internet.fr

2010 International Kharkov Symposium on Physics and Engineering of Microwaves, Millimeter and Submillimeter Waves (MSMW'2010) and Workshop on Terahertz Technologies and Spectroscopy of Complex Media (TERATECH'2010)

V. N. Karazin Kharkov National University, Ukraine, June 21 - 26, 2010

Abstract

MSMW'2010 Symposium took place at the V. N. Karazin Kharkov National University, Ukraine on June 21-26, 2010. It was organized by the Scientific Council of the National Academy of Sciences of Ukraine (NASU) on Radio-Physics and Microwave Electronics, in co-operation with the following organizations: A. Usikov Institute of Radiophysics and Electronics of NAS of Ukraine (IRE NASU), Institute of Radio Astronomy of NAS of Ukraine (IRA NASU), V. Karazin Kharkov National University (KhNU), Kharkov National University of Radio Electronics (KhNURE), Institute of Magnetism of NAS and MES of Ukraine (IMAG NASU and MESU), Young Scientists Council of IRE NASU, IEEE AP/MTT/ED/AES/GRS/NPS/EMB Societies East Ukraine Joint Chapter, IEEE "IRE-Kharkov" Student Branch, IEEE "IRE-Kharkov MTT-S" Student Chapter, IEEE "IRE-Kharkov ED-S" Student Chapter and the National URSI Committee of Ukraine. It was technically co-sponsored by: URSI Commissions B and K, IEEE AP/MTT/ED/AES/GRS/NPS/EMB Societies East Ukraine Joint Chapter and sponsored by IEEE AP, MTT, ED, and NPS Societies, IEEE Electron Devices Society, URSI Commission and the European Microwave Association (EuMA).

The working days of the Symposium were June 22 to 25. Every day the program started with a plenary session of five 35-min invited lectures in a large auditorium. After that, four or three parallel day-long sessions of 15-min contributed papers had been working. The working language of the Symposium was English. June 26 was filled in with social events. The number of registered participants was 166 including 110 from Kharkov, 15 from the rest of Ukraine, 15 from Russia, 5 from Germany, 4 from Mexico, 3 from Turkey, 2 from France, China, Iran, and Lithuania each, 1 from USA, the United Kingdom, Sweden, Japan, Israel, and Belarus each, and also from Canada, Czech Republic, India. The total number of papers presented during the Symposium was about 212, included 28 invited ones.

CD-ROM version of the MSMW'2010 Proceedings had been prepared before the Symposium. MSMW'2010 Symposium program contains papers submitted world-known experts in microwaves and shorter wavelength science and technology, so participation in the Symposium has become a unique experience to Ukrainian participants. The holding of the Symposium became possible thanks to the support of sponsors: URSI, IEEE AP, MTT, ED, and NPS Societies as well as efforts of the traditional founders and organizers of MSMW. The European Microwave Association has donated a special grant for the funding of the EuMA-MSMW Microwave Prizes awarded to the young scientists who presented outstanding papers during the Symposium.

As three years ago, on the MSMW'07, this year the Workshop on Terahertz Technologies and Spectroscopy of Complex Media (TERATECH'10) was organized in the

Figure 1. The opening ceremony of the MSMW'20010 Symposium. From left to right: Dr. A. V. Boriskin (IRE NASU, Kharkov), Prof. Ni. I. Slipchenko (KhNURE), Prof. S. N. Shulga (KhNU), Prof. L. M. Lytvynenko (IRA NASU, Kharkov), Prof. V. M. Yakovenko (IRE NASU, Kharkov), Prof. A. N. Pogorily (IMAG NASU and MESU), Prof. S. I. Tarapov, Dr. A. A. Kostenko, Prof. A. I. Nosich (IRE NASU, Kharkov)

Figure 2. Poster session. From left to right: Prof. L. P. Yatsuk (KhNU, Kharkov), Dr. V. V. Yachin (IRA NASU, Kharkov), Dr. T. L. Zinenko (IRE NASU, Kharkov)

framework of the MSMW'2010 Symposium in the format of a special two-day session. We strongly hope that it will have remarkable impact on the on-going and future R&D in this novel area. This is fully in line with traditionally strong emphasis placed by MSMW program on the mm and sub-mm wave physics and technology. Extremely captivating and challenging area of nanophysics and nanoelectronics, considered as the key technology of the current century, has been also included into the agenda of the workshop.

Also, were organized IEEE Chapter Chair Conference, IEEE ED Society Mini-Colloquium, and the 10-th Kharkov Young Scientists Conference (YSC*10) "Electromagnetics, Photonics, and Biophysics" in the framework of the MSMW'2010 Symposium.

MSMW'2010 started at 9:00 on June 22, 2010 by the opening ceremony at the "Large Chemical" auditorium of the Kharkov National University. The first to address the participants was MSMW'2010 Chairman, Director of IRE NASU, Vice-Chairman of the Ukrainian National URSI Committee Prof. Vladimir M. Yakovenko. He was followed by the welcome words from the other organizations behind MSMW'2010: Head of the Department of Thin Films Physics of IMAG NASU and MESU Prof. Anatolii N. Pogorily, Dean of the School of Radio Physics of KhNU Prof. Sergei N. Shulga and Vice-Rector of KhNURE Prof. Nikolai I. Slipchenko. The next to make a welcoming speech was MSMW'2010 Co-Organizer Prof. Alexander I. Nosich of IRE NASU, who spoke in the name of the IEEE AP/MTT/ED/AES/GRS/NPS/EMB Societies East Ukraine Joint Chapter.

At the first morning a plenary session was held, consisting of five invited talks:

Development Of Powerful Terahertz Gyrotrons, M. Glyavin, A. Luchinin, V. Manuilov, M. Moiseev, A. Sedov, V. Zapevalov. Nizhny Novgorod, Russia

260 Ghz Quasioptical Setup For Epr And Dnp Experiments On The 9.2 Tesla Dnp/Nmr/Epr Spectrometer, V. Denysenkov, V. K. Kiseliov, M. Prandolini, M. Gafurov, A. Krahn, F. Engelke, V. I. Bezborodov, Ye. M. Kuleshov, P. K. Nesterov, M. S. Yanovsky, T. F. Prisner. Kharkov, Ukraine; Frankfurt am Main, Rheinstetten, Germany

Microwave Emission Properties Of A Precipitating Atmosphere With Respect To Remote Sensing Of Precipitation From Space By Means Of Microwave Radiometry, B. G. Kutuza, Moscow, Russia

Measurement Of Dielectric Properties Of Liquid Ctystals In The Millimeter And Thz Ranges, V. V. Meriakri, E. E. Chigray, I. P. Nikitin., L. C. Pan, R. P. Pan, M. P. Parkhomenko. Fryazino, Russia; Hsinchu, Taiwan

Sources Of Intense Impulse Microwave Emission, I. I. Magda, Kharkov, Ukraine.

After the lunch, the symposium continued working with four simultaneous sessions:

Session W. Workshop on Terahertz Technologies and Spectroscopy of Complex Media.

Session A. Electromagnetic Theory and Numerical Simulation.

Session C. Wave propagation, Radar, Remote Sensing and Signal Processing.

Session G. Scientific, Industrial and Biomedical Applications.

In session W the following invited papers were presented:

High Power Thz Technologies Opened By High Power Radiation Sources – Gyrotrons, T. Idehara, T. Saito, I. Ogawa, S. Mitsudo, Y. Tatematsu, Fukui, Japan

Anderson Localization in Metamaterials, N. M. Makarov, F. M. Izrailev, E. J. Torres-Herrera, Puebla, Mexico

In session A the following invited paper was presented:

Resonant Radiation Of Electron Beam, Moving Near Periodic Boundary Of Metamaterial, P. Melezhik, A. Poyedinchuk, N. P. Yashina, G. Granet, Kharkov, Ukraine; Clermont-Ferrand, France

After the sessions, all the participants were invited to enjoy the concert provided by Ukrainian *folk instruments* Ensemble "Vesela Banda" of the I. Kotlyarevsky Kharkov State University of Arts. Later that evening, at 8:00 p.m., a welcome party was organized at the university restaurant. At the welcome party, Ukrainian sparkling wine was served. This event created a perfect atmosphere to relax and shake off the troubles of long and sometimes tiring journeys that participants had to undertake to reach MSMW'2010.

At the plenary session on June 23, the following invited papers were presented:

Electromagnetic Analysis Of Lamellar Diffraction Gratings Using A Spectral Method Based On Spline Expansion With A Non Uniform Sampling Scheme, A. M. Armeanu, L. B. Andriamanampisoa, K. Edee, G. Granet, P. Schiavone, Aubиre, France

Trapped Mode Resonances Of Metal-Dielectric Arrays, S. L. Prosvirnin, A. V. Gribovsky, V. V. Khardikov, P. L. Mladyonov, E. O. Iarko, Kharkov, Ukraine

Resonance Responses Of Compound Screens With Below-Cutoff Holes And Eigenoscillation Intercoupling As Its Forward Base, A. O. Perov, N. G. Kolmakova, A. A. Kirilenko, Kharkov, Ukraine

Algan/Gan Microwave Transistors For Wireless Communication Systems And Advanced Nanostructures For High-Speed Sensor Applications, S. Vitusevich, Juelich, Germany

Stochastic Scattering Due To Random Inhomogeneities In Shf Oscillation Systems, E. M. Ganapolskii, Z. E. Eremenko, Yu. V. Tarasov, Kharkov, Ukraine

That day regular sessions of contributed papers consisted of:

Session W. Workshop on Terahertz Technologies and Spectroscopy of Complex Media.

Session B. Microwave solid State Physics and Applications

Session F. Radio Astronomy and Earth's Environment Study

In session B the following invited papers were presented:

Josephson Waveform Synthesizers, J. Niemeyer, O. Kieler, F. Müller, J. Kohlmann, R. Behr, L. Palafox, Braunschweig, Germany

Microwave Study Of $Fese_{0.3}te_{0.7}$ Thin Film By Te_{011}-Mode Sapphire Dielectric Resonator, Yun Wu, Shuyu Zhou, Xiyuan Wang, Lixin Cao, Xueqiang Zhang, Yusheng He, A. A. Barannik, N. T. Cherpak, V. N. Skresanov, Beijing, China; Kharkov, Ukraine

Superconducting Gap Structure Of Iron Pnictides From Radiofrequency Penetration Depth And Thermal Conductivity, M. A. Tanatar, D. C. Canfield, R. Prozorov, Ames, USA

In session F the following invited papers were presented:

Influence Of Hf Powerful Radio Waves On The Ozone Number Density In The Earth's Atmosphere, Yu. Yu. Kulikov, V. L. Frolov, Nizhny Novgorod, Russia

The Use Of Precise Spectroscopy For Detailed Studies Of Star Forming Regions And Fundamental Priperties Of The Universe, A. V. Lapinov, Nizhny Novgorod, Russia

On this day, a bus city tour was organized, enabling participants to get acquainted with the history of Kharkiv, the second-largest Ukrainian city. Remarkable historical buildings and monuments, such as the Assumption Cathedral, WW II Memorials, and the "Gosprom" complex built in the 1920s in the constructivism style of the early Soviet period were visited.

On the third day, the plenary session looked as follows:

System Aspects Of A Low-Cost Coherent Radar System With Aesa Antenna For Maritime Applications, T. Bertuch, M. Pamies, C. Löcker, P. Knott, H. Erkens, R. Wunderlich, S. Heinen, Wachtberg, Germany

Figure 3. MSMW'2010 Banquet. From left to right: Dr. A. A. Kostenko (IRE NASU, Kharkov), Prof. A. N. Vystavkin and Dr. S. V. Shitov (V. A. Kotelnikov Institute of Radio Engineering and Electronics of RAS, Moscow, Russia)

Lasers With Free Nonrelativistic Electrons, V. A. Buts, A.M. Egorov, Kharkov, Ukraine

Reliability, Degradation And Breakdown Of Advanced Gate Stacks, E. Miranda, Barcelona Spain

Nanocrystalline Silicon Thin Film Transistors. A. Nathan, London, United Kingdom

Two parallel sessions of regular papers that day went along the following topics:

Session E. Microwave and mm wave engineering.

Session H. R-functions, atomic functions, wavelets, fractals.

During those sessions the following invited papers were presented:

Characteristics Of The Wavegude To Quasioptical Or Dielectric Resonator Couplings, V.N. Skresanov, V.V. Glamazdin, M.P. Natarov, A.I. Shubny, Kharkov, Ukraine

Reconstruction And Super-Resolution Algorithms Of 2D-3D Images And Objects, V.I. Ponomaryov, Mexico-city, Mexico

That evening, the Symposium banquet was held at the university restaurant. This was a lovely event accompanied with live music, dancing and informal speeches. The dominant tone, however, was the joy of meeting the old friends and colleagues and making new ones.

On June 25, the following invited topics were presented:

Microwave And Thz Applications Of Ferroelectrics And Multiferroics, S. Gevorgian, A. Vorobiev, Moelndal, Sweden

Two Terminal And Multiterminal Efficient Planar Silicon Light Emitting Devices (Si-Led's) Fabricated By Standard Ic Technology As Components For All Silicon Monolithic Integrated Optoelectronic Systems, Herzl Aharoni, Beer-Sheva, Israel

New Measurement Method For Two-Port Noise

Figure 4. The closing ceremony of MSMW'2010: Prof. V. M. Yakovenko congratulates Dr. V. A. Sydoruk (Institute of Bio- und Nanosystems, Forschungszentrum Juelich, Germany) with seccessful presentation on the Symposium. On the right – Dr. O. V. Shramkova

Parameters, D. Pasquet, C. Andrei, D. Lesénéchal, P. Descamps, Caen, France

Fifty Years of Noise Radar, K.A. Lukin, R.M. Narayanan, Kharkov, Ukraine; Pennsylvania, USA

On the last working day, the symposium continued working with only one session:

Session D. Vacuum and solid state devices & IEEE EDS Mini-Colloquium

The closing ceremony of MSMW'2010 took place in the "Large Physical Auditorium" of KhNU at 15:00. At first, the winners of the Young Scientist Paper Contest were announced and awarded with the EuMA-MSMW prizes and certificates. This year the European Microwave Association established a 1000 Euro fund to be awarded to the winners of the Young Scientist Paper Contest. They were divided into 6 prizes: one First Prize, two second prizes, and three third prizes. The International Awards Jury consisted of 9 members: G. Granet, Aubiure, France, T. Idehara, Fukui, Japan, B. G. Kutuza, Moscow, Russia, S. Vitusevich, Juelich, Germany, A. I. Nosich, N. T. Cherpak, O. V. Shramkova, and D.M. Vavriv, Kharkov, Ukraine, and F. I. Yanovsky, Kiev; Ukraine.

The First Prize was awarded to:

Nikolay I. Avtomonov, Mechanisms Of Oscillations Excitation In The Spatial-Harmonic Magnetron With Cold Secondary-Emission Cathode Ira Nasu, Kharkov, Ukraine.

Two Second Prizes were awarded to:

Vitaly S. Bulygin, Visibility Of A Spherical Disk Illuminated By A Plane Wave Under The Grazing Incident, Khnu, Kharkov, Ukraine

Vyacheslav L. Semenenko, Parametric Instability Of Mobile Elastic Gate In Tera- And Nano- High Electron Mobility Transistor, Moscow Institute Of Physics And Technology (State University), Moscow, Russia

Three Third Prizes were awarded to

Sergey A. Prikolotin, Spectral Characteristics Of Step-Bended Bar In A Rectangular Waveguide, Ire Nasu, Kharkov, Ukraine

Vadim V. Vashchenko, On Mathematical Modeling Of A Triangular Building Block In The Analysis Of E-Plane Waveguide Structures, Zaporizhzhya National Technical University, Zaporizhzhya, Ukraine

Sergey V. Nedukh, Magnetoresonance Features Of Strontium-Doped Lanthanum Manganites-Perovskites In Microwave Band, Ire Nasu, Kharkov, Ukraine

Besides, 5 Honorary Mentions were awarded for the "Next to the best papers":

Evgeny A. Gurnevich, The Possibility Of Cherenkov Radiation Generation In A Photonic Crystal Formed By Parallel Metallic Threads, Research Institute For Nuclear Problems, Belarus

Anna M. Linkova, Double Frequency Sounding Of Liquid Precipitation, Ire Nasu, Kharkov, Ukraine

Dmitry V. Churikov, Analytical Kravchenko Wavelets In The Digital Uwb Signal PROCESSING, Kotel'nikov Institute of Radio Engineering and Electronics of RAS, Moscow, Russia

Evgeny A. Serov, Atmosphere Continuum Absorption Investigation At Mm Waves, Institute Of Applied Physics Russian Academy Of Science, Nizhny Novgorod, Russia

Olga V. Shapoval, Backscattering From Thin Magneto-Dielectric Strips At The Edge-On Incidence Of The H-Polarized Plane Wave, Ire Nasu, Kharkov, Ukraine

The colorful certificates of the EuMA-MSMW Prizes, signed by Dr. Oksana V. Shramkova, Ukrainian Delegate at the European Microwave Association and Prof. Vladimir M. Yakovenko, MSMW'2010 Chairman, were handed to the winners.

Additionally, another Young Scientist Award was granted by the IEEE East Ukraine Joint Chapter for the best poster paper presented at the symposium. It consisted of certificate and 100 USD money prize. This award was given to

Hossein Farhang, Optimization Of An X-Band Twta Using Magic Pic-Fdtd Code, Microwave Tubes Laboratory, Moghtader Tech Co., Tehran, Iran

The final closing address was done by Prof. Vladimir M. Yakovenko. He announced that the next Symposium, MSMW'2013, will be held again in Kharkov in June, 2013, thanked the participants and organizers for creating unprecedented forum for scientific discussions, and expressed a hope that the MSMW Symposia series will be continued. He also expressed gratitude to international institutions such as IEEE, URSI, EuMA, which rendered valuable and timely support.

In the weekend following this Symposium, the participants were proposed a social program in order to relax after four days of intensive work and strengthen the links originated at the Symposium. On Saturday, June 26 a full-day field trip with refreshments was organized from Kharkov to the S. Braude Radio Astronomy Observatory of the IRA NAS of Ukraine. The observatory is located about 80 km southwards from Kharkov. It operates the world-largest decameter-wavelength radio telescope involved into international research programs including the investigations of solar activity, Jupiter magnetic field and others. Nice weather and hospitality of the hosts helped finish the symposium agenda.

Prof. Vladimir M. Yakovenko
MSMW'2010 Chairman

SCOSTEP 12th Quadrennial Symposium on Solar Terrestrial Physics (STP-12)

Berlin, Germany, July 12 -16, 2010

The 12th quadrennial SCOSTEP symposium on Solar Terrestrial Physics was held in Berlin on July 12-16, 2010, dates chosen so that participants could also attend the COSPAR meeting in Bremen the following week. The previous symposium was held in Rio de Janeiro in March 2006. The meeting attracted more than 250 participants, including 45 students, from 32 countries. The location was the brand new Seminaris hotel and conference center, near the Free University of Berlin. The organization of the meeting was excellent and Professor F.J. Lübken, Chairman of the organizing committee, and his team have to be congratulated for their work.

SCOSTEP has a responsibility to promote interdisciplinary programs in Solar-Terrestrial Physics, and is currently in the middle of probably the most extensive research program that it has ever organized, namely the Climate and Weather in the Sun-Earth System (CAWSES-II). This multidisciplinary approach has been reflected in the scientific program of the symposium with the morning sessions devoted to tutorial and keynote lectures. These allowed participants to learn the latest developments in varied scientific topics ranging from solar physics to magnetosphere, ionosphere and lower atmosphere physics. For example, the five tutorial lectures approached some of the hot topics in Solar-Terrestrial physics and climate change studies, namely (1) new view of the Sun from the Hinode satellite, (2) economical and societal impacts of Space Weather, (3) solar influences on climate, (4) reconstruction of solar activity with applications in climate change, and (5) lessons about planet Earth learnt by studying other magnetospheres and ionospheres.

Given the large number of submitted papers, the afternoon sessions had to be organized with two sets of parallel talks. The number of oral talks was then over 110, while about 150 posters were presented in 1-hr long sessions organized at the time of coffee breaks. One of the most noticeable sessions was devoted to solar influences on climate, a scientific topic highly debated in relation to global warming. One important conclusion is that the solar influence alone cannot explain the rise in temperature observed in the 20th century. Moreover, the evolution of solar cycles indicates that the Sun might be entering a new grand minimum. A session was also devoted to Space Weather and its impact on our society, depending ever more every day on space technologies. Other topics of interest ware space climatology, waves and instabilities in the atmosphere and ionosphere and, importantly, the various couplings occurring in the Earth's environment from the solar wind to the mesosphere and then lower atmosphere, but also from the troposphere upwards. As a matter of fact, it appears that important transfers of energy occur both 'top-down' and 'bottom-up'.

The STP-12 symposium has undoubtedly been a success and the SCOSTEP Bureau has decided to continue this series of symposium now spanning over 40 years. The next STP-13 symposium should be held in 2013 in a location to be defined.

The 9th Nordic Shortwave Conference HF 10

Fårö, August 17 -19, 2010

HF 10, with the attached long-wave symposium LW 10, was held in August on the small island of Fårö, just north of Gotland in the Baltic Sea. It gathered about a hundred participants from Europe, USA, Canada, and Australia. Some 30 papers were presented and discussed. The conference was a great success, confirmed by the answers to the questionnaire.

Figure 2. Bishop Lennart Koskinen opening the conference. HF 10 Chair Carl Walde (tie) and NRS President Mats Nilson (crossed arms) stood by

Figure 1. The Täby Spa Octet, just before the flag hoisting.

Apart from URSI, the main sponsors were SNRV, the Swedish National Committee of URSI, and NRS, the Nordic Radio Society, a foundation cooperating with SNRV and responsible for the conference. All participants received a bilingual booklet, “SAA Karlskrona Radio 100 years,” sponsored by ÅF-Consult AB.

After a morning session by the Täby Spa Octet (Figure 1), the conference was opened by Bishop Lennart Koskinen, of the Visby (Gotland) diocese, who is also responsible for the activities of the Church of Sweden abroad (“In my diocese, the sun never sets”). The speech was received cum laude (Figures 2 and 3). The URSI representative, Åke Blomquist, honorary fellow of SNRV and honorary president of NRS, introduced the conference (Figure 4). The keynote speaker was professor L. W. (Les) Barclay, OBE, on “Ionospheric Communication – Opportunities and Barriers” (Figure 5).

The prize for best paper/presentation went to Mari-Anne Meister of Estonia (Figure 6), for her contribution, “Results of the Practical Research for HF Communication in Estonia.” Incidentally, the Nordic National Committees of URSI have joined to get Estonia, Latvia, and Lithuania into the URSI family: we hope to have them with us in near time.

Figure 4. URSI representative Åke Blomquist, Honorary President of NRS, introducing HF 10 in the auditorium.

Figure 5. Prof. Les Barclay delivering his keynote (at 0800 am).

Dear Friends!

Welcome to Gotland and Fårö, only one of many centers in the universe, but definitely the most central place in the Baltic sea.

My name is Lennart Koskinen, and I am the Bishop of the diocese of Visby, the smallest och biggest diocese in the Baltic sea area. It consists of Gotland with less than 60000 inhabitants, but also of all the parishes of Church of Sweden abroad, in 119 places around the world. We try to be everywhere were there are many Swedes, from Australia to California. So we can say that the sun never sets in the diocese of Visby. We also collaborate closely with the foreign ministry to help our citizens when they for one reason or another are in trouble abroad. The tsunami in Thailand was perhaps the most striking example of that where more than 800 Swedes were killed by the waves.

This means that we are very dependent on communications. I have been sailing and racing a lot on most of the big oceans, and know the value of shortwave signals. Even if I don't understand the technology I can understand the importance of your conference in both peace and war, and specially in extra-ordinary situations which we all know can occur at any time. What you are improving here prevents us from being blind and deaf when we need to communicate the most. I congratulate you for having the opportunity to take part in this conference.

But communication is more than sending and receiving messages. In the church we communicate both horizontally and vertically, sometimes even without words. I hope you will also find new ways of communication here in Fårö.

You will definitely meet new friends and learn from one another. But try also to communicate without any technology with the marvelous nature here. I have been looking at your program, and you will have some spare time to do that. Silent communication with oneself and perhaps something bigger than our own selves is sometimes called meditation. You cannot find a more suitable place for that than the nature here.

Sometimes when I am staring at the sea from the shore and perhaps longing for going out sailing, I can ask myself: But is it really the sea I am looking at? It is and it is not. What I see, and what you see when you are looking out is not the real sea, it is only the surface. The sea itself is hidden there beneath the surface in the depths. That is a suitable metaphor for the life itself. Life is more than what you can immediately see on the surface. Depths beneath depths. And it is really deep here outside. Life is more than the obvious.

Another metaphor in line with your conference, is here just in front of us. What do you see here in front of me. Air, yes, but you know better than I, that this is no empty space. The air is full of signals, and if you have the right equipment, for example a simple mobile phone can pick up messages and even pictures, a radio even more, a portable television with an antenna can easily find moving pictures and music, right here in this seemingly empty space. My message to you is: make the invisible and silent visible and audible. Use your days and nights here in this magic island not only for a conference like many others, but for an expansion of your selves and your senses, and this will be one of your best weeks for a long time.

With that a wish you luck and all my blessings. With these words I declare this conference opened.

Lennart Koskinen

Figure 3. The Bishop's speech.

HF 10 included an exhibition (Figure 7), a foxhunt (radio direction finding), a concert in the nearby Fårö church where the famous film director Ingmar Bergman is laid to rest, a banquet (Figure 8), and a bus tour of Fårö (Figure 9), all to create and maintain networks on VLF/LF/HF.

Figure 6. Mari-Anne Meister of Estonia receiving her prize for best-paper presentation, with Karl-Arne Markström, Technical Program Committee Chair.

Figure 7. The HF 10 banquet, Gotland style.

Figure 8. At the exhibition: A Swedish Navy communications shelter and van.

Figure 9. A rauk (limestone created by erosion) at Fårö.

The HF series is triennial, another being IRST, the IET Ionospheric Radio Systems and Techniques in the UK (presumably, in 2012). There is also a series of industry meetings sponsored by HFIA, the High Frequency Industry Association. The last one was in Solna on the Swedish mainland, just after HF 10. The tenth conference of our series since 1986, HF 13/LW 13, will be in 2013. However, it may be somewhat earlier than the traditional week 33 in August. To keep informed, please visit http://www.nordichf.org, where you will also find more about HF 10.

Carl Walde
Secretary of SNRV and NRS, HF 10 Chair
E-mail: info@walde.se

CONFERENCE ANNOUNCEMENTS

URSI Commission F Triennial Symposium on Wave Propagation and Remote Sensing

Garmisch-Partenkirchen, Germany, March 8 - 11, 2011

Conference Objective

The next URSI Triennium Symposium of Commission – F will provide a forum that will feature state-of-the-art developments and scientific activities in the general areas of wave propagation and remote sensing. The conference intends to build a closer cooperation between the two related scientific streams, namely, wave propagation and remote sensing. Leading experts from both areas will present review lectures that will augment topical contributions from researchers currently engaged in the developing front of the areas of wave propagation and remote sensing. The symposium will also field several short courses in the two areas as an addendum to the main conference. This meeting will be a sequel to a very successful meeting held earlier in Garmisch – Partenkirchen in 2002. The conference venue is nestled in the picturesque alpine landscape at the foot of Germany's highest mountain.

Organisation and Technical Committee

General Chair: Wolfgang Keydel

Chairmen of the Organisation and Technical Committee:
Madhu Chandra, Chemnitz University of Technology, Chemnitz, Germany & Alberto Moreira, DLR, Wessling, Germany

Members of the Organisation Committee:
All members of the German National Committee for URSI Commission-F

Members of the Technical Committee:
All national representatives of URSI Commission-F

Conference Highlights

The scientific meeting will address scientific and technological aspects of wave propagation and scattering in communication, microwave remote sensing, navigation and other information systems. The conference programme will include a series of ***review and keynote presentations*** suited for both young scientists and experts. The conference programme will feature the state-of-the-art developments in areas of propagation, remote sensing and related areas.

In addition, on the *sidelines* of the meeting on Monday, 7th March, tutorial workshops/short courses on topics of radar remote sensing and wave propagation will be featured. These ***workshops/short courses*** will offer excellent opportunities to newcomers and professionals alike to acquaint or re-acquaint themselves with technical knowledge required in dealing with issues of the current state-of-the-art. The workshop presentations will be specially tailored to match the knowledge requirements of scientists from diverse backgrounds, engineering or non-engineering alike.

Young Scientists Programme

In keeping with the established URSI tradition, the Triennial Symposium will offer limited bursaries to support the participation of deserving young scientists from developing and developed countries. Indeed, the planned review presentations will strike a tutorial tone to especially cater to the needs of young scientists. The conference aims to offer a value educational experience to newcomers in the field.

Important dates

Deadline for submitting abstracts	10th January 2011
Notification to authors:	20th January 2011
Submission of extended abstracts:	20th February 2011
Conference presentation:	8th -11th March 2011
Submission of full post-conference papers:	20th June 2011

All extended abstracts will appear on a conference CD-ROM. All full post-conference papers submitted will be considered for publication in a special issue of the Journal of Radio Science.

Contact

Prof. Dr. M. Chandra
Department of Microwave Engineering and Photonics
Chemnitz University of Technology,
Chemnitz, Germany
E-Mail: madhu.chandra@etit.tu-chemnitz.de
Website: To be announced shortly

ICEAA - APWC

Torino, Italy, September 12 - 17, 2011

The thirteenth edition of the International Conference on Electromagnetics in Advanced Applications (ICEAA 2011) is supported by the Politecnico di Torino, by the Istituto Superiore Mario Boella and by the Torino Wireless Foundation, with the principal technical co-sponsorship of the IEEE Antennas and Propagation Society and the technical co-sponsorship of the International Union of Radio Science (URSI). It is coupled to the first edition of the IEEE-APS Topical Conference on Antennas and Propagation in Wireless Communications (APWC 2011). The two conferences consist of invited and contributed papers, and share a common organization, registration fee, submission site, workshops and short courses, and social events. The proceedings of both conferences will be published on IEEE Xplore.

Topics for the International Conference on Electromagnetics in Advanced Applications (ICEAA 2011)

Adaptive antennas
Complex media
Electromagnetic applications to biomedicine
Electromagnetic applications to nanotechnology
Electromagnetic education
Electromagnetic measurements
Electromagnetic modeling of devices and circuits
Electromagnetic packaging
Electromagnetic properties of materials
Electromagnetic theory
EMC/EMI/EMP
Finite methods
Frequency selective surfaces
Integral equation and hybrid methods
Intentional EMI
Inverse scattering and remote sensing
Metamaterials
Optoelectronics and photonics
Phased and adaptive arrays
Plasma and plasma-wave interactions
Printed and conformal antennas
Radar cross section and asymptotic techniques
Radar imaging
Random and nonlinear electromagnetics
Reflector antennas
Technologies for mm and sub-mm waves

Topics for the IEEE-APS Topical Conference on Antennas and Propagation in Wireless Communications (APWC 2011)

Active antennas
Antennas and arrays for security systems
Channel modeling
Channel sounding techniques for MIMO systems

Cognitive radio
Communication satellite antennas
DOA estimation
EMC in communication systems
Emergency communication technologies
Indoor and urban propagation
Low-profile wideband antennas
MIMO systems
3.5G and 4G mobile networks
Multi-band and UWB antennas
OFDM and multi-carrier systems
Propagation over rough terrain
Propagation through forested areas
RFID technologies
Signal processing antennas and arrays
Small mobile device antennas
Smart antennas and arrays
Space-time coding
Vehicular antennas
Wireless mesh networks
Wireless security
Wireless sensor networks

Information for Authors

Authors must submit a full-page abstract electronically by **February 25, 2011**. Authors of accepted contributions must submit the full paper, executed copyright form and registration electronically by June 3, 2011. Instructions can be found on the Web site. Each registered author may present one paper at ICEAA and one paper at IEEE APWC. One additional paper may also be accepted if space permits, but will incur a supplemental publication fee of 100 Euro. All papers must be presented by one of the authors. Please refer to the Web site for details.

Deadlines

Abstract submission:	February 25, 2011
Notification of acceptance:	April 8, 2011
Full paper and presenter registration:	June 3, 2011

Contact

Prof. Roberto D. Graglia
Chair of Organizing Committee
Dipartimento di Elettronica
Politecnico di Torino
Corso Duca degli Abruzzi, 24
10129 Torino, Italy
E-mail: roberto.graglia@polito.it

Prof. Piergiorgio L. E. Uslenghi
Chair of Scientific Committee
Department of ECE (MC 154)
University of Illinois at Chicago
851 South Morgan Street
Chicago, Illinois 60607-7053, USA
E-mail: uslenghi@uic.edu
Web site: http://www.iceaa.net

39TH COSPAR SCIENTIFIC ASSEMBLY

Mysore, India, July 14 - 22, 2012

The 39th COSPAR Scientific Assembly will be held at the Global Education Centre, 2 Infosys Training Centre Mysore, Karnataka India from 14 - 22 July 2012.

Topics

Approximately 100 meetings covering the fields of COSPAR Scientific Commissions (SC) and Panels:

- SC A: The Earth's Surface, Meteorology and Climate
- SC B: The Earth-Moon System, Planets, and Small Bodies of the Solar System
- SC C: The Upper Atmospheres of the Earth and Planets Including Reference Atmospheres
- SC D: Space Plasmas in the Solar System, Including Planetary Magnetospheres
- SC E: Research in Astrophysics from Space
- SC F: Life Sciences as Related to Space
- SC G: Materials Sciences in Space
- SC H: Fundamental Physics in Space
Panel on Satellite Dynamics (PSD)
- Panel on Scientific Ballooning (PSB)
- Panel on Potentially Environmentally Detrimental Activities in Space (PEDAS)
- Panel on Radiation Belt Environment Modelling (PRBEM)
- Panel on Space Weather (PSW)
- Panel on Planetary Protection (PPP)
- Panel on Capacity Building (PCB)
- Panel on Education (PE)
- Panel on Exploration (PEX)
- Special events: interdisciplinary lectures, round table, etc

Selected papers published in *Advances in Space Research*, a fully refereed journal with no deadlines open to all submissions in relevant fields.

Contact

COSPAR Secretariat, c/o CNES
2 place Maurice Quentin, 75039 Paris Cedex 01, France
Tel: +33 1 44 76 75 10
Fax: +33 1 44 76 74 37
cospar@cosparhq.cnes.fr
http://www.cospar-assembly.org

Scientific Program Chair

Prof. U.R. Rao
Department of Space, India

Abstract Deadline

Mid-February 2012

URSI CONFERENCE CALENDAR

September 2010

ISTC2010 - International Symposium on Turbo Codes
Brest, France, 6-10 September 2010
cf. Announcement in the Radio Science Bulletin of December 2009, p. 34-36.
Contact: Ms. Karine Amis, Télécom Bretagne, International Symposium on Turbo Codes, Département: Électronique, Technopôle Brest Iroise, CS83818, 29238 BREST Cedex, FRANCE, Tel: +33 2 98 00 10 28, Fax : +33 2 98 00 11 84, Email : karine.amis@telecom-bretagne.eu, Web: http://conferences.telecom-bretagne.eu/turbocodes/

CAOL 2010 – International conference on Advanced Optoelectronics and Lasers
Sevastopol, Ukraine, 10-14 September 2010
Contact: http://caol.kture.kharkov.ua/

Metamaterials 2010 - The Fourth International Congress on Advanced Electromagnetic Materials in Microwaves and Optics
Karlsruhe, Germany, 13-16 September 2010
Contact : Prof. R.W. ZIOLKOWSKI, Dept. of Electrical and Computer Engineering, University of Arizona, 1230 E. Speedway Blvd., Tucson, AZ 85721-0104, USA, Phone : +1 520 621-6173, Fax : +1 520 621-8076, E-mail ziolkowski@ece.arizona.edu

VERSIM Workshop
Prague, Czech Republic, 13-17 September 2010
Contact: Dr. Ondrej Santolik, Institute of Atmospheric Physics, Bocni II/1401, 14131 Praha 4, Czech republic, Fax +420 272-762 528, E-mail: os@ufa.cas.cz

ISSSE 2010 - International Symposium on Signals Systems and Electronics
Nanjing, China, 16-19 September 2010
Contact: Guangqi Yang, State Key Lab of Millimeter Waves, School of Information Science and Engineering, Southeast University, Nanjing, 210096, China, Tel: +86 (25) 8379 4364, Fax: +86 (25) 8379 2096, E-mail: issse2010@emfield.org, Web: http:// www.emfield.org/issse2010

ICEAA 2010 - International Conference on Electromagnetics in Advanced Applications
Sydney, Australia, 20-24 September 2010
cf. Announcement in the Radio Science Bulletin of September 2009, p. 62-63.
Contact: Dr. R. Graglia, Department of Electronics, Politecnico di Torino, 600 Duco\a Abruzzi 24, 10129 Torino, Italy, E-mail : roberto.graglia@polito.it, http://www.iceaa-offshore.org

AP-RASC - 2010 Asia-Pacific Radio Science Conference
Toyama, Japan, 22-26 September 2010
cf. Announcement in the Radio Science Bulletin of December 2009, p. 6-8.
Contact: Prof. K. Kobayashi, Vice President for International Affairs, Chuo University, 1-13-27 Kasuga, Bunkyo-ku, Tokyo 112-8551, JAPAN, Fax: +81-3-3817-1847, E-mail: kazuya@tamacc.chuo-u.ac.jp

October 2010

URSI Commission F Microwave Specialist Symposium on Microwave Remote Sensing of the Earth, Oceans, Ice, and Atmosphere
Florence, Italy, 4-8 October 2010
Contact: Prof. P. Pampaloni, IFAC/CNR, Via Madonna Del Piano 10, 50019 Sesto Fiorentino, Florence, Italy, Phone: +390 554 235 205, Fax +390 554 410893, E-mail: P.Pampaloni@ifac.cnr.it

November 2010

ESWW7 - Seventh European Space Weather Week
Brugge, Belgium, 15-19 November 2010
Contact: Dr. R. Vanderlinden, Royal Observatory of Belgium, Ringlaan 3, B-1180 Ukkel, Belgium. E-mail: Ronald.VanderLinden@oma.be

December 2010

APCM 2010 - 2010 Asia-Pacific Microwave Conference
Yokohama, Japan, 7-10 December 2010
Contact: Prof. Kenji Itoh, Kanazawa Institute of Technology, 7-1 Ohgigaoka, Nonoichi, Ishikawa, 921 8501, Japan, fax +81 76-294-6711, E-mail: itoh.kenji@ieee.org

ICMARS 2010 - International Conference on Microwaves, Antenna, Propagation and Remote Sensing
Jodhpur, India, 14-17 December 2010
Contact: Prof. O.P.N.Calla, International Centre for Radio Science, OMNIWAS, A-23 Shastri Nagar, Jodhpur 342003, India, Fax +91 0291-2626166, opncalla@yahoo.co.in, info@radioscience.org

March 2011

12th International Com F Triennial Open Symposium on Radio Wave Propagation and Remote Sensing
Garmisch-Partenkirchen, Germany, 8-11 March 2011
cf. Announcement in the Radio Science Bulletin of September 2010, p. 76-77.
Contact: Prof. M. Chandra, Microwave Engineering and Photonics, Electrical Eng & Information, T.U. Chemnitz, Reichenhainer Strasse 70, D-09126 CHEMNITZ, GERMANY, Fax : +49 371 531 24349, E-mail : madhu.chandra@etit.tu-chemnitz.de

April 2011

JURSE 2011 - Joint Urban Remote Sensing Event 2011 (formerly URBAN)
Munich, Germany, 11-13 April 2011
Contact: Photogrammetry & Remote Sensing, Technische Universitaet Muenchen, Arcisstr. 21, D-80333 München, Germany, Fax: +49 89 2809573, E-mail: pf at bv.tum.de, Web: http://www.pf.bv.tum.de/jurse2011/

CEM 2011 - Eight International Conference on Computation in Electromagnetics
Wroclaw, Poland, 11-14 April 2011
Contact: Prof. Jan K. Sykulski, Chairman of CEM 2011, Electrical Power Engineering Research Group, School of Electronics and Computer Science, University of Southampton, Southampton, SO17 1BJ United Kingdom, Fax +44 23-8059 3709, E-mail: jks at soton.ac.uk, Web: http:// www.cem2011.com

August 2011

XXXth URSI General Assembly and Scientific Symposium
Istanbul, Turkey, 13-20 August 2011
Contact: URSI Secretariat, c/o INTEC, Sint-Pietersnieuwstraat 41, B-9000 Gent, Belgium, Fax +32 9 264 4288, E-mail: info@ursi.org and ursigass2011@ursigass2011.org , http://www.ursigass2011.org/

September 2011

ICEAA-APWC 2011 - International Conference on Electromagnetics in Advanced Applications
Torino, Italy, 12-17 September 2011
cf. Announcement in the Radio Science Bulletin of September 2010, p. 77-7!.
Contact: Prof. P.L.E. Uslenghi, Dept. of ECE (MC 154), University of Illinois at Chicago, 851 S. Morgan Street, CHICAGO, IL 60607-7053, USA, Tel : +1 312 996-6059, Fax : +1 312 996 8664, E-mail : uslenghi@uic.edu , http://www.iceaa.net

October 2011

ISAP 2011 - 2011 International Symposium on Antennas and Propagation
Jeju, Japan, 25-28 October 2011
cf. Announcement in the Radio Science Bulletin of June 2010, p. 53-54.
Contact: 5F Daehan Bldg., #1018 Dunsan-Dong, Seo-Gu, Daejeon 302-120, Korea, Tel : +82-42-472-7463, Fax : +82-42-472-7459, isap@isap2011.org, *http://*www.isap2011.org

July 2012

COSPAR 2012 - 39th Scientific Assembly of the Committee on Space Research (COSPAR) and Associated Events
Mysore, India, 14 - 22 July 2012
cf. Announcement in the Radio Science Bulletin of September 2010, p. 78-79.
Contact: COSPAR Secretariat, c/o CNES, 2 place Maurice Quentin, 75039 Paris Cedex 01, France, Fax: +33 1 44 76 74 37, cospar@cosparhq.cnes.fr , http://www.cospar-assembly.org/

URSI cannot be held responsible for any errors contained in this list of meetings.

An up-to-date version of this Conference Calendar, with links to various conference web sites can be found at www.ursi.org/Calendar of supported meetings

News from the URSI Community

BOOKS PUBLISHED FOR URSI RADIOSCIENTISTS

The Design of CMOS Radio-Frequency Integrated Circuits, Second Edition

by Michael Thomas H. Lee, Cambridge, Cambridge University Press. 2009, Hardcover

ISBN 978-0-521-83539-8; 797 pp., USD 94.00.

This book is an expanded and revised version of the first edition, published in 1998. Since the date of the first edition, much progress and numerous developments have been made in the field of RF CMOS, at both the academic and industrial levels. This edition intends to cover the design principles, techniques, and applications of gigahertz RF integrated circuits. One remarkable evolution in the second edition is to provide a bridge between system and circuit issues, as well as to cover the principles of wireless systems in a completely new chapter. The book is organized in 20 chapters over 797 pages. The lengths of the chapters are roughly between 12 and 60 pages. Most of the chapters are completed by a set of quite useful problems for students.

The first chapter (39 pages) provides a historical overview of the development of radio technology. It presents many historical aspects, stories, and actors connected to the birth and the growth of radio technology. This chapter has more than a cultural reason, as it helps the reader to understand the principles and the foundation of radio technology.

Chapter 2 (46 pages) is dedicated to an overview of wireless principles. After a brief presentation of the history of wireless systems, the first, second, and third generations of cellular systems are discussed. Modern technologies, like Wi-Fi, Bluetooth, and WPAN are then presented. The important common aspects of wireless systems, such as channel capacity, analog and digital modulations, and atmospheric propagation are also discussed.

Chapter 3 (26 pages) discusses the main properties of passive RLC networks. The reason for this is the preponderance of RLC circuits in RF technology. Many basic configurations, such as π, T, and L networks are detailed. A set of 16 problems concludes this chapter.

Chapter 4 (52 pages) concerns the characteristics of passive IC components. It surveys the passive components largely used in CMOS processes. Among these are single interconnections, capacitors, inductors, and transformers. Skin-depth and coupling effects are considered in the determination of closed-form formulas presented in the chapter. A set of 10 problems concludes this chapter.

Chapter 5 (35 pages) is a review of MOS device physics. The MOSFET configuration is studied, and static and dynamic electrical signals and models are discussed. Different regimes of operations and useful models are given and detailed. A set of 10 problems concludes this chapter.

Chapter 6 (18 pages) is entitled "Distributed Systems." It is mainly focused on transmission lines and their main properties. Specific RF parameters, such as the characteristic impedance and the propagation constant, are briefly introduced and used to study the behavior of finite-length transmission lines. A set of 10 problems concludes this chapter.

Chapter 7 (12 pages) is entitled "Smith Chart and S-Parameters." Two RF concepts are briefly introduced. One is the Smith-chart diagram, and the other is the concept of *S* parameters. The chapter contains some useful comments on power and impedance values in RF systems. A set of 10 problems concludes this chapter.

Chapter 8 (38 pages) is entitled "Bandwidth Estimation Techniques." It presents several methods for estimating the bandwidth of high-order systems. The MOSFET model is considered, and many useful formulas are presented and discussed. The connections among rise time, delay, and bandwidth are discussed, too. A set of 10 problems concludes this chapter.

Chapter 9 (44 pages) is entitled "High-Frequency Amplifier Design." It concerns the detailed design of a high-frequency amplifier. Both broadband and narrowband, and single- and cascaded-stage configurations are studied. Many practical design rules are presented. A set of 12 problems concludes this chapter.

Chapter 10 (20 pages) is dedicated to voltage references and biasing. This is mainly a review of diode characteristics. It surveys many biasing methods in the context of CMOS integration. A set of 12 problems concludes this chapter.

Chapter 11 (30 pages) is dedicated to noise. Different kinds of noise are introduced, such as thermal, shot, flicker, and popcorn noise. The classical two-port noise theory and the noise-factor parameter are then presented and illustrated in examples of noise calculations. A set of 14 problems concludes this chapter.

Chapter 12 (40 pages) is dedicated to low-noise amplifiers (LNAs). This chapter exploits the concepts presented in the three previous chapters, in order to introduce the design of a low-noise amplifier having the best noise performance. The dynamic range and large-signal linearity limits are also discussed. A set of 12 problems concludes this chapter.

Chapter 13 (36 pages) is dedicated to mixers. Mixer fundamentals as well as characteristic parameters are presented. The concept of nonlinear systems as linear mixers is developed. Numerous mixer topologies are then examined. A set of nine problems concludes this chapter.

Chapter 14 (52 pages) is entitled "Feedback Systems." It provides the concepts of system control and feedback. It does not contain any RF matter. However, these concepts are exploited in the following chapters, and especially for the PLL device. A set of 14 problems concludes this chapter.

Chapter 15 (67 pages) is entitled "RF Power Amplifier." It presents numerous topologies for building RF amplifiers, each with its specific domain of application. Tradeoff issues among gain, linearity, and efficiency are studied. The load-pull experimental approach is developed, too. A set of 11 problems concludes this chapter.

Chapter 16 (60 pages) is entitled "Phase Locked Loops." It presents the basic operating theory in detail. The analysis of both first- and second-order loops is presented. The loop stability is detailed, as well as the sensitivity to power and noise. A set of 10 problems concludes this chapter.

Chapter 17 (49 pages) is entitled "Oscillators & Synthesizers." It presents in detail the issue of oscillators and frequency synthesizers. Relaxation and tuned configurations are presented. Prediction of amplitude and criteria for stability and start-up are all studied. A set of 11 problems concludes this chapter.

Chapter 18 (35 pages) is entitled "Phase Noise." It concerns the noise of oscillators. General criteria for optimizing the noise performance of oscillators are discussed. A theory of phase noise is presented and applied to oscillators based on noisy MOSFET devices. A set of 10 problems concludes this chapter.

Chapter 19 (70 pages) is entitled "Architectures." This chapter exploits the concepts introduced in the previous chapters in order to built transmitters and receivers. Rules are developed for predicting system performance. Super-heterodyne architectures are examined. The merits and limitations of each configuration are studied in detail. A set of seven problems concludes this chapter.

Chapter 20 (12 pages) is entitled "RF Circuits Trough the Ages." This is a description of some fundamental RF circuits, selected by the author as important milestones in RF/radio design. The focus is more on early consumer-radio circuits. The chapter discusses five fundamental configurations.

In summary, this book is an excellent textbook for the design of RF CMOS integrated circuits. It covers all the aspects needed for the design process, including the foundations of RF analysis, as well as feedback and control theory. The organization into 20 chapters is logical, and helps the reader to quite easily acquire the subject matter of each chapter. Many practical circuits that can be seen as worked examples are given in all the chapters. In addition, the length of the chapters is quite good, as well as the proposed set of problems at the end of the chapters. I suspect that this book will be most useful for undergraduate/graduate students, or as an introduction to RF CMOS circuits. In that sense, it is an excellent source for students, and professors could recommend it.

Two points should contribute to improving the audience of the book in future editions. Some annexes giving basic formulas and important data for RF and CMOS should be added. Solutions or tricks for the proposed problems should also be included.

Smail Tedjini
Grenoble-inp/Lcis
E-mail: Smail.tedjini@lcis.grenoble-inp.fr

Nanotechnologies for Future Mobile Devices

by Tapani Ryhänen, Mikko A. Uusitalo, Olli Ikkala, and Asta Kärkkäinen (eds.), Cambridge University Press, 2010, Hardcover ISBN-13: 9780521112161; 282 pp.; USD 73.99.

Nanotechnologies are meant to be one of the disruptive technologies that will change the way we understand mobile and Internet communications today. Thanks to their features in terms of cost, size, and energy consumption, nanotechnologies are currently changing the way we think of mobile devices and communication paradigms, and open a new era in innovation and manufacturing processes.

Through its practical orientation, *Nanotechnologies for Future Mobile Devices* provides the state of the art of nanotechnologies and the future trends. The book is intended for experts wanting to know the future evolution of nanotechnologies, and for readers interested in learning about this disruptive technology. For those professionals who want to go more deeply into technical aspects, each chapter includes a vast list of up-to-date references.

This book is a result of a research collaboration between industry (Nokia) and academia (Helsinki University of Technology and University of Cambridge), so the technical contents are fully complemented with business analysis and open innovation. This practical perspective is evident when reading the book.

The book is organized in nine chapters that cover from technological aspects to manufacturing and commercialization. This is preceded by an introductory chapter, explaining how nanotechnologies can transform future mobile and Internet communications and networks. It depicts the challenges that nanotechnologies will face in the near future.

Chapter 2 focuses on how nanotechnologies can provide capabilities for tailoring materials at the molecular level in order to develop new specific materials with well-defined functions under a bottom-up approach. A number of interesting examples for nanocomposites to tune mechanical properties, as well as for synthesizing organic and inorganic nanocomposites, are shown in the chapter.

Chapter 3 explains how nanotechnologies can solve the increasing energy needs of future mobile devices by developing more-efficient storage and energy-harvesting solutions, very light materials for transport, and very-low-cost fuel cells for portable devices. The limits of scaling, computing, architectures for nanosystems, and future options for memory technologies are discussed in Chapter 4. After reading the last section, it is very clear what the features are of diverse architectures and physical-implementation alternatives, and how future mobile devices will benefit from nanotechnologies.

Complementing computing and storage solutions, Chapter 5 reviews sensing and actuation concepts for nanotechnologies, towards future Internet and cognitive systems. In Chapter 6, nanotechnology is presented as an enabling technology for the Internet of Things. New forms of mobile-communication concepts, such as location-based services, will be possible only under stringent cost, size, and low-power-consumption requirements that can be achieved using nanowire structures, and graphene and carbon nanotubes, for example.

Chapter 7 particularizes the analysis for flat-panel devices, with a focus on emerging display technologies and their role in human interaction. The last two chapters deal with the commercialization of nanotechnologies. Chapter 8 discusses how value can be created and extracted from nanotechnologies under the perspectives of commercialization of emerging technologies, innovation, and manufacturing. Chapter 9 derives the economic impact of the first nanotechnology generation (denoted as “Nanotech 1.0”) under technology-development tools: the hype cycle and the S curve. Examples from automotive applications to the electronics and power industries are provided to show the entering of Nanotech 1.0 technologies into the market. The last chapter draws the main conclusions of the book, with emphasis on technology, applications, open innovation, and how nanotechnologies will change our ways of communication and interaction with the physical world.

Finally, it is my opinion that the contents of the book are essential to understanding the key aspects that nanotechnology must focus on in order to continue being a disruptive technology in the areas of mobile communications and devices, electronics, and the Internet.

Ramón Martínez
Universidad Politécnica de Madrid
E-mail: ramon@gr.ssr.upm.es

2010 GROTE REBER MEDAL AWARDED TO ALAN ROGERS

The 2010 Grote Reber Gold Medal for outstanding and innovative contributions to radio astronomy has been awarded to Dr. Alan Rogers, a Research Affiliate at the Massachusetts Institute of Technology Haystack Observatory. Rogers was honored for his many pioneering developments in radio and radar interferometry, radio spectroscopy, and for his application of radio-astronomy techniques to society.

The medal was presented July 7, 2010, in Hobart, Tasmania, at the annual meeting of the Astronomical Society of Australia. The Reber Medal was established by the Trustees of the Grote Reber Foundation to honor the achievements of Grote Reber. It is administered by the Queen Victoria Museum in Launceston, Tasmania.

The previous winners of the Grote Reber Medal have been Prof. Bill Erickson (University of Maryland, 2005); Prof. Bernard Mills (University of Sydney, 2006); Prof. Govind Swarup (Tata Institute of Fundamental Research, 2007); Dr. Sander Weinreb (Caltech – JPL, 2008); and Dr. Barry Clark (NRAO, 2009).

Alan Rogers received his BSc in Mathematics and Physics from the University College of Rhodesia in 1962, and his SM and PhD in Electrical Engineering from MIT in 1964 and 1967, respectively. Following a year as a Lecturer at the University of Zimbabwe in 1968, he has since been at the Haystack Observatory, where he was the Associate Director until his retirement in 2006.

Rogers is best known for his contributions over many decades to the techniques of very-long-baseline interferometry. More recently, he developed an innovative radio array, which he successfully used to detect the 327 MHz line of interstellar deuterium, capping a 40-year quest for this important astrophysical atomic gas. He was also the leader of a program to apply radio-astronomy techniques to locate emergency calls from mobile telephones.

Rogers is now working with Judd Bowman of Caltech on an Epoch-of-Reoinization project, the Experiment to Detect the Global EoR Signature (EDGES). This NSF-funded experiment uses a single low-frequency dipole antenna and a high-dynamic-range radio spectrometer. The aim is to detect the cosmological epoch of reionization (EoR), a significant but poorly understood period in the history of the universe. The experiment measures the all-sky radio spectrum between 100 and 200 MHz, in order to probe the global evolution of 21-cm emission from neutral hydrogen gas at high redshift. In this type of measurement, reionization should produce a faint, step-like contribution to the spectrum that is superimposed on the much-brighter galactic synchrotron foreground. The observed frequency of the "step" and its sharpness encode both the redshift and duration of the reionization epoch. The EDGES antenna and receiver were deployed in August 2009 at the Murchison Radio-astronomy Observatory in Western Australia (Australia and New Zealand's candidate site for the SKA core). The first three-month deployment of EDGES was successful, and yielded constraints on reionization that have implications for future EoR experiments.

Who Was Grote Reber?

Who was Grote Reber? For almost a decade – 1937 to 1946 – he was the world's sole radio astronomer. Born in Wheaton, Illinois, in 1911, he moved to Tasmania in 1954, and spent more than half of his long life there. (He died in 2002.) Reber's achievements include:

- In 1937, he built the world's first purpose-built radio telescope (a 9.75 m diameter dish).

- In the late 1930s and early 1940s, he made the world's first detailed radio map of the sky (published in 1944). This was done at 160 MHz, and showed for the first time the galactic center in Sagittarius, the radio source Cassiopeia A, and the first observational evidence for spiral arms in our Milky Way Galaxy.

- In the early 1940's, he was the first to publish the detection of radio emission from the "quiet" sun, and the intense radio emission associated with solar activity.

- In the early 1950s, he became the first astronomer to build a high-altitude observatory in Hawaii (on Mt. Haleakala).

- From the mid-1950s, he built the first "Square Kilometre Array:" an array of dipoles covering an area of one square kilometer in central Tasmania. This operated at a frequency of 2.13 MHz. In the 1960s, Reber mapped the southern sky with this telescope.

Next year, 2011, is the 100th anniversary of Grote Reber's birth.

Call for Nominations

Nominations for the 2011 prize close on October 15, 2010. To nominate an achiever in radio astronomy for the medal, please send a covering letter and supporting material (e.g., CV and bibliography) to

Martin George
Queen Victoria Museum and Art Gallery
PO Box 403
Launceston, Tasmania 7250, Australia

or by e-mail to martin.george@qvmag.tas.gov.au. For more information, please see the Grote Reber Medal home page at http://www.qvmag.tas.gov.au/?articleID=539.

Helen Sim
CSIRO Astronomy and Space Science
and Australian Astronomical Observatory
Tel: +61 2 9372 4251

Information for authors

Content

The *Radio Science Bulletin* is published four times per year by the Radio Science Press on behalf of URSI, the International Union of Radio Science. The content of the *Bulletin* falls into three categories: peer-reviewed scientific papers, correspondence items (short technical notes, letters to the editor, reports on meetings, and reviews), and general and administrative information issued by the URSI Secretariat. Scientific papers may be invited (such as papers in the *Reviews of Radio Science* series, from the Commissions of URSI) or contributed. Papers may include original contributions, but should preferably also be of a sufficiently tutorial or review nature to be of interest to a wide range of radio scientists. The *Radio Science Bulletin* is indexed and abstracted by INSPEC.

Scientific papers are subjected to peer review. The content should be original and should not duplicate information or material that has been previously published (if use is made of previously published material, this must be identified to the Editor at the time of submission). Submission of a manuscript constitutes an implicit statement by the author(s) that it has not been submitted, accepted for publication, published, or copyrighted elsewhere, unless stated differently by the author(s) at time of submission. Accepted material will not be returned unless requested by the author(s) at time of submission.

Submissions

Material submitted for publication in the scientific section of the *Bulletin* should be addressed to the Editor, whereas administrative material is handled directly with the Secretariat. Submission in electronic format according to the instructions below is preferred. There are typically no page charges for contributions following the guidelines. No free reprints are provided.

Style and Format

There are no set limits on the length of papers, but they typically range from three to 15 published pages including figures. The official languages of URSI are French and English: contributions in either language are acceptable. No specific style for the manuscript is required as the final layout of the material is done by the URSI Secretariat. Manuscripts should generally be prepared in one column for printing on one side of the paper, with as little use of automatic formatting features of word processors as possible. A complete style guide for the *Reviews of Radio Science* can be downloaded from http://www.ips.gov.au/IPSHosted/NCRS/reviews/. The style instructions in this can be followed for all other *Bulletin* contributions, as well. The name, affiliation, address, telephone and fax numbers, and e-mail address for all authors must be included with All papers accepted for publication are subject to editing to provide uniformity of style and clarity of language. The publication schedule does not usually permit providing galleys to the author.

Figure captions should be on a separate page in proper style; see the above guide or any issue for examples. All lettering on figures must be of sufficient size to be at least 9 pt in size after reduction to column width. Each illustration should be identified on the back or at the bottom of the sheet with the figure number and name of author(s). If possible, the figures should also be provided in electronic format. TIF is preferred, although other formats are possible as well: please contact the Editor. Electronic versions of figures *must* be of sufficient resolution to permit good quality in print. As a rough guideline, when sized to column width, line art should have a minimum resolution of 300 dpi; color photographs should have a minimum resolution of 150 dpi with a color depth of 24 bits. 72 dpi images intended for the Web are generally *not* acceptable. Contact the Editor for further information.

Electronic Submission

A version of Microsoft *Word* is the preferred format for submissions. Submissions in versions of T$_E$X can be accepted in some circumstances: please contact the Editor before submitting. *A paper copy of all electronic submissions must be mailed to the Editor, including originals of all figures.* Please do *not* include figures in the same file as the text of a contribution. Electronic files can be send to the Editor in three ways: (1) By sending a floppy diskette or CD-R; (2) By attachment to an e-mail message to the Editor (the maximum size for attachments *after* MIME encoding is about 7 MB); (3) By e-mailing the Editor instructions for downloading the material from an ftp site.

Review Process

The review process usually requires about three months. Authors may be asked to modify the manuscript if it is not accepted in its original form. The elapsed time between receipt of a manuscript and publication is usually less than twelve months.

Copyright

APPLICATION FOR AN URSI RADIOSCIENTIST

I have not attended the last URSI General Assembly, and I wish to remain/become an URSI Radioscientist in the 2009-2011 triennium. Subscription to *The Radio Science Bulletin* is included in the fee.

(please type or print in BLOCK LETTERS)

Name : Prof./Dr./Mr./Mrs./Ms. ____

Family Name First Name Middle Initials

Present job title: ____

Years of professional experience: ___________

Professional affiliation: ____

I request that all information be sent to my ☐ home ☐ business address, i.e.:

Company name: ____

Department: ____

Street address: ____

City and postal/zip code: ____

Province/State: ____________________ Country: ____________________

Phone: ____________________ ext. ________ Fax: ____________________

E-mail: ____

Areas of interest (Please tick)

☐ A Electromagnetic Metrology
☐ B Fields and Waves
☐ C Radio-Communication Systems & Signal Processing
☐ D Electronics and Photonics
☐ E Electromagnetic Environment & Interference
☐ F Wave Propagation & Remote Sensing
☐ G Ionospheric Radio and Propagation
☐ H Waves in Plasmas
☐ J Radio Astronomy
☐ K Electromagnetics in Biology & Medicine

I prefer (Please tick)

☐ An electronic version of the RSB downloadable from the URSI web site
(The URSI Board of Officers will consider waiving the fee if a case is made to them in writing.) 40 Euro

☐ A hard copy of the RSB sent to the above address 100 Euro

Method of payment : VISA / MASTERCARD (we do not accept cheques)

Credit card No ☐☐☐☐ ☐☐☐☐ ☐☐☐☐ ☐☐☐☐ Exp. date ____________

CVC Code: ____________ Date : ____________________ Signed ____________________

Please return this signed form to :

The URSI Secretariat
c/o Ghent University / INTEC
Sint-Pietersnieuwstraat 41
B-9000 GHENT, BELGIUM
fax (32) 9-264.42.88